6-23-2021 10:45 AM

Brain Signatures of Human Skill Learning: From Single Movements to Movement Sequences

Eva Berlot, *The University of Western Ontario*

Supervisor: Diedrichsen, Jörn, *The University of Western Ontario*

A thesis submitted in partial fulfillment of the requirements for the Doctor of Philosophy degree in Neuroscience

ABSTRACT

Sequences of finger movements, such as making a cup of coffee or playing the piano, have a key role in our lives. An important neuroscientific question is how such movement sequences are represented in the brain. The central goal of this thesis was to investigate how different brain regions represent individual movements, and how these representations change when learning sequences of movements. To that end, we used 1) high-field functional magnetic resonance imaging (fMRI) to measure brain activation in humans while they produced finger movements on a keyboard-like device, and 2) advanced multivariate analyses to characterize the brain representations underlying the acquisition and control of finger movements. First, we examined the functional architecture of individual finger movements (Chapter 2). To dissociate sensory processing from movement, we designed an experiment including active finger movements and passive finger stimulation. We found that while the contralateral hemisphere represented individual fingers equally well during active movement and passive stimulation, the ipsilateral hemisphere represented fingers more clearly during active movement. Next, we assessed how brain representations for sequences of finger movements develop with learning (Chapters 3 and 4). Healthy volunteers were trained to execute a set of finger presses over five weeks and underwent repeated fMRI sessions. The results revealed widespread learning-related changes in premotor and parietal regions, including overall reduction in activation and a reorganization of how individual sequences are represented (Chapter 3). Contrary to previous research, none of these changes were observed in the primary motor cortex (M1). This distinction in learning between M1 and association regions was further supplemented by utilizing repetition suppression analysis and multivariate pattern analysis (Chapter 4). We demonstrate that M1 primarily represents the starting finger of the sequence, an effect which diminishes upon repeated sequence execution, but does not further represent sequence-specific features. Conversely, association regions reflect sequence identity and remain more stable across repetitions. Altogether, these studies revealed that M1 and association regions are differentially involved in execution and

learning of movement sequences. The broad implication of this research is that premotor and parietal regions are likely fundamental to learning sequential skills, extending beyond finger movements.

KEYWORDS

Movement, Learning, Motor learning, Hand Control, M1, fMRI, MVPA, Representational analysis

SUMMARY FOR LAY AUDIENCE

Our everyday lives are composed of sequences of movements – from the routine of making a cup of coffee to playing piano. With repeated practice, the execution of sequences like these becomes more fluid and efficient. What changes in the brain during learning that leads to such skillful control of movement sequences? To address this question, we investigated how the brain represents single finger movements and assessed what brain regions are involved in the acquisition of skilled finger movement sequences. We utilized functional magnetic resonance imaging (fMRI), a non-invasive technique that allowed us to measure brain activation in humans while they performed finger movements. One brain region that is of particular interest to motor neuroscientists is the primary motor cortex (M1). It sends commands to the muscles which then initiate the execution of movements. Prior research has established that hand movements are primarily controlled by the contralateral hemisphere (i.e., M1 in the left part of the brain controls right-hand movements), but the role of the ipsilateral hemisphere is not well understood. By contrasting brain activation during active finger movements and passive stimulation of fingers (analogous to depressing a piano key vs. the touch sensation from the key on the fingertip), we show that, while the contralateral hemisphere represents both of those conditions equally, the ipsilateral hemisphere represents active movement more than passive stimulation. Next, we asked how brain representations change as individuals learn sequences of finger movements over weeks of training. The activity of M1 during movement execution related most to the starting finger of the movement sequence, and did not show any learning-related changes. In contrast, brain regions that are typically implicated in movement planning showed activity decreases throughout learning, and represented different sequences as more distinct from one another. This altogether suggests that when learning a sequential skill, activity in areas supporting the skill decreases, perhaps reflecting increased efficiency, and is supplemented by more subtle changes of how patterns of activity represent individual sequences. These types of learning-related changes may apply more broadly to different types of learning, from sewing to touch-typing.

CO-AUTHORSHIP STATEMENT

Chapter 1 and **5** contain sections from an opinion article. I wrote the paper with helpful input from Nicola Popp and Jörn Diedrichsen. The citation is:

Berlot, E., Popp, N.J. and Diedrichsen, J., 2018. In search of the engram, 2017. *Current Opinion in Behavioral Sciences*, *20*, pp.56-60.

Chapter 2 has been published. George Prichard, Jill O'Reilly, Naveed Ejaz and Jörn Diedrichsen collected and preprocessed the data. I performed all subsequent analyses, produced figures and wrote the manuscript. All co-authors provided comments on the manuscript. The citation is:

Berlot, E., Prichard, G., O'Reilly, J., Ejaz, N. and Diedrichsen, J., 2019. Ipsilateral finger representations in the sensorimotor cortex are driven by active movement processes, not passive sensory input. *Journal of Neurophysiology*, *121*(2), pp.418-426.

Chapter 3 has been published. The experiment was conceptualized and designed by myself, Nicola Popp and Jörn Diedrichsen. Nicola Popp and I collected the data. I analyzed the data and wrote the manuscript, with comments from Nicola Popp and Jörn Diedrichsen. The citation is:

Berlot, E., Popp, N.J. and Diedrichsen, J., 2020. A critical re-evaluation of fMRI signatures of motor sequence learning. *Elife*, *9*, e55241.

Chapter 4 is under revision and has been posted on the bioRxiv preprint server. It contains analysis on the data acquired for Chapter 3. I analyzed the data, created the figures and wrote the manuscript. All co-authors contributed to interpretation of results. The citation is:

Berlot, E., Popp, N.J., Grafton, S.T. and Diedrichsen, J., 2020. Combining repetition suppression and pattern analysis provides new insights into the role of M1 and parietal areas in skilled sequential actions. *bioRxiv*.

ACKNOWLEDGEMENTS

Thanks to my supervisor, Dr Jörn Diedrichsen. My journey over the years has been guided by his incredible knowledge and brilliant insights. I am particularly grateful for the confidence he has in me as a scientist, even at times when I lack that myself.

Thanks to all of the members of the Diedrichsen lab, and more broadly the Sensorimotor Superlab (past and present), for being wonderful colleagues and friends, and for providing valuable feedback over the years. I would specifically like to express my thanks to Nicola Popp for the help with the monstrous amounts of data collection and for all the coffee breaks.

Thanks to Drs Andrew Pruszynski, Jody Culham, Brian Corneil, Ryan Stevenson, Naveed Ejaz, Federico De Martino and Marieke Mur for their pivotal mentorship over the years, and for being excellent role models.

Thanks to Joe Gati, Trevor Szekeres and Scott Charlton for all the help with the MRI data collection. Without them, this research would not have been possible.

Thanks to the Brain and Mind Institute community as a whole for fostering a warm and stimulating research environment.

Thanks to my partner Cason for making me happy, for being my sounding board when I needed it, and for everything else.

Thanks to my family. It is difficult to articulate how much their consistent presence throughout my academic life has meant to me. My brother, Rok – a steady source of encouragement that helps keep me composed. And his family, Jasna, Zora and Val, for bringing laughter that lifts the strain of intense studies. Lastly, my parents, Marija and Boris, for their unwavering support every step of the way. They instilled in me the curiosity for knowledge and taught me the importance of tenacity in life. I dedicate this work to them.

TABLE OF CONTENTS

LIST OF FIGURES

LIST OF ABBREVIATIONS

ANOVA	Analysis of variance
BA	Brodmann area
BF	Bayes Factor
BOLD	Blood-oxygen-level-dependent
Exe	Execution
fMRI	Functional magnetic resonance imaging
FS	Full speed
G	Second moment matrix
GLM	General linear model
GRAPPA	GeneRalized Autocalibrating Partial Parallel Acquisition
ITI	Inter-trial-interval
LH	Left hand
M1	Primary motor cortex
MDS	Multidimensional scaling
MEG	Magneto-encephalography
MPRAGE	Magnetization Prepared - RApid Gradient Echo
MRI	Magnetic resonance imaging
MT	Movement time
MVPA	Multi-voxel pattern analyses
N	Newton
PCM	Pattern component modelling
PFC	Prefrontal cortex
PM	Premotor cortex
PMd	Dorsal premotor cortex
PMv	Ventral premotor cortex
RH	Right hand
ROI	Region of interest
RS	Repetition suppression

RSA	Representational similarity analysis
S1	Primary somatosensory cortex
SD	Standard deviation
SEM	Standard error of the mean
SMA	Supplementary motor area
SPL	Superior parietal cortex
SPLa	Anterior superior parietal cortex
SPLp	Posterior superior parietal cortex
T	Tesla
TE	Echo time
TR	Repetition time
V1	Primary visual cortex

APPENDIX

CHAPTER 1

1 General Introduction

1.1 Preamble

The human hand has been a chief engine driving the development of humanity. When the hand became liberated from locomotion by our adoption of upright bipedal posture, it gained its own functions which became the foundation for nearly all of humanity's subsequent achievements (Darwin, 1871). After that decisive crossroad, humans became toolmakers, which opened a new world of possibilities fostering creativity, triggering a huge expansion of the brain. This allowed humans to grasp more complex ideas and become sophistical social beings, which then led to the development of language, culture, civilization as we know it today (McGinn, 2015). This central role of the hand in humanity's ascension to Earth's dominant lifeform is also captured in visual arts. Interestingly, paintings of hands may be the oldest form of visual art in human history and have since remained an important cultural motif, depicting developments of skills, insights and society (**Figure 1.1**). Today, hands play an essential role in nearly all of our endeavours – from writing to buttoning a shirt, drawing, sewing, cutting an apple, or browsing the internet.

The foundation of this enhanced dexterity in humans is set by how the brain controls finger movements, with direct projections from the primary motor cortex (M1) to parts of the spinal cord which innervate finger muscles (Rathelot and Strick, 2009). This allows us to perform individuated finger movements. Most actions, however, require more than one individual finger movement. Movements are often executed in a sequential order, whereby, over time and with practice, the set of sequential movements become performed faster, more efficiently and fluently, as if they were executed as a single long action. This is known as motor sequence learning. Many everyday activities fall under the family of

motor sequence skills, but arguably no example depicts the capacity to learn sequences of finger movements better than professional piano playing. A pianist must bimanually execute up to 1,800 note per minute (Munte et al., 2002). The key neuroscientific question that stems from such feats of human behaviour is: what brain changes can sculpt such astonishing behavioural improvements in the production of motor sequences?

In this introductory chapter, I will first review the neural organization that underlies hand movements. I will then present a theoretical framework summarizing the possible ways of how the neural circuitry could support complex sequential movements. After that, I will discuss the brain changes that occur during learning of complex motor sequences, and review the techniques needed to address such questions in humans. Last, I will provide an overview of the data chapters of this thesis.

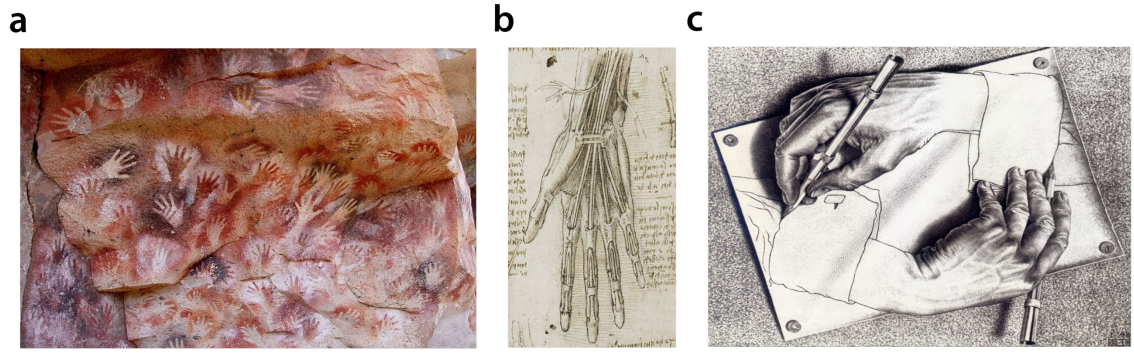

Figure 1.1. Fascination with the hand in visual arts.

a) Cueva de las Manos (Cave of Hands), Argentina, c. 11000 BC, is one of the earliest remainders of wall art. **b)** Leonardo da Vinci, c. 1510, Royal Collection Trust, studied the hands from both an artistic and scientific point of view. **c)** M. C. Escher, Drawing Hands, 1948. In the 20th century, the art questions itself, with the hand being part of that self-reflection.

1.2 Neural organization of hand movements

1.2.1 The role of M1 in hand control

How do we move our hands? For decades, the answer to this question seemed simple: the primary motor cortex (M1) represents parts of the human body in the form of a somatotopic map (Penfield and Jasper, 1954). If we want to move our hand, the neurons of the hand area of M1 become active, sending the motor commands to the spinal cord, which in turn sends signals to the hand muscles, resulting in overt hand movement (Lawrence and Kuypers, 1968; Tower, 1940). This conceptualization implies a direct connection between subparts of M1 and individual hand muscles, with the brain moving the body as a puppeteer moves a marionette.

However, evidence suggests that M1's organization is not as clear-cut. While it broadly follows a somatotopic gradient, the representation within the hand area is less clearly defined. The borders between neuronal populations for different fingers are fuzzy with lots of overlap. Electrophysiological studies (Schieber and Hibbard, 1993) show that neurons in primate M1 are broadly tuned to multiple finger movements – in other words, instead of a single finger, or an individual muscle, they commonly represent several fingers. Moreover, stimulating a specific part of M1 leads to coordinated and complex postures, such as making a fist or opening a hand (Graziano et al., 2002) This suggests that M1's functional map might be organized based on how the body parts are used in actions encountered in everyday life.

Studies in humans have supplemented these observations. To measure brain activation non-invasively in humans, researchers commonly utilize functional magnetic resonance imaging (fMRI). fMRI measures the indirect consequences of neural activity, with blood-oxygen-level-dependent imaging (BOLD; Ogawa et al., 1990) relying on regional differences in cerebral blood flow to delineate activity in different brain areas. Using fMRI, Ejaz and colleagues (2015) examined brain activation while healthy volunteers performed individuated finger movements. They reported that the spatial layout

of M1's activation for individual fingers was highly variable across individuals. However, on closer inspection they observed some common features across participants: for example, the evoked activity patterns for the middle and ring fingers were more similar to each other than either were to the thumb pattern. Thus, the relative similarity between activity patterns across different finger pairs was preserved across individuals. By further probing what underlies this similarity structure, the authors found that it is well explained by how hands are used in everyday life. Fingers that are commonly used together evoke a more similar activity pattern in M1, whereas fingers that are used independently are represented more dissimilarly. This finding of M1's activation being possibly shaped by natural usage indicates a degree of plasticity in its functional organization. Altogether this suggests that M1 is better understood as a best-fit rendering of the natural motor repertoire onto a cortical sheet (Graziano et al., 2002), rather than a puppet-and-puppeteer analogy of the somatotopic map.

1.2.2 Motor control is supported by a distributed mosaic of brain regions

While M1 sends commands for voluntary movements, this alone is not enough to interact with the world in a meaningful way. Instead, our actions need to be planned depending on what the environment affords. This often requires decisions be made between alternative options, and rapid adjustments based on the feedback received from the environment. Achieving these goals involves interactions between a mosaic of highly distributed brain areas, commonly referred to as the motor system (**Figure 1.2a**). Below I will briefly describe the functions of individual areas of the motor system.

Posterior to M1, in the postcentral gyrus, sits the primary somatosensory cortex (S1), which receives afferent sensory signals from the spinal cord. These sensory signals need to be processed to evaluate if the current actions are achieving the desired sensory consequences, and if not, adjust the outgoing actions (Scott et al., 2015). S1 and M1 are commonly seen as two sides of the same coin – with S1 processing sensory input, whereas M1 focusing on its outputs. However, these neighbouring bits of the cortex are much more interlinked than that. Sensory signals about finger digits and their motor commands are

tightly intertwined in M1's activity patterns (Wiestler et al., 2011), supporting the idea that M1 and S1 are together involved in feedback control to deftly move in a complex world (Scott et al., 2015).

While M1 and S1 need to provide instantaneous signals about ongoing actions, higher-order regions, commonly referred to also as the 'associative regions', provide more contextual information to frame the movements for overall behavioural goals. These can broadly be divided into two main functions: 1) sensory-motor transformations and 2) decision processes that lead to action initiation. Parieto-prefrontal interactions are pivotal in computing a series of sensory-motor transformations. For visually-guided movements, visual signals are transmitted from the primary visual cortex (V1) through the dorsal visual stream (Milner and Goodale, 2008) to posterior and superior parietal cortices (Andersen and Buneo, 1993; Cui and Andersen, 2011). There, information is integrated and transformed from sensory reference frames to motor-relevant reference frames, and communicated to premotor regions (Scott et al., 1997). Premotor cortex is involved in the decisional process of which action to select. To that pursuit, the received input from the prefrontal cortex can play a biasing role by signalling context-specific factors, such as motivation, behavioural relevance, and payoff of actions (Miller, 2000; Schultz, 2004; Tanji and Hoshi, 2001). Besides the premotor cortex, motor areas on the medial surface, specifically supplementary motor area (SMA) and pre-SMA, can also bias which actions are executed, how they are temporally organized, and when the movement is initiated (Nachev et al., 2008; Shima et al., 2007). Together, these cortical regions subserve the goal of providing the necessary context to M1 to plan and execute the relevant movements.

Outside of the neocortex, subcortical structures play important roles in influencing human behaviour – with cerebellum and basal ganglia particularly relevant for motor control (Middleton and Strick, 2000). The basal ganglia are a cluster of subcortical structures which form parallel loops with the neocortex, where cortical input is received through the striatum, and propagates back to the neocortex via the thalamus (Alexander et al., 1986). These signals are critical for movement selection, initiation, stopping, and segmenting of longer actions (Graybiel and Grafton, 2015; Jin and Costa, 2015). Cerebellum also interacts with the neocortex through parallel loops, and is thought to be

particularly essential for coordination and fine tuning of movements during execution (Wolpert et al., 1998).

Altogether, each of these functionally and anatomically distributed brain regions plays a specific role in motor control. Despite distinctions between them, it is important to stress that different motor functions are not entirely compartmentalized with inflexible boundaries between regions. Instead, natural interactive behaviour requires all of these brain systems to continuously interact. Thus, reciprocal signals between these brain regions are continuously integrated to achieve successful behaviour.

1.2.3 Ipsilateral vs. contralateral control

Many of the associative regions of the neocortex represent higher-order aspects of motor control. These can be relevant to the movement of either hand, and are modulated during bimanual control of actions (Swinnen and Wenderoth, 2004; **Figure 1.2b**). In contrast, M1 and S1 show a much stronger lateralization, primarily representing the contralateral hand (**Figure 1.2b**). M1's ipsilateral input to the spinal cord lacks the capacity to produce hand and finger movements (Brinkman and Kuypers, 1973), an observation which has led to the questioning of its relevance in movement control. Yet, during bimanual reaching movements, the activity of M1 neurons represents the direction of the ipsilateral arm (Donchin et al., 1998). Evidence from humans likewise suggests that ipsilateral M1 represents aspects of ongoing actions. While ipsilateral activity is suppressed below resting baseline during unimanual movements, individual fingers of the ipsilateral hand can nevertheless be decoded (Diedrichsen et al., 2013). This evidence challenges the classic view that M1 controls only the contralateral side of the body.

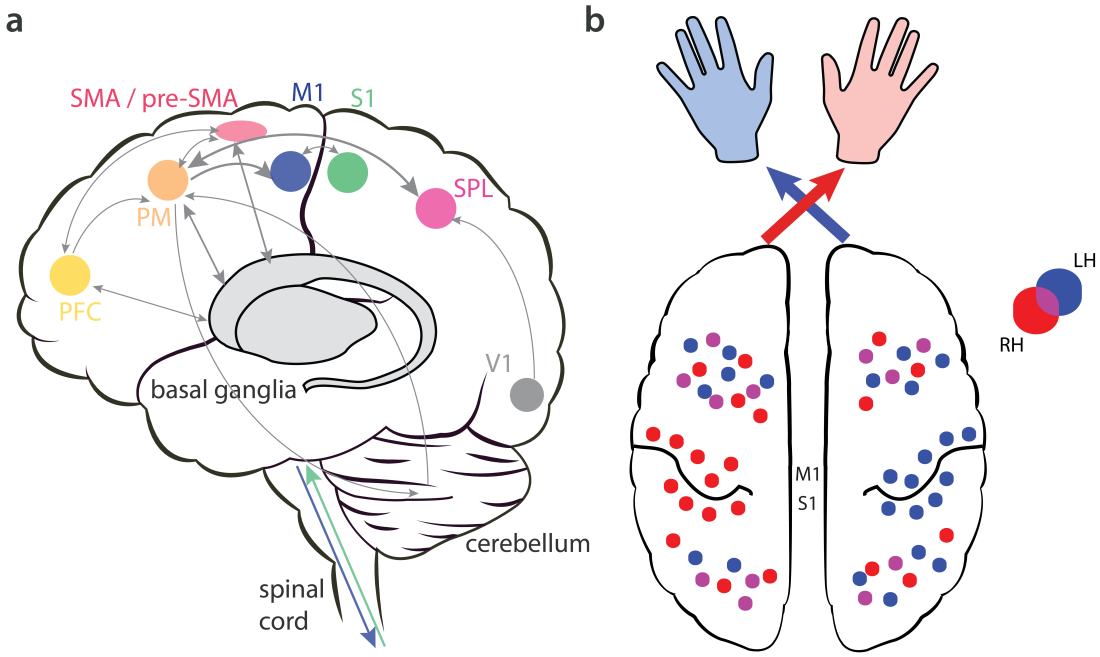

Figure 1.2. Schematic depiction of motor systems in the brain.

a) Sketch of a human brain, shown from the lateral side, depicting the cerebral cortex, cerebellum, and basal ganglia. Grey arrows represent connections between brain regions in the processes of sensory-motor transformation and action specification. Blue arrow shows efferent motor commands from the primary motor cortex (M1) through the spinal cord. Green arrow depicts afferent sensory signals from the spinal cord to the primary somatosensory cortex (S1). Abbreviations: primary visual cortex (V1), superior parietal lobule (SPL), supplementary motor area (SMA), premotor cortex (PM), prefrontal cortex (PFC). **b)** Lateralization of brain regions, shown through a superior view on the brain with both hemispheres. Neuronal populations in M1 and S1 primarily represent the contralateral effector, hand, shown here with dots in the colour of the respective hand (red for right hand – RH, blue for left hand – LH). Premotor and parietal regions contain neuronal populations which represent both the contralateral as well as the ipsilateral hand. Additionally, activity patterns in these regions are commonly modulated for bimanual usage of hands (shown in purple dots).

If ipsilateral M1 represents parameters of ongoing actions, what is the functional relevance of this representation, and where do these signals originate? One possibility is that activity in the ipsilateral M1 reflects a spillover from the contralateral M1 through transcallosal connections (Asanuma and Osamu, 1962). The proposed functional implications of these connections are largely based on studies of stroke patients, and form the basis of the interhemispheric competition account (Murase et al., 2004; Ward and Cohen, 2004). This account proposes that the two hemispheres normally communicate, exerting mutual inhibition on one another. After stroke this communication becomes imbalanced with unopposed inhibition from the healthy hemisphere, which is thought to impede the recovery (see also Xu et al., 2019). These clinical studies showcase potential functional significance of the ipsilateral hemisphere.

Still, to date the origin and functional relevance of ipsilateral M1 representations has remained much more elusive than for their contralateral counterparts. One possible way to make progress in understanding what aspects of movements ipsilateral representations represent is to try dissecting finger movements into their constituent components. A prominent distinction is one between active components of movements vs. sensory processing of the received feedback signals. An experimental dissociation of the two components would allow one to address whether ipsilateral sensorimotor cortices are primarily involved in active components of movements, such as initiation or planning, or whether they contribute to fine feedback control, incorporating incoming sensory signals from the periphery. This could refine our understanding of how the ipsilateral hemisphere is functionally involved in hand control in healthy individuals, in turn forming a springboard for further investigations of clinical significance.

1.3 Sequences of finger movements

1.3.1 Why study motor sequences?

So far I have discussed the brain circuitry involved in motor control and making an action, such as a finger movement. Virtually any goal-directed behaviour, however, depends on the ability to produce not only a single action, but a sequence of actions. This applies broadly – from playing Chopin's Revolutionary Etude, to the routine of making a cup of coffee, or inserting your PIN on a phone. These overarching actions are composed of smaller movement elements, often referred to as motor primitives, which are strung together in a serial order to create a new behaviour. Performing these activities in a wrong order can lead to disappointing consequences, such as a cacophony of sounds, a cold beverage, or a locked phone. Through practice, humans learn to produce such sequences of actions successfully and fluidly, as if they are executed as a single longer action. The key question is how the brain sculpts such behaviours where isolated movements are combined into one smooth, coherent action.

One possibility is that executing a movement sequence (e.g. pressing a PIN's digits 5-4-2-3) relies on a one-by-one process, whereby each motor primitive is initially selected and executed (e.g. digit 5), before processing the next upcoming element (e.g. digit 4), then the one after, etc. (**Figure 1.3a**). This could possibly account for behaviour of newly encountered sequences (e.g. when receiving a new PIN). However, once these sequences are repeatedly executed, they seem to be performed very fluidly and in a rapid succession, which does not seem to match such a slow one-by-one process of sequential selection and execution for each motor primitive. What is even more problematic for this account is that individual elements of skilled sequential actions often seem to be performed in an overlapping manner, with a primitive starting to be executed before the one before is finished (Verwey, 1995). Thus, the one-by-one serial execution of each motor primitive does not capture aspects of skilled sequential behaviour.

Instead, it could be that the sequence of primitives (5-4-2-3) become bound together, forming a new motor primitive (5423; **Figure 1.3b**). This could occur through

statistical learning, or binding (Lashley, 1951; Verwey, 1996), whereby individual presses become predictive of upcoming presses over time. In the specific example of a PIN sequence, “5” becomes predictive of “4”, which is in turn predictive of “2”, and that of “3”. Such a mechanism could account for observations that the speed of execution of complex finger tapping sequences increases over time (Abrahamse et al., 2013), as a bound sequence representation would free up the time-consuming process of selection of individual presses. The speed of execution could be even further improved by optimizing the details of the movements specific to the sequence (i.e. depending on the preceding and following elemental movements). This optimization would behaviourally be portrayed as coarticulation, which is commonly observed in complex sequence production (Ben-Shaul et al., 2004). Yet, there are limitations of this account too. Forming a primitive for each sequence would require immense computational capacity to represent all of the movement sequences used in everyday life. Moreover, this deterministic representation of a sequence could render the organism inflexible – for instance upon a perturbation encountered during sequence execution, the system would always have to restart the sequence and would not be able to continue where it left off. Yet, people can adapt their behaviours on-the-go: for example, pianists can improvise after making a mistake without having to restart the piece they are playing. Thus, an extreme version of representing each sequential action as a singular primitive also seems unfeasible. This all goes to show how the execution of motor sequences represents a challenging problem for the motor system. On the one hand, the brain needs to somehow resolve this tension between representing a sequence as a serially ordered concatenation of motor primitives, while on the other hand representing them as a singular continuous action.

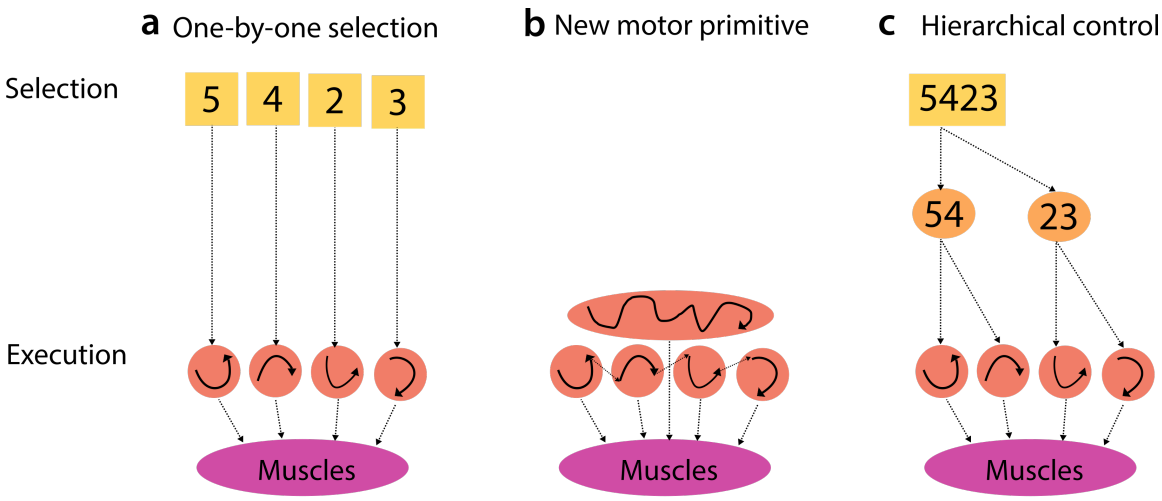

Figure 1.3. Production of a sequence of movements.

a) Sequence production relying on a slow one-by-one selection procedure, where each element is separately selected and executed before moving on to a different element (5-4-2-3). **b)** Representations related to execution of individual elements might bind over time, forming a novel sequence representation, or a new motor primitive. **c)** Alternatively, a complex sequence could be represented at various levels of abstraction (chunks and individual sequences), with the execution level remaining unchanged and evoked for individual elements of the sequence.

1.3.2 Does M1 bind finger movements into a sequence?

Where in the brain are motor sequences represented? In an earlier section of this introduction, I discussed the evidence that the representational structure of M1's activity patterns is shaped according to the usage of fingers in everyday life (Ejaz et al., 2015). This evidence indeed hints that M1's code might be malleable rather than predetermined. Could M1 represent complex movement sequences once these become commonly encountered in everyday life (**Figure 1.3b**)?

Computational work has provided proof-of-principle demonstration that a single neural network, like M1, could in theory learn to independently generate complex sequential patterns (such as writing full words, Laje and Buonomano, 2013). Such a code would allow M1 to autonomously generate complex activity patterns necessary for the production of motor sequences (**Figure 1.3b**). Some indirect experimental evidence for M1's involvement in skilled movement sequences comes from a study, where participants were trained for four weeks to perform a sequence of finger movements. Afterwards they underwent fMRI scanning while performing the trained sequence or a control sequence (Karni et al., 1995). Execution of the trained sequence evoked more expanded activation in M1 compared to the control sequence, which the authors interpreted as indicative of M1 forming a new, more extensive representation dedicated to the trained sequence – i.e. a motor 'engram'. Several other motor learning studies also reported increased M1 activation for trained, compared to control, sequences (Floyer-Lea & Matthews, 2005; Karni et al., 1995, 1998; Lehéricy et al., 2005; Penhune & Doyon, 2002). Despite the tenuous link between change in overall activation and a formation of a bound sequence representation, these studies altogether support the idea that M1 might be involved in the production of skilled sequences of movements.

More recent evidence has, however, cast some doubt on this idea that M1's functional architecture changes with learning. Beukema and colleagues (2019) have tested the specific hypothesis that M1's representation of individual fingers become bound together with motor learning. They trained participants over five weeks on a sequence of finger movements, and afterwards assessed their brain activation during execution of

elemental finger movements using fMRI. The authors reasoned that a newly formed sequence representation should alter representation of elemental movements, i.e. individual fingers. Specifically, fingers that are executed repeatedly in the trained sequence, should show more similar activation patterns after learning. Their findings, however, did not depict any such learning-related change in the similarity of finger-specific activation patterns in M1 (or in any other region). This instead suggests that representation of individual elements for sequence execution does not change with learning. Similarly, another study assessing brain activation during skilled sequence production (Yokoi et al., 2018) reported that M1's activity patterns are better explained as a combination of individual fingers than an integrated sequence representation. This together hints that M1 contains a rather stable organization which is inflexible to learning conditions.

An alternative explanation for these null findings is that the spatial resolution afforded by fMRI is not sufficient to observe learning-related changes in M1. Could it be that new motor primitives for skilled sequences form on a smaller spatial scale, such as at the level of single M1 neurons? This question was posed by Matsuzaka and colleagues (2007) who trained macaques on a sequential reaching task. In this task, animals had to reach to a target presented on the screen, with presentation order being either in a random or a structured sequence. After two years of practice, monkeys learned to perform the task and could anticipate the target order in the structured sequence without relying on the presentation of visual cues. Comparing activity of M1 neurons during the two task modes revealed that over 40% of neurons were differentially active for the trained vs. the random sequence. They interpreted these findings as M1's neurons reflecting sensitivity to the skilled context. The issue, however, is that performance of random sequences was visually guided while trained sequences were executed from memory, introducing a visual confound that could explain the differential responsivity. Moreover, findings from other recent electrophysiological studies suggest that M1 only represents individual elements of a sequence rather than the sequence itself (Russo et al., 2020; Zimnik and Churchland, 2021). In one of these recent studies (Zimnik and Churchland, 2021), the authors compared monkey's activity patterns during skilled two-reach sequences (e.g. reach to target A, then target B) to single reaches (e.g. reach to target A). If the system demonstrates sequence dependency, then the activation state for a given element should differ depending on the

context – i.e., movement towards A should evoke different activity patterns if it is preceded, or followed by movement towards B, compared to when it is executed alone. In contrast, the observed activity prior to the two-reach execution did not differ from those observed for the single reach. This illustrates that even on the level of single neurons M1 might not form a linked sequence representation, or a new motor primitive, but instead reflects the execution-related activity for ongoing elementary movements of a sequence.

1.3.3 Hierarchical control of sequences of finger movements

Instead of forming a new sequence-specific motor primitive in M1, sequential behaviour could be organized hierarchically, with sequence-specific features represented at higher levels of the motor hierarchy. This would still call upon M1's neuronal populations for elementary movement executions. A specific flavour of this idea is a hierarchical organization of motor sequences, where several elementary movements are combined into motor "chunks" (Lashley, 1951; Rosenbaum et al., 1983), which would in turn get bound into still longer "sequence" representations (**Figure 1.3c**). Production of a movement sequence would be achieved by activating the sequence representation, which would in turn evoke the corresponding chunks, and these would trigger generation of the elementary movements.

Evidence for such hierarchical organization of motor sequences comes from behavioural analysis of how individual finger presses are executed in a sequence. Over the course of learning, the inter-press intervals of presses within a sequence become more consistent. The increasingly more consistent gaps in performance between successive elements indicate formation of chunks, with the time needed to execute successive elements across chunk boundaries longer than for elements within a chunk (Popp et al., 2020; Rosenbaum et al., 1983; Sakai et al., 2003). The reason for this difference in execution time is that the time-consuming selection process is needed only at the beginning of each chunk, but not within chunk. One of the advantages of forming a chunk representation is the possibility to generalize it to new settings. For instance, when presenting new sequences to individuals – some which are either completely random and

others which contain a rearranged order of chunks, participants retain the performance advantage for the chunked sequences (Sakai et al., 2003). This indicates that they can make use of the previously learnt chunks to execute new sequences more successfully. Thus, this type of hierarchical representation enables efficient and flexible generalization across context, which is not achievable with a single motor primitive per entire sequence (**Figure 1.3b**).

The level of hierarchy employed for a sequence execution could of course exceed the simple element-chunk-sequence organization and be composed of more levels of abstraction – from single finger movements and their first-level transitions to complexities on the level of a piano concert, or other complex behaviours encountered in everyday lives. While such a hierarchical representation of sequences seems a plausible account to support flexible and efficient sequential behaviour, it is not so clear how such a hierarchical organization maps onto the brain anatomy (Yokoi and Diedrichsen, 2019). Even less is known about how activation of brain regions would change over the course of learning to reflect such hierarchical sequence organization.

1.4 Brain changes during sequence learning

1.4.1 Tracking learning-related changes longitudinally

Most prior studies have examined brain activity after motor training has been completed, commonly by comparing activation elicited for performance of trained sequences to control sequences. This provides a mapping between processes that have emerged throughout learning and the resultant brain activity. However, this offers only a static snapshot of brain function in the skilled state, which belies the plastic and changing nature of the nervous system. As a more direct approach, brain activity can be measured at different timepoints throughout learning. Such longitudinal assessments of brain activity can provide a much richer description of how learning of novel skills is shaped by the nervous system. Besides having richer data, this longitudinal assessment can even lead to qualitatively different

conclusions than relying on a single measurement point. For instance, activation in a given area can undergo non-linear changes throughout learning (Wymbs and Grafton, 2015), where a direct contrast of control vs. skilled sequence might indicate only minimal, or even no change. Longitudinal studies also open the door to address the questions of how the functional organization underlying execution of motor sequences emerges, and changes over a prolonged training period (**Figure 1.3** longitudinally). Does skill learning progress from a hierarchical organization to a more execution-oriented representation? Or do higher-order representations of individual sequences become altered, perhaps strengthened, with learning?

1.4.2 Measuring learning-related changes: activation vs. representation

To inspect brain activation related to learning in humans, several different measurement techniques can be employed. fMRI is a particularly suitable technique to investigate brain localization and mapping due to the high spatial resolution of measurements it affords. In recent years, more studies have moved from conventional imaging field strengths (1.5 / 3 T) to high-field imaging (7 T; or even higher, ultra-high-field, imaging) (De Martino et al., 2018). One of the reasons for this is that higher magnet strength increases the accuracy of the mapping with respect to the site of neuronal activity. This is for two reasons: 1) greater spatial resolution afforded with increasing field strength, and 2) higher specificity to the signal coming from smaller vessels (Ugurbil, 2016; Vaughan et al., 2001). These reasons make BOLD fMRI at high field strengths an appropriate tool for assessing where in the human brain changes occur with learning.

Longitudinal fMRI experiments have attempted to study motor learning by correlating improvements in performance with changes in the overall activity in different brain areas (see Hardwick et al., 2013 for a review). One common observation is that early in learning, the production of motor sequences evokes extended activity in a network of cortical motor, premotor, and association regions. This activity commonly decreases over the course of learning in the majority of cortical regions, while focal activation increases have been observed in M1 (for a review see Dayan and Cohen, 2011), sensorimotor regions

of the cerebellum (Doyon et al., 2002), basal ganglia (Lehéricy et al., 2005) and the spinal cord (Vahdat et al., 2015). This has been interpreted as evidence that well-learnt motor sequences are represented in a more execution-oriented code, or stored in these areas, with a decreasing role of neocortical association areas in the skilled behaviour (**Figure 1.4a**) (Dayan and Cohen, 2011). The fundamental problem with this argument, however, is that decreases in fMRI activation do not necessarily reflect that an area is no longer involved in the task. It could be that the region still performs the same function, but does so more efficiently, which would result in lower fMRI activation (Picard et al., 2013). This also means that greater neuronal recruitment and more efficient coding could cancel each other out, resulting in no net change in activation. Therefore, average changes in BOLD activity with sequence learning make interpretations of change difficult, limiting our understanding of the underlying neuronal changes.

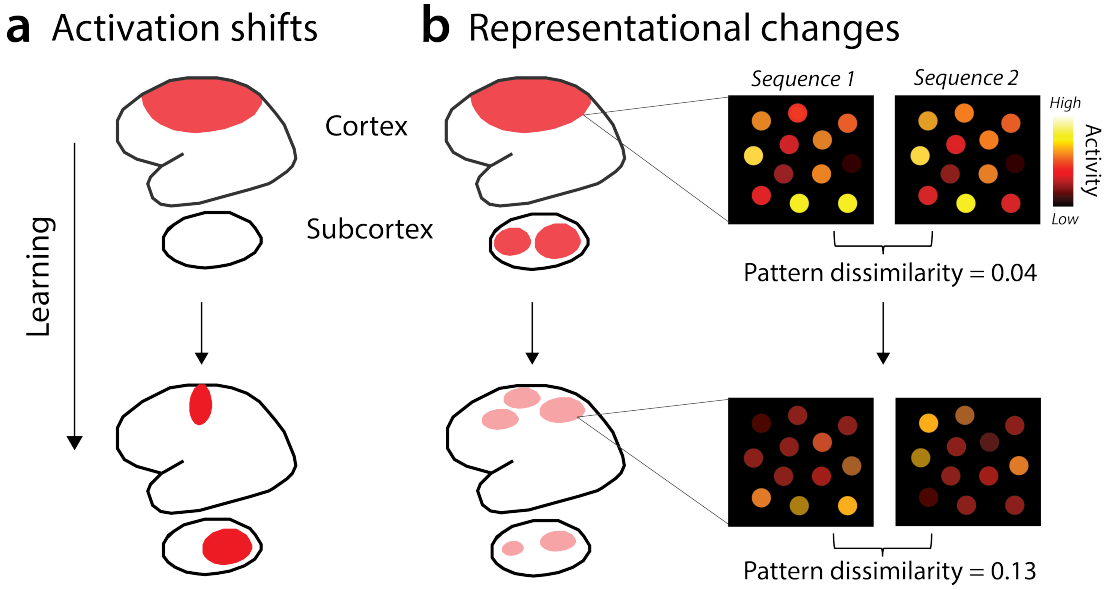

Figure 1.4. Assessing changes in activation vs. representation in motor sequence learning.

a) Many studies propose that motor skills transfer from a widespread recruitment of cortical areas to a more circumscribed locus of more execution-related areas (the primary motor cortex, subcortical structures) with learning. **b)** Changes in representational structure with learning. Neuronal population in a given area might respond very similarly during two finger tapping sequences at the beginning of learning (indicated by similar pattern of activation of activation units and a low pattern dissimilarity). With training, units become less active, but also differentially recruited for each of the two sequences. Thus, early in learning a downstream-connected area would receive identical input for production of either sequence, but later it receives a unique input for each of them, further leading to recruitment of specific motor pools for each action. (Figure adapted from Berlot et al., 2018).

To understand how neuronal activity contributes to motor skill, it is therefore necessary to look at what information neuronal populations encode, moving beyond average activation by using methods which assess the fine-grained activity patterns for different conditions. Multi-voxel pattern analyses (MVPA; Norman et al., 2006) are a family of methods which investigate the relationship between multivariate activity patterns evoked by different conditions (e.g. different movement sequences) instead of just overall average evoked activity. One emerging method for assessing multi-voxel activation patterns is representational similarity analysis (RSA; Kriegeskorte et al., 2008; **Figure 1.4b**), which makes inferences based on the similarity, or dissimilarity, with which voxel patterns represent different conditions, e.g. different motor sequences. It is important to note that while the existence of representation of one or more task-relevant variables is not sufficient evidence for concluding a functional role of the region, it is a necessary condition. Namely, only if the regional pattern of activity represents some important task variables (i.e. with different neuronal state for different versions / times of the task), will the region be able to influence a downstream-connected area in a task-specific fashion, and hence contribute to the improvement of the skill. Application of this representational similarity analysis tool to motor skills comes from a study by Wiestler and Diedrichsen (2013), demonstrating that the activity patterns for trained sequences are more distinguishable than those for untrained sequences across several higher-order cortical regions, but not M1. Yet, this is another example of a cross-sectional study which only assessed one specific timepoint of learning and did not test for how sequence representations become more distinguishable with learning (**Figure 1.4b**).

Besides representational similarity analysis, a different approach to assess regional representation is through repetition suppression (RS) (Grill-Spector et al., 2006; Gross et al., 1967; Henson et al., 2003). This method relies on comparing evoked activation when a given condition is repeated (e.g. A-**A**) to when it is preceded by a different stimulus (e.g. B-**A**). If activation after a repetition is reduced compared to a non-repetition, this is taken as evidence that the region represents different conditions as distinct from one another (i.e. A as distinct from B). Therefore, both representational analysis tools and RS assess multivoxel activity patterns across the different conditions, thereby informing the researcher about whether a region represents individual conditions, such as different motor

sequences. To reveal further what aspects of performed motor sequences contribute to regional representational structure, this can be examined by constructing different representational models, based on the underlying features of experimental conditions (e.g. performed fingers, sequence identity, etc.). The observed multivoxel regional activity patterns can then be compared to these models to see which representational models best account for the observed activity patterns.

Applying such representational tools to longitudinal datasets of motor sequence learning has, with the exception of an RS study (Wymbs and Grafton, 2015), not been done. Yet, to better understand the types of changes that underlie motor sequence learning, it is pivotal to assess how regional representations change with learning. This would allow us to move beyond mapping of observable behavioural improvements onto brain areas with average activation changes and understand better what types of fine-grained activity changes underlie motor sequence learning. There are several specific questions this would allow addressing. Do higher-order regions show reduced representation of sequences as learning progresses, in line with the notion of decreasing role of associative regions? Does sequence representation increase in the motor execution areas? Or could it be that learning strengthens the hierarchical organization of how sequences are represented in the brain?

1.4.3 The learning and performance conundrum

While longitudinal studies present unique opportunities for assessing learning-related changes in the brain, they also come with drawbacks which can seriously complicate the interpretation of findings. The biggest concern in learning studies is attributing whether observed changes in brain activity truly reflect the underlying learning process, or just a difference in performance. For motor learning, one of the most problematic factors is the speed of execution. Speed is often the most pronounced behavioural change with learning, but parametric manipulation of speed, independent of learning, also modulate activation across brain areas (Arbuckle et al., 2019; Ashe and Georgopoulos, 1994; Churchland et al., 2006; Orban et al., 2010). It is virtually impossible to disentangle which changes in brain activation genuinely reflect motor learning from changes that purely reflect a basic motor

implementation of a faster performance. This conundrum of how to study learning while accounting for changing performance has puzzled cognitive neuroscientists attempting to study brain plasticity.

One possible remedy to the performance confound is to constrain behaviour to remain constant across different stages of learning. This can be done by, for instance, pacing the participants at a slower speed in all sessions (Karni et al., 1995; Lehéricy et al., 2005). Yet, blocking the expression of the learnt behaviour in this way might not tap into the brain circuitry that changed during learning. Thus, this control of performance might represent a confound itself. For this reason, some studies examine performance at full speed with the hope that this provides a more direct window into the functional neuroanatomy responsible for the skilled performance (van Mier et al., 2004; Wiestler and Diedrichsen, 2013; Wymbs and Grafton, 2015). Choosing either of these two strategies results in compromises; therefore, if possible, combining both approaches might be most fruitful – i.e. including some scans where performance is controlled and others where participants are allowed to fully express their newly acquired skill. Such a combination allows to address what changes in brain representation are speed- vs. learning-dependent.

1.5 Objectives and overview

The central objective of this thesis is to examine how brain processing changes when learning sequences of finger movements. To that end, this thesis aimed to develop a comprehensive overview of what aspects of finger movements are represented across different brain areas in humans, and how that changes with learning. We employed high-field (7T MRI) functional neuroimaging to assess brain activation in humans at high spatial resolution, allowing for analysis of fine-grained distribution of activation, focussing on the primary sensorimotor and higher-order cortical association regions. In this thesis, I first examine activation of these regions during simple individuated finger movements to investigate the basis of the functional architecture across these regions. I then go on to assess how function of these regions changes during the acquisition of skilled sequential movements. A major theme developed through this series of projects is the distinction

between M1 and higher-order association regions. Even after extensive training, M1 only reflects execution of individual fingers and does not form a sequence representation (**Figure 1.3b**). In contrast, premotor and parietal cortices change substantially during learning, supporting the hierarchical notion of motor sequence learning (**Figure 1.3c**).

Chapter 2 examines the functional architecture underlying individuated finger movements, contrasting contralateral and ipsilateral cortical regions. While finger movements are mostly controlled by the contralateral cortical regions, the role and function of the ipsilateral regions during movements is less clear. Ipsilateral activation is suppressed during movements below resting baseline; however, movements can still be decoded from it – exemplifying a case where overall BOLD and MVPA provide independent insights into its function. We investigated the overall activation and representation of individual fingers in contralateral and ipsilateral regions while participants performed single finger presses or had their fingers passively stimulated. This allowed us to examine to what extent these representations are driven by sensory feedback vs. active movement components, providing some hints into the involvement of the ipsilateral hemisphere during finger movements.

Chapter 3 investigates brain changes accompanying learning of sequential finger movements. While several different neuroimaging correlates of motor learning have been proposed, there is little agreement about what metrics reflect learning, and where in the brain to expect changes during motor sequence learning. In this study, we systematically reinvestigate different proposed correlates of learning by assessing brain activity across four scanning sessions over a five-week training period. We additionally utilize control, untrained, sequences to compare brain activation for trained sequences against. We assess changes in average activation for trained, compared to untrained sequences, as well as how fine-grained sequence-specific representation form during learning. Specifically, the investigation was focussed on learning-related changes in the primary motor cortex (M1), and contrasting those to changes in cortical association regions (premotor and parietal regions). Additionally, this chapter offers an inspection on how the speed of performance affects evoked activation, a common methodological problem in studying learning, by

contrasting two sessions at the end of behavioural training – one in which participants perform at a paced speed compared to another one where they perform at full speed.

Chapter 4 further investigates how learning changes representation across different regions by combining representational similarity analysis with RS. RS is commonly used in cognitive neuroscience as a tool for investigating brain representation, with the rationale that if overall regional activation reduces upon repetition of a stimulus, then that region must be sensitive to differences between presented stimuli. We combined RS with multivariate analyses methods to assess how representations of sequences change with learning, and vary with repetition, across different regions. To understand RS effect in more detail, the activity patterns evoked during performance of motor sequences were decomposed into different representational components (e.g. sequence identity, starting finger, combination of fingers), to assess how the representational structure of a region changes with repetition.

Altogether, the projects of this thesis generated both methodological as well as theoretical advances. Methodologically, I present and assess several techniques that can be applied to investigate plasticity in the human brain. Theoretically, I characterize the roles of primary sensorimotor and higher-order cortical association regions in simple finger movements and examine learning-related changes during acquisition of sequences of finger movements.

1.6 References

Abrahamse, E.L., Ruitenberg, M.F.L., de Kleine, E., Verwey, W.B., 2013. Control of automated behavior: Insights from the discrete sequence production task. Front. Hum. Neurosci. 7, 82.

Alexander, G.E., Delong, M.R., Strick, P.L., 1986. Parallel Organization Of Functionally Segregated Circuits Linking Basal Ganglia And Cortex. Annu. Rev. 9, 357–381.

Andersen, R.A., Buneo, C.A., 2003. Sensorimotor integration in posterior parietal cortex. Adv. Neurol. 93, 159–177.

Arbuckle, S.A., Yokoi, A., Pruszynski, J.A., Diedrichsen, J., 2019. Stability of representational geometry across a wide range of fMRI activity levels. Neuroimage 186, 155–163.

Asanuma, H., Osamu, O., 1962. Effects of transcallosal volleys on pyramidal tract cell activity of cat. J. Neruophysiology 25, 198–208.

Ashe, J., Georgopoulos, A.P., 1994. Movement Parameters and Neural Activity in Motor Cortex and Area 5. Cereb. Cortex 4, 590–600.

Ben-Shaul, Y., Drori, R., Asher, I., Stark, E., Nadasdy, Z., Abeles, M., 2004. Neuronal Activity in Motor Cortical Areas Reflects the Sequential Context of Movement. J. Neurophysiol. 91, 1748–1762.

Berlot, E., Popp, N.J., Diedrichsen, J., 2018. In search of the engram, 2017. Curr. Opin. Behav. Sci. 20, 56–60.

Beukema, P., Diedrichsen, J., Verstynen, T.D., 2019. Binding During Sequence Learning Does Not Alter Cortical Representations of Individual Actions. J. Neurosci. 39, 6968–6977.

Brinkman, J., Kuypers, H.G.J.M., 1973. Cerebral control of contralateral and ipsilateral arm, hand and finger movements in the split-brain rhesus monkey. Brain 96, 653–674.

Churchland, M.M., Santhanam, G., Shenoy, K. V., 2006. Preparatory activity in premotor and motor cortex reflects the speed of the upcoming reach. J. Neurophysiol. 96, 3130–3146.

Cui, H., Andersen, R. a., 2011. Different Representations of Potential and Selected Motor Plans by Distinct Parietal Areas. J. Neurosci. 31, 18130–18136.

Darwin, C., 1871. The descent of man and selection in relation to sex. Murray, London.

Dayan, E., Cohen, L.G., 2011. Neuroplasticity subserving motor skill learning. Neuron 72, 443–454.

De Martino, F., Yacoub, E., Kemper, V., Moerel, M., Uludag, K., De Weerd, P., Ugurbil, K., Goebel, R., Formisano, E., 2018. The impact of ultra-high field MRI on cognitive and computational neuroimaging. Neuroimage 168, 366–382.

Diedrichsen, J., Wiestler, T., Krakauer, J.W., 2013. Two distinct ipsilateral cortical representations for individuated finger movements. Cereb. Cortex 23, 1362–1377.

Donchin, O., Gribova, A., Steinberg, O., Bergman, H., Vaadia, E., 1998. Primary motor cortex is involved in bimanual coordination. Nature 395, 274–278.

Doyon, J., Song, A.W., Karni, A., Lalonde, F., Adams, M.M., Ungerleider, L.G., 2002. Experience-dependent changes in cerebellar contributions to motor sequence learning. Proc. Natl. Acad. Sci. U. S. A. 99, 1017–22.

Ejaz, N., Hamada, M., Diedrichsen, J., 2015. Hand use predicts the structure of representations in sensorimotor cortex. Nat. Neurosci. 18, 1034–1040.

Floyer-Lea, A., Matthews, P.M., 2005. Distinguishable brain activation networks for short- and long-term motor skill learning. J. Neurophysiol. 94, 512–518.

Graybiel, A.M., Grafton, S.T., 2015. The striatum: Where skills and habits meet. Cold Spring Harb. Perspect. Biol. 7, 1–14.

Graziano, M.S.A., Taylor, C.S.R., Moore, T., 2002. Complex Movemnets Evoked by Microstimulation of Precentral Cortex. Neuron 34, 841–851.

Grill-Spector, K., Henson, R., Martin, A., 2006. Repetition and the brain: Neural models of stimulus-specific effects. Trends Cogn. Sci. 10, 14–23.

Gross, C.G., Schiller, P.H., Wells, C., Gerstein, G.L., 1967. Single-unit activity in temporal association cortex of the monkey. J. Neurophysiol. 30, 833–843.

Hardwick, R.M., Rottschy, C., Miall, R.C., Eickhoff, S.B., 2013. A quantitative meta-analysis and review of motor learning in the human brain. Neuroimage 67, 283–297.

Henson, R.N., Ganel, T., Otten, L.J., 2003. Electrophysiological and Haemodynamic Correlates of Face Perception , Recognition and Priming 793–805.

Jin, X., Costa, R.M., 2015. Shaping action sequences in basal ganglia circuits. Curr. Opin. Neurobiol. 33, 188–196.

Karni, A., Meyer, G., Jezzard, P., Adams, M.M., Turner, R., Ungerleider, L.G., 1995. Functional MRI evidence for adult motor cortex plasticity during motor skill learning. Nature 377, 155–8.

Karni, A., Meyer, G., Rey-Hipolito, C., Jezzard, P., Adams, M.M., Turner, R., Ungerleider, L.G., 1998. The acquisition of skilled motor performance: fast and slow experience-driven changes in primary motor cortex. Proc. Natl. Acad. Sci. U. S. A. 95, 861–8.

Kriegeskorte, N., Mur, M., Bandettini, P., 2008. Representational similarity analysis – connecting the branches of systems neuroscience. Front. Syst. Neurosci. 2, 4.

Laje, R., Buonomano, D. V., 2013. Robust timing and motor patterns by taming chaos in recurrent neural networks. Nat. Neurosci. 16, 925–933.

Lashley, K.S., 1951. The Problem of Serial Order in Behavior. Oxford, United Kingdom: Bobbs-Merrill.

Lawrence, D.G., Kuypers, H.G.J.M., 1968. The Functional Organization Of The Motor System In The Monkey. Brain 91, 1–14.

Lehéricy, S., Benali, H., Van de Moortele, P.-F., Pélégrini-Issac, M., Waechter, T., Ugurbil, K., Doyon, J., 2005. Distinct basal ganglia territories are engaged in early and advanced motor sequence learning. Proc. Natl. Acad. Sci. U. S. A. 102, 12566–12571.

Matsuzaka, Y., Picard, N., Strick, P.L., 2007. Skill representation in the primary motor cortex after long-term practice. J. Neurophysiol. 97, 1819–1832.

McGinn, C., 2015. Prehension: The Hand and the Emergence of Humanity. The MIT Press.

Middleton, F. A., Strick, P.L., 2000. Basal ganglia and cerebellar loops. Brain Res. Rev. 31, 236–250.

Miller, E.K., 2000. The prefontral cortex and cognitive control. Nat. Rev. Neurosci. 1, 59–65.

Milner, A.D., Goodale, M.A., 2008. Two visual systems re-viewed. Neuropsychologia 46, 774–785.

Munte, T.F., Altenmüller, E., Jancke, L., 2002. The musician's brain as a model of neuroplasticity. Nat. Rev. 3, 3–8.

Murase, N., Duque, J., Mazzocchio, R., Cohen, L.G., 2004. Influence of interhemispheric interactions on motor function in chronic stroke. Ann. Neurol. 55, 400–409.

Nachev, P., Kennard, C., Husain, M., 2008. Functional role of the supplementary and pre-supplementary motor areas. Nat. Rev. Neurosci. 9, 856–869.

Norman, K.A., Polyn, S.M., Detre, G.J., Haxby, J. V., 2006. Beyond mind-reading: multi-voxel pattern analysis of fMRI data. Trends Cogn. Sci. 10, 424–430.

Ogawa, S., Lee, T.M., Kay, A.R., Tank, D.W., 1990. Brain magnetic resonance imaging with contrast dependent on blood oxygenation. Proc. Natl. Acad. Sci. U. S. A. 87, 9868–9872.

Orban, P., Peigneux, P., Lungu, O., Albouy, G., Breton, E., Laberenne, F., Benali, H., Maquet, P., Doyon, J., 2010. The multifaceted nature of the relationship between performance and brain activity in motor sequence learning. Neuroimage 49, 694–702.

Penfield, W., Jasper, H., 1954. Epilepsy and the functional anatomy of the human brain - Western University. Oxford, England: Little, Brown & Co.

Penhune, V.B., Doyon, J., 2002. Dynamic cortical and subcortical networks in learning and delayed recall of timed motor sequences. J. Neurosci. 22, 1397–406.

Picard, N., Matsuzaka, Y., Strick, P.L., 2013. Extended practice of a motor skill is associated with reduced metabolic activity in M1. Nat. Neurosci. 16, 1340–7.

Popp, N.J., Yokoi, A., Gribble, P.L., Diedrichsen, J., 2020. The effect of instruction on motor skill learning. J. Neurophysiol. 124, 1449–1457.

Rathelot, J.A., Strick, P.L., 2009. Subdivisions of primary motor cortex based on cortico-motoneuronal cells. Proc. Natl. Acad. Sci. U. S. A. 106, 918–923.

Rosenbaum, D.A., Kenny, S.B., Derr, M.A., Laboratories, B., Hill, M., 1983. Hierarchical Control of Rapid Movement Sequences. J. Exp. Psychol. Hum. Percept. Perform. 9, 86–102.

Russo, A.A., Khajeh, R., Bittner, S.R., Perkins, S.M., Cunningham, J.P., Abbott, L.F., Churchland, M.M., 2020. Neural Trajectories in the Supplementary Motor Area and Motor Cortex Exhibit Distinct Geometries, Compatible with Different Classes of Computation. Neuron 107, 745–758.e6.

Sakai, K., Kitagushi, K., Hikosaka, O., 2003. Chunking during human visuomotor sequence learning. Exp. Brain Res. 152, 229–242.

Schieber, M.H., Hibbard, L.S., 1993. How somatotopic is the motor cortex hand area? Science 261, 489–492.

Schultz, W., 2004. Neural coding of basic reward terms of animal learning theory, game theory, microeconomics and behavioural ecology. Curr. Opin. Neurobiol. 14, 139-147.

Scott, S.H., Cluff, T., Lowrey, C.R., Takei, T., 2015. Feedback control during voluntary motor actions. Curr. Opin. Neurobiol. 33, 85–94.

Scott, S.H., Sergio, L.E., Kalaska, J.F., 1997. Reaching Movements With Similar Hand Paths but Different Arm Orientations. II. Activity of Individual Cells in Dorsal Premotor Cortex and Parietal Area 5. J. Neurophysiol. 78, 2413–2426.

Shima, K., Isoda, M., Mushiake, H., Tanji, J., 2007. Categorization of behavioural sequences in the prefrontal cortex. Nature 445, 315–318.

Swinnen, S.P., Wenderoth, N., 2004. Two hands, one brain: Cognitive neuroscience of bimanual skill. Trends Cogn. Sci. 8, 18–25.

Tanji, J., Hoshi, E., 2001. Behavioral planning in the prefrontal cortex. Curr. Opin. Neurobiol. 11, 164–170.

Tower, S.S., 1940. Pyramidal Lesion In The Monkey. Brain 63, 36–90.

Ugurbil, K., 2016. What is feasible with imaging human brain function and connectivity using functional magnetic resonance imaging. Philos. Trans. R. Soc. B Biol. Sci. 371, 20150361.

Vahdat, S., Lungu, O., Cohen-Adad, J., Marchand-Pauvert, V., Benali, H., Doyon, J., 2015. Simultaneous Brain-Cervical Cord fMRI Reveals Intrinsic Spinal Cord Plasticity during Motor Sequence Learning. PLoS Biol. 13, e1002186.

van Mier, H.I., Perlmutter, J.S., Petersen, S.E., 2004. Functional changes in brain activity during acquisition and practice of movement sequences. Motor Control 8, 500–520.

Vaughan, J.T., Garwood, M., Collins, C.M., Liu, W., DelaBarre, L., Adriany, G., Andersen, P., Merkle, H., Goebel, R., Smith, M.B., Ugurbil, K., 2001. 7T vs. 4T: RF power, homogeneity, and signal-to-noise comparison in head images. Magn. Reson. Med. 46, 24–30.

Verwey, W.B., 1995. A forthcoming key press can be selected while earlier ones are executed. J. Mot. Behav. 27, 275–284.

Verwey, W.B., 1996. Buffer Loading and Chunking in Sequential Keypressing. J. Exp. Psychol. Hum. Percept. Perform. 22, 544–562.

Ward, N.S., Cohen, L.G., 2004. Mechanisms underlying recovery of motor function after stroke. Arch. Neurol. 51, 1844–1848.

Wiestler, T., Diedrichsen, J., 2013. Skill learning strengthens cortical representations of motor sequences. Elife 2, e00801.

Wiestler, T., McGonigle, D.J., Diedrichsen, J., 2011. Integration of sensory and motor representations of single fingers in the human cerebellum. J. Neurophysiol. 105, 3042–3053.

Wolpert, D.M., Miall, R.C., Kawato, M., 1998. Internal models in the cerebellum. Trends Cogn. Sci.

Wymbs, N.F., Grafton, S.T., 2015. The human motor system supports sequence-specific representations over multiple training-dependent timescales. Cereb. Cortex 25, 4213–4225.

Xu, J., Branscheidt, M., Schambra, H., Steiner, L., Widmer, M., Diedrichsen, J., Goldsmith, J., Lindquist, M., Kitago, T., Luft, A.R., Krakauer, J.W., Celnik, P.A., Group, S., 2019. Rethinking Interhemispheric Imbalance as a Target for Stroke Neurorehabilitation. Ann. Neurol. 85, 502–513.

Yokoi, A., Arbuckle, S.A., Diedrichsen, J., 2018. The role of human primary motor cortex in the production of skilled finger sequences. J. Neurosci. 38, 1430–1442.

Yokoi, A., Diedrichsen, J., 2019. Neural Organization of Hierarchical Motor Sequence Representations in the Human Neocortex. Neuron 103, 1178–1190.e7.

Zimnik, Andrew J., Churchland, M.M., 2021. Independent generation of sequence elements by motor cortex. Nat. Neurosci. 24, 412–424.

CHAPTER 2

2 Ipsilateral finger representations in the sensorimotor cortex are driven by active movement processes, not passive sensory input

2.1 Introduction

The primate hand is controlled mainly by descending projections from the motor areas in the contralateral cerebral hemisphere (Brinkman and Kuypers, 1973). While the hand also receives input from ipsilateral motor regions through uncrossed corticospinal projections, these projections lack the capacity to produce overt movement (Soteropoulos et al., 2011). If, and to what degree, the ipsilateral hemisphere directly or indirectly contributes to hand movements is currently debated (Chen et al., 1997; Verstynen et al., 2005). It is clear, however, that neural activity in ipsilateral motor regions is modulated during hand movements. Overall, there is a global suppression of activity as evidenced by a reduction in BOLD (blood-oxygen-level-dependent) signal measured using functional magnetic resonance imaging (fMRI) (Cramer et al., 2011; Verstynen et al., 2005). Below this suppressive effect, there are clear task-specific changes. For example, one can decode the identity of the moved effector (e.g. finger) from ipsilateral activity alone (electrocorticography: Scherer et al., 2009; Fujiwara et al., 2017; fMRI: Diedrichsen et al., 2013). These ipsilateral activity patterns appear to be weaker, but otherwise identical versions of the pattern elicited by movement of the mirror-symmetric finger in the opposing hand (Diedrichsen et al., 2013; Diedrichsen, Yokoi, & Arbuckle, 2017). Altogether, these studies show that the ipsilateral hemisphere *represents* aspects of finger movements. The origin and functional relevance of these representations, however, remain unclear.

One puzzle regarding the function of these ipsilateral representations is whether they reflect processes involved in active motor planning and execution, or whether they are a consequence of re-afferent sensory input. In the contralateral hemisphere, passive

somatosensory stimulation of individual fingers has been shown to evoke activity patterns that are very similar to those associated with active finger movements (Wiestler et al., 2011). This is even the case on the single-finger level; cortical patches that are especially activated by movement of the index finger are also activated by index finger stimulation. The tight match between tuning for active and passive conditions is unsurprising given the importance of accurate sensory information for fine movement control (Augurelle et al., 2003; Pruszynski et al., 2016), and is consistent with the characterisation of primary motor cortex as a *feedback* controller (Scott, 2004).

Here we ask whether ipsilateral sensorimotor cortex plays a role in the fine feedback control of finger movements. If so, we should see that ipsilateral representations can also be activated by passive sensory stimulation. Indeed, we would expect that passive finger stimulation recruits ipsilateral finger-specific circuits to approximately the same degree as active finger presses, as they do in the contralateral sensorimotor cortex. Alternatively, if the ipsilateral hemisphere is primarily recruited during movement planning, we would predict that ipsilateral representations are more pronounced during active presses, and either weaker or absent during passive finger stimulation.

To test between these two possibilities, we used high-field fMRI (7T) to measure ipsilateral activity patterns during active single finger presses and passive finger stimulation. We contrasted the overall activity during active and passive conditions in both the contralateral and ipsilateral hemisphere. Using multivariate pattern analysis, we also analyzed how strongly different conditions activated finger-specific circuits, i.e. the degree to which finger information is represented in these areas (Diedrichsen & Kriegeskorte, 2017). This analysis allowed us to determine the extent to which representations in the contralateral and ipsilateral motor areas are driven by sensory input alone (passive condition), or by a combination of sensory input and active planning and execution processes (active condition). We further examined these representations using a fine-grained analysis across the subfields of the sensorimotor cortices.

Overall, we found that active and passive conditions recruited contralateral and ipsilateral sensorimotor areas differently. While contralateral finger representations were

equally strong for active and passive conditions, the corresponding ipsilateral finger representations around the central sulcus were stronger for the active than passive condition. Our results demonstrate that motor areas in ipsilateral and contralateral hemispheres are differentially recruited during active and passive finger presses. This differential recruitment of contralateral and ipsilateral motor areas points to a difference in neurophysiological origin of movement representation.

2.2 Methods

2.2.1 Participants

Seven volunteers participated in the experiment. The average age was 26.1 years (SD = 2.5 years), and the sample included four women and three men. All participants were right-handed. The experimental procedures were approved by the Ethics Committee of University College London and Oxford University.

2.2.2 Apparatus

Participants placed their two hands on an MRI-compatible keyboard (**Figure 2.1a**), which was positioned on their lap, secured with a foam pillow. The keyboard had 10 elongated keys, with a groove for each fingertip. Force applied during finger press execution was measured with force transducers mounted underneath each key. The keys were non-movable and therefore finger presses were not associated with overt movements. Nonetheless, these isometric presses still involved voluntary activation of muscles, as well as sensory feedback from the pressure on the fingertip. To generate a sensory stimulation protocol that was matched as closely as possible to the sensory input during active finger presses, we applied isometric force presses through pneumatic pistons embedded in each key of the keyboard. Upward movement of the finger was prevented by a stiff foam pad which held the fingers securely in place (**Figure 2.1b**). The force to the fingertip in the

passive condition was closely matched to that in the active condition by generating force pulses at the same inter-press interval and with the same average peak force as those produced during the active condition. The mean peak force was 4.3 N in the active and 4.5 N in the passive condition. Therefore, the two conditions differed mainly in terms of the motor command (i.e. the efference), and were matched as closely as possible in terms of sensory afference. It is of course never possible to exactly match sensory feedback across active and passive conditions, as the efferent outflow itself will alter the incoming sensory information (Blakemore et al., 1999). Therefore, our conclusions on the source of representation did not rely on a direct comparison of passive and active conditions in a single region, but rather on a difference in their relative weighting across the two hemispheres (i.e. passive vs. active responses in contra- vs. ipsilateral sensorimotor regions).

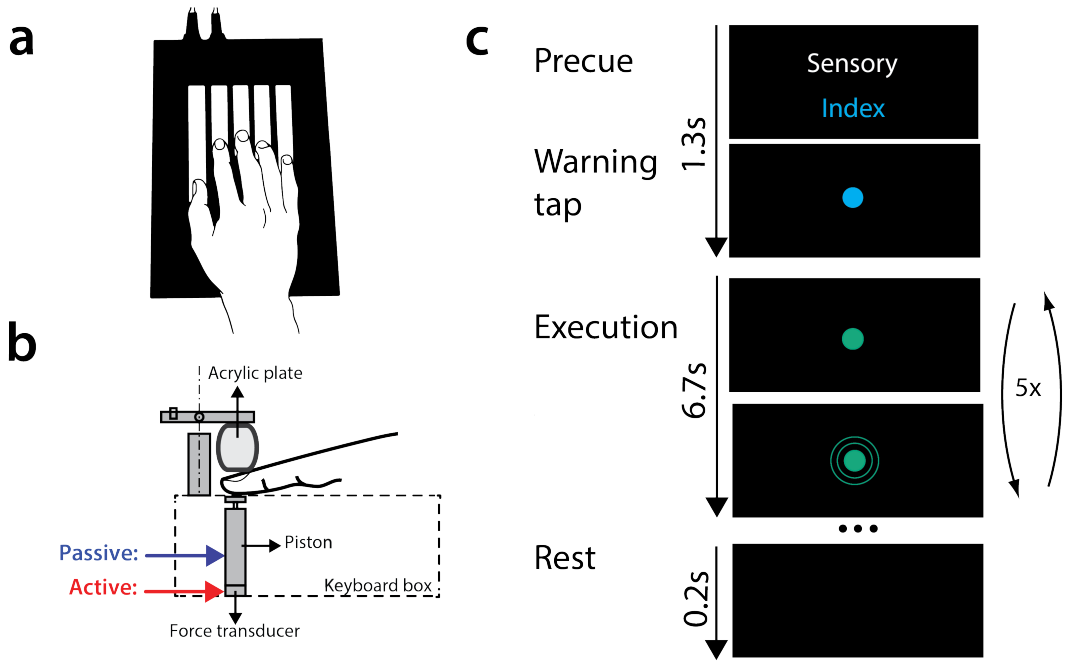

Figure 2.1. Apparatus and experimental design.

a) Keyboard used in the task – the left hand was positioned on a mirror-symmetric keyboard. **b)** An adjustable foam pillow was sitting on the top of each finger, preventing any overt finger motion. In the active condition, participants pressed one of the keys and the force applied was recorded through the force transducer. In the passive condition, the force was applied to the finger using a pneumatic piston. **c)** Each trial started with a cue denoting which condition and finger are implicated in the trial. This was followed by a warning press to the finger, after which each participant either received five finger presses (in the passive condition), or pressed the key five times (active condition). Each trial lasted for a total of 8.2 seconds. Both active and passive conditions involved only the right hand.

2.2.3 Experimental design

We employed a slow event-related design, randomly intermixing active and passive conditions in each imaging run. Every trial lasted for 8.2 seconds, during which participants either performed five isometric presses with one of the fingers (active condition) or had a finger stimulated five times (passive condition). Both conditions involved only the right hand. Each trial was divided into the instruction phase (1.3 s) and the execution phase (6.7 s). First, the instructional cue was presented on the screen, specifying which finger is to be pressed or stimulated (e.g. Sensory / Index, **Figure 2.1c**). Next, the fixation circle appeared in blue and a warning press was applied to the finger which was to be pressed or stimulated. Afterwards, the central circle turned green which was a 'go' cue for participants to perform the five presses in the active condition, or to have force applied to their finger five times. For every press with the correct finger, the central fixation circle expanded with green circles, whereas in the rare case of an incorrect press, the surrounding circles turned red. To control for visual feedback and predictability of presses, the visual display in the passive condition was the same as in the active condition. Each run contained three repetitions of each of ten conditions (five fingers in passive / active tasks), and there were seven or eight imaging runs per participant. Thus, the number of repetitions was equal across all conditions for each participant. Five rest phases of 13 to 16 seconds each were randomly interspersed in each imaging run to obtain a reliable estimate of baseline activation. We ensured that our participants performed the task nearly perfectly. Three out of seven participants never pressed the key with an incorrect finger throughout the entire session, and the mean error rate across all participants was 1.3% of trials. Even in these cases, typically only one of the five presses performed in the trial was incorrect. Because of near-perfect performance and for consistency across participants, we have included all the trials in the analysis.

2.2.4 Image acquisition

Data was acquired on a 7-T Siemens Magnetom scanner with a 32-channel head coil. An anatomical T1-weighted scan was acquired using a magnetization-prepared rapid gradient

echo sequence (MPRAGE) with voxel size of 0.7 mm isotropic (field of view = 224x224x180 mm). Functional data was acquired in 7-8 runs (depending on the participant), using a 2D echo-planar imaging sequence (GRAPPA 2, repetition time [TR] = 3.0 s, echo time [TE] = 25 ms). We acquired 47 slices with isotropic voxel size of 1.4 mm.

2.2.5 First-level analysis

Functional data were analyzed using SPM12 and custom-written code in MATLAB (The MathWorks). Differences in acquisition timing of slices were corrected for by aligning all slices to the middle slice of each volume. Functional images were corrected for geometric distortions using field map data (Hutton et al., 2002), and aligned to the first image of the first run, resulting in correction for head movements during the scan (three translations: x, y, z directions and three rotations: pitch, roll, and yaw). Finally, the data were co-registered to the anatomical scan. No smoothing or normalisation to an atlas template was performed at this stage.

Preprocessed data were analyzed using a general linear model. Since participants performed the active finger tapping task almost perfectly (average error rate=1.3±1.7% of trials), we included all of the trials in the analysis. For each trial type, we defined one regressor per imaging run, resulting in 10 regressors per run (five fingers for each condition: passive / active). The regressor was a boxcar function which started with the beginning of the trial and lasted for the trial duration. This function was convolved with a hemodynamic response function, with a time-to-peak of 4.5 s, manually adjusted to best fit the average timeseries. The analysis resulted in one activation estimate (beta image) for each of the 10 conditions per run. We calculated average percent signal change for the passive and active conditions (averaged across all fingers) as the mean evoked response relative to the baseline in each run, averaged across runs.

2.2.6 Surface-based analysis and searchlight approach

To carefully characterize activation patterns across different cortical areas, we obtained a reconstruction of individual subjects' cortical surfaces using Freesurfer (Dale et al., 1999). All individual surfaces were aligned to the symmetrized atlas template of Freesurfer (using xhemireg, Fischl et al., 1999) via spherical registration.

To detect finger-specific representations for the active and passive conditions across the cortex (see section 2.2.8 Multivariate analysis), we used a surface-based searchlight approach (Oosterhof et al., 2011). For each surface node, we selected a surrounding circular region of 120 voxels (i.e. in 3D volume), which on average resulted in a searchlight radius of 6.5 mm. To avoid contamination of signals across the central sulcus, we excluded all voxels that contained gray matter from the other side. We extracted the activation estimates (betas) of selected voxels from the first-level analysis and then computed the dissimilarity between activity patters for the passive and active finger pairs (see section 2.2.8 Multivariate analysis). The resulting distance was assigned to the center of the searchlight sphere. By moving the searchlight across the cortical surface, we obtained a map of distances for active and passive condition patterns, representing how well each patch of cortex represented individual finger active and passive conditions.

2.2.7 Regions of interest (ROI) and cross-section

To compare finger representations across different subfields of the sensorimotor cortex, we defined seven regions of interest (ROIs). The ROIs were defined using Brodmann maps derived from post-mortem histology, aligned to the cortical surface atlas (Fischl et al., 2008). Each cortical node was assigned to the region that had (across analyzed brains) the highest probability. Primary motor cortex (M1), or Brodmann area 4, was split into anterior (BA4a) and posterior (BA4p) components. ROIs for primary somatosensory cortex (S1) were Brodmann areas 3a, 3b, 1, and 2. Additionally, the premotor cortex was defined as the lateral aspect of Brodmann area 6 (BA6). To exclude mouth and leg representations in all these areas, we included only cortical nodes within 2.5 cm above and below the hand knob, the point of greatest curvature in the central sulcus (Yousry et al., 1997).

We performed the analysis on percent signal change and distance estimates (see section 2.2.8 Multivariate analysis) for cortical surface patches in a cross-section across the surface sheet, running from the rostral end of BA6 to the posterior end of BA2. For the pattern component modelling analysis (described in section 2.2.9 Pattern component analysis), we used all voxels within each ROI, and further joined BA4a and BA4p into BA4, and BA3a and BA3b into BA3.

2.2.8 Multivariate analysis

The overall activation across fingers does not provide insight into finger-specific processes (i.e. finger representations; Diedrichsen et al., 2013). While finger representations can be visualized in terms of their rough somatotopic arrangement on the cortical surface (Indovina and Sanes, 2001; Wiestler et al., 2011), a fuller description can be obtained by taking into account the entire fine-grained activity pattern for each finger (Ejaz et al., 2015). We therefore calculated distances between activation patterns for different fingers, separately for each subject. We first standardized the beta-image for each voxel by dividing it by the standard deviation of its residual, as obtained from the first-level GLM. Such univariate prewhitening has been shown to increase the reliability of distance estimates as compared to non-standardized images (Walther et al., 2016). For active and passive conditions separately, we then calculated the crossvalidated squared Mahalanobis distance (crossnobis estimator, Nili et al., 2014; Walther et al., 2016; Diedrichsen and Kriegeskorte, 2017) between each finger pair. Because the expected value of this estimator is zero if the two conditions only differ by measurement noise, the crossnobis estimate can be used to test whether an area "*represents*" a certain parameter by testing it against zero (Diedrichsen, Provost, & Zareamoghaddam, 2016).

2.2.9 Pattern component analysis

To quantify the correspondence between active and passive activity patterns, we used pattern component modelling (PCM; Diedrichsen et al., 2017). A naïve way to assess the

correlation would be to simply correlate corresponding finger patterns, after subtracting the mean pattern, for the passive and active condition. However, the raw correlations severely underestimate the true correlation between patterns as the correlations are lowered by measurement noise. Even cross-validated correlations are severely biased (see example 2, Diedrichsen et al., 2017). Instead, we can use PCM to test between different models on the strength of the correlation between the finger-specific patterns in the active and passive condition: a *'null' model* where active and passive conditions are unrelated, a *'flexible correlation' model* where the two conditions share some correlation, and a *'perfect correlation' model* in which the passive finger-specific patterns are simply scaled version of the active patterns. We compared these models by calculating for each subject the log-Bayes factor of the flexible and perfect model against the null model. Subsequent group inferences were performed using parametric statistics (t-test) on the individual log-Bayes factors.

2.2.10 Statistical analysis

To statistically assess how activity or distances differ between conditions in either hemisphere, we performed a condition x ROI ANOVA, followed by post-hoc t-tests on distance estimates of passive and active conditions in each region individually. To directly contrast the distance estimates of the two conditions across the two hemispheres, we conducted a hemisphere x condition ANOVA. We further quantified the spatial distribution of distances across regions of the two hemispheres using a hemisphere x ROI ANOVA on estimates of distances in the active condition. To statistically assess the correspondence between active and passive patterns, we contrasted the obtained correlation estimates against 0 using one-sample t-tests, and conducted a model type x ROI ANOVA on log-Bayes factors of the flexible and perfect correlation models. Our ANOVAs were followed by post-hoc t-tests, using Bonferroni correction for multiple comparisons for adjusting the significance value. Given the small sample size (N=7), we replicated each test using non-parametric statistics (rank-sum test, not reported here), which yielded qualitatively similar results. All of the plots presenting results are group averages per condition (N=7) – the cross-sectional plots in **Figure 2.2** and **Figure 2.3** for each surface node, the matrices in

Figure 2.4 are a group average across seven subjects, and **Figure 2.5** for each of the dots in the barplot (so 7 values per ROI).

2.3 Results

2.3.1 Contralateral finger representations are equally strong in active and passive conditions

Before looking at the contribution of sensory and motor processes to the ipsilateral representations, we carefully quantified the passive and active finger representations in the contralateral hemisphere. As a first proxy for contralateral recruitment during the two conditions, we investigated the overall BOLD activation across sensorimotor regions. The sensory input was similar in both tasks, but the active condition additionally required planning and initiation of the press. These additional motor demands were predicted to evoke higher levels of activation in the active compared to the passive task. Figure **2.2a** shows the percent signal change on the flattened contralateral cortical surface related to the active (red) and passive condition (blue). Both conditions evoke activity in highly overlapping cortical patches (purple). For statistical evaluation, we used a series of anatomically defined ROIs, running from premotor cortex (BA6) posterior into BA2 (separated by dashed white lines), and tested the evoked activity of each region against zero with a one-sample t-test. Significance at $p<0.001$ was reached in all subfields for both passive and active conditions (blue and red bars in **Figure 2.2b**). To examine differences between active and passive conditions, we performed a condition x ROI ANOVA. Both the main effects of condition and ROI were significant (condition: $F_{(1,6)}=23.791$, $p=0.0028$, ROI: $F_{(1,6)}=4.833$, $p=9.0e^{-4}$), as was the interaction between them ($F_{(1,6)}=8.19$, $p=1.3e^{-5}$). Post-hoc t-tests comparing activation during passive and active conditions within each ROI revealed that the active condition elicited higher activation than the passive condition in every region (Bonferroni-corrected significance level: $p=0.0071$ – black stars in **Figure 2.2b**).

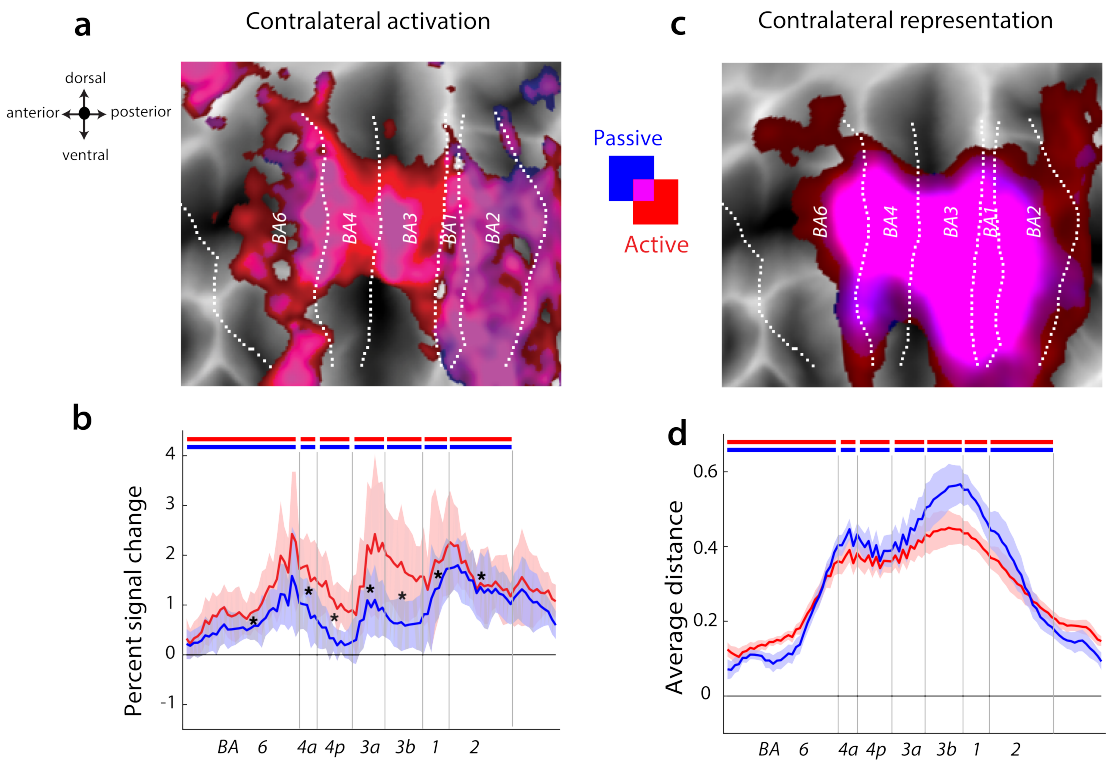

Figure 2.2. Average contralateral evoked activation and distances between finger patterns during active and passive tasks across subfields of sensorimotor cortex.

a) Evoked activity for the active (red) and passive (blue) conditions on the flattened contralateral cortical surface. The two conditions activated similar cortical areas, with the overlap indicated by purple areas. Regions of interest (ROIs) were defined based on the probabilistic cyto-architectonic atlas (Fischl et al., 2008), with each node assigned the area of the highest probability. Borders between regions are indicated with white dotted lines. **b)** Percent signal change for active and passive tasks was sampled in a cross-section from anterior (BA6) to posterior (BA2), along a rectangular strip with a width of 26 mm. Horizontal red and blue bars indicate significant activation during the active and passive task, respectively. Significant differences between the activation for active and passive tasks are indicated by black stars (p<0.0071 – Bonferroni correction). **c)** Average distance between finger patterns for the active (red) and passive (blue) tasks on the flattened contralateral cortical surface. The two conditions evoked similar distances, which is indicated by the purple overlap. **d)** Distances in the contralateral hemisphere were significantly higher than zero for both tasks, as indicated by the red and blue bars. There was no difference in distances between the two conditions in any ROI. Shaded areas in **b** and **d** reflect the standard error of the group mean.

Next, we evaluated how strong representations for different fingers were in each of these ROIs, independent of the overall activity. It is possible to observe large activation without any representation of individual fingers (implying the activation is induced by processes not specifically related to finger control), or to observe lower activation with very clear finger representation. For a region to perform a specific function, a clear representation is more important than high activation (Diedrichsen & Kriegeskorte, 2017). We evaluated the strength of representation using the cross-validated squared Mahalanobis distance estimate (crossnobis, Diedrichsen et al., 2016) between activity patterns of individual fingers, separately for active presses and passive finger stimulation. As expected, we found strong finger representations for both passive and active conditions (**Figure 2.2c**), confirmed by a t-test on distance estimates of each condition across all cortical sensorimotor regions combined (passive: $t_{(6)}$=13.82, p=8.93e^{-6}, active: $t_{(6)}$=9.76, p=6.65e^{-5}). Distances were particularly large in the depths of the central sulcus, peaking in area 3b, and decreased anteriorly in premotor area (BA6) and posteriorly in BA2 (**Figure 2.2d**). We quantified this observation statistically by performing a condition x ROI ANOVA on the distance estimates. The main effect of condition was not significant ($F_{(1,6)}$=3.183, p=0.125), but both the main effect ROI and the interaction between the ROI and condition were (ROI: $F_{(1,6)}$=37.288, p=5.1e^{-14}, interaction: $F_{(6,36)}$=12.183, p=1.9e^{-7}). Post-hoc t-tests on the effect of condition within each region revealed a trend for larger distances in the passive compared to active condition in BA3b and BA1, but this difference did not reach significance after Bonferroni correction.

In summary, we found that both active and passive conditions activated the finger-specific representations to the same extent in contralateral M1 and S1. In contrast, the average overall activity was significantly higher in the active condition. This means that the additional neuronal processes in the active condition were not finger specific, but instead increased activity in a general fashion for all fingers.

2.3.2 Ipsilateral finger representations are stronger in active than passive condition

Having quantified the amount of passive and active digit representations in the contralateral hemisphere, we next turned to the ipsilateral hemisphere. We again first quantified the overall percent signal change of elicited activity. Consistent with previous research (Diedrichsen et al., 2013; Verstynen et al., 2005) we found significant BOLD modulation across ipsilateral ROIs during the active condition, as confirmed by a one-way ANOVA with the main effect of region ($F_{(6,36)}$=16.26, p=5.9e^{-9}). Activation in the depth of the sulcus was suppressed below resting baseline (**Figure 2.3b**, grey background), and this suppressive effect was significant in areas 4p and 3a (BA4p: $t_{(6)}$=-4.89, p=0.0027; BA3a: $t_{(6)}$=-4.28, p=0.005). Only premotor (BA6) and parietal areas (BA2) exhibited significant increases in BOLD signal (BA6: $t_{(6)}$=6.57, p=5.94e^{-4}; BA2: $t_{(6)}$=4.51, p=0.004).

To quantify the activation and deactivation profiles across both active and passive conditions, we used a condition x ROI ANOVA. The main effect of condition was not significant ($F_{(1,6)}$=0.095, p=0.769), but there was a significant main effect of ROI ($F_{(1,6)}$=19.55, p=5.4e^{-10}), and a significant interaction between the two factors ($F_{(6,36)}$=8.13, p=1.4e^{-5}). Post-hoc t-tests demonstrated that this interaction was driven by higher activity in the premotor cortex during the active condition ($t_{(6)}$=4.23, p=0.006), which is in line with its bilateral involvement during action preparation (Cisek et al., 2003). Other areas showed no significant difference in activity between the two conditions. Thus, regions located in the depth of the central sulcus in the ipsilateral hemisphere were significantly suppressed during both passive and active conditions.

We have previously found that despite the suppression of BOLD activity, the ipsilateral hemisphere contains information about individual finger movements (Diedrichsen et al., 2013). Here we asked whether the ipsilateral hemisphere represents individual fingers only during active movement, or also during passive finger stimulation. We first examined individual finger representations during the active condition. The average distance among active finger presses was higher than zero in every region (all $t_{(6)}$>2.721, p<0.034; **Figure 2.3d**), replicating our prior results (Diedrichsen et al., 2013). Next we tested whether the ipsilateral hemisphere represents individual fingers in the

passive condition to the same extent as during active movement (similar to the contralateral hemisphere). The main effect of condition on the distance estimates was significant ($F_{(1,6)}$=24.36, p=0.0026), and post-hoc t-tests revealed that the average distance was lower in the passive than in the active task in the depth of the sulcus (black stars in **Figure 2.3d**). Subfields 4p, 3a, and 3b which all showed significant distances during active finger presses, did not show finger representation for passive finger stimulation, as confirmed by one-sample t-tests against 0 (no blue bars in **Figure 2.3d**). These findings suggest that ipsilateral representations in these areas are driven by processes involved in the active generation of movement, but not by the sensory input arising from passive stimulation.

Last, we quantified whether the relative amount of finger representation across the passive and active tasks differs across the two hemispheres. This test is critical to determine whether the source of contralateral and ipsilateral finger information is identical or different. A hemisphere x condition ANOVA combined across all regions revealed a clear interaction effect ($F_{(1,6)}$=64.481, p=2.0e^{-4}), demonstrating that the relative magnitude of finger-specific representation during the active and passive conditions differs significantly across the two hemispheres. This can also be observed in the representational dissimilarity matrices (**Figure 2.4**), that show the distances between digits during active and passive conditions for the contra- and ipsilateral M1. While the contralateral sensorimotor circuit represents individual finger presses and stimulation to the same extent (or, if anything, more for the passive condition), finger representation on the ipsilateral side was stronger during the active condition. This demonstrates that the contribution of sensory information to the neural activation patterns is much smaller in the ipsilateral as compared to the contralateral sensorimotor areas.

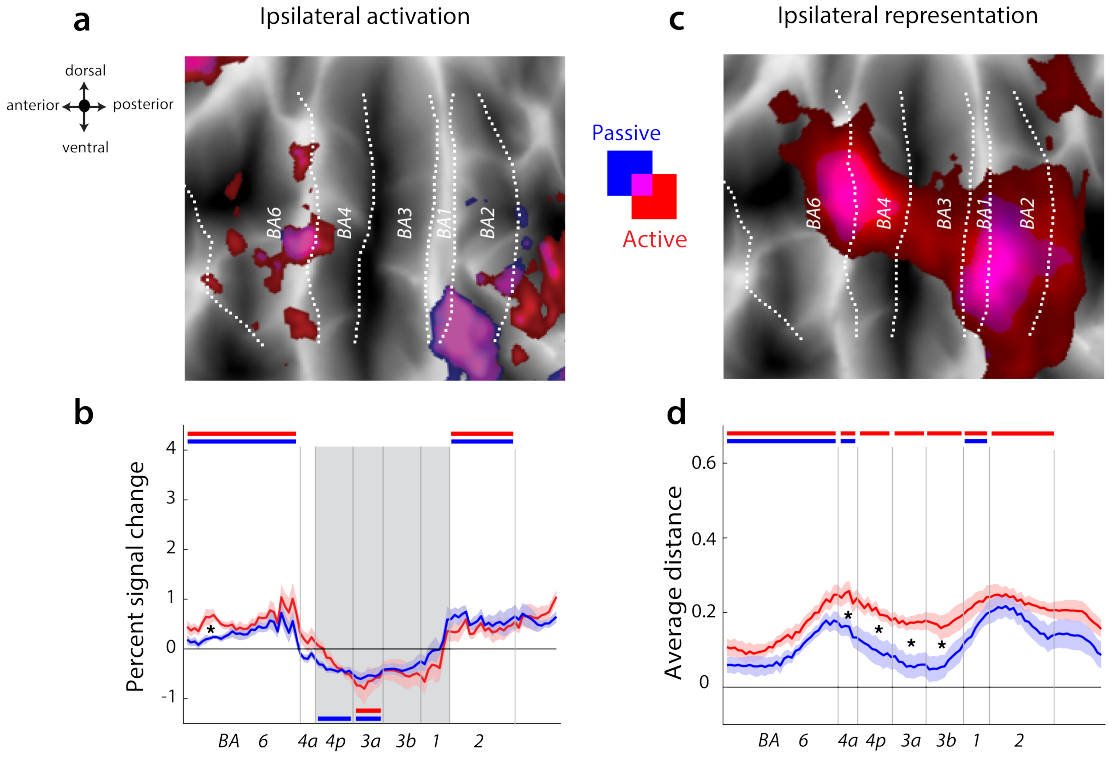

Figure 2.3. Average ipsilateral evoked activation and distances between finger patterns during active and passive tasks across subfields of sensorimotor cortex.

a) Evoked activity above resting baseline for the two conditions on the flattened ipsilateral hemisphere. **b)** Ipsilateral hemisphere showed suppression of activity below resting baseline around the central sulcus for both conditions, indicated with grey background. BA6 displayed more activation for the active than passive condition, but all other areas responded similarly for the two conditions. **c)** Average passive and active distances in the ipsilateral hemisphere. The active condition elicited higher distances than the passive condition, which is reflected in the predominately red blobs, especially in the depth of the central sulcus. **d)** Ipsilateral hemisphere displayed higher distances for the active than the passive task. This difference was significant in areas BA4a, 4p, 3a and 3b (asterisks, $p<0.0071$). Shaded area in **b** and **d** reflects standard error of the group mean.

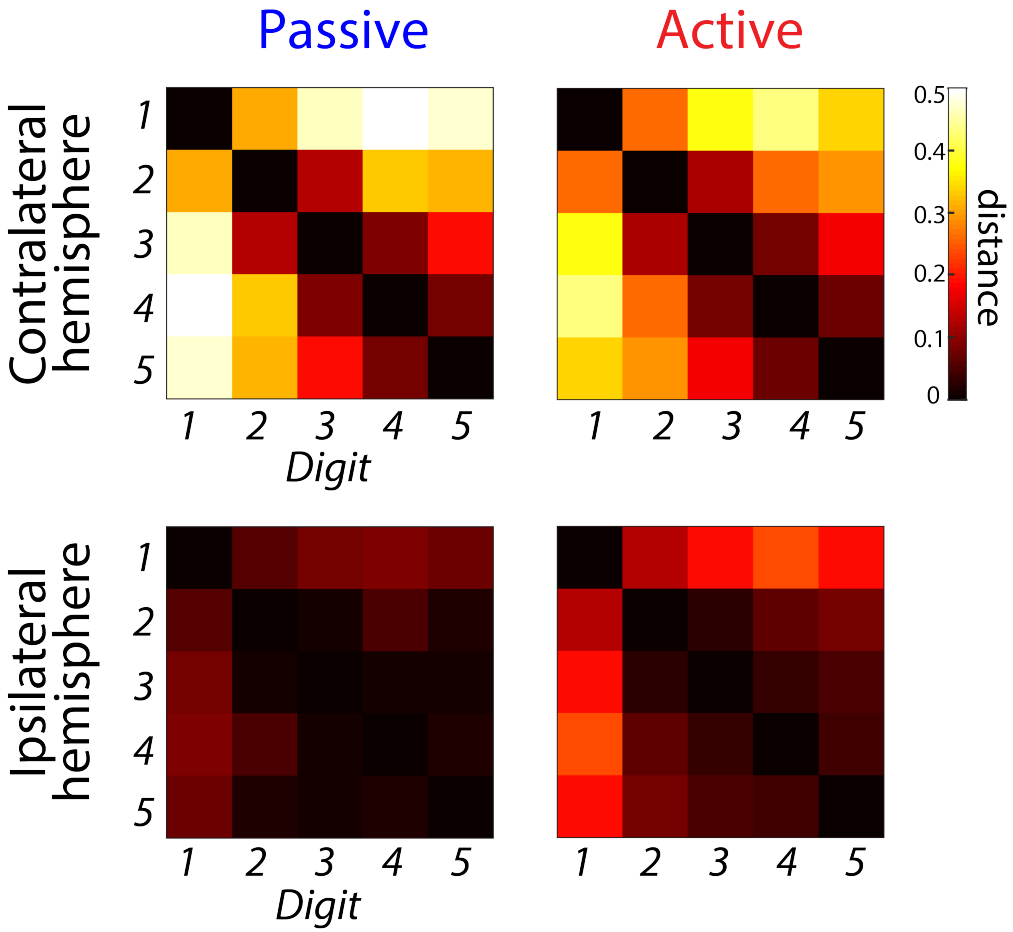

Figure 2.4. Representational dissimilarity matrix for distances between patterns of digit pairs in contralateral and ipsilateral M1 (BA4a and BA4p combined), for passive and active conditions.

The distances are averaged across the seven participants. The structure of dissimilarity matrix (see Ejaz et al., 2015) is preserved across hemispheres and conditions.

2.3.3 Spatial distribution of active representations is different across hemispheres

An additional important insight about ipsilateral representation can also be gained by considering the spatial distribution of representations across subfields of sensorimotor cortices. We compared the distribution of active distances across the cross-section of ROIs in the contralateral and ipsilateral hemisphere (i.e. the profile of red lines in **Figure 2.2d** versus **Figure 2.3d**). Our results showed that the ipsilateral profile of distances for the active condition is not just a scaled-down version of the contralateral distances. For example, contralateral distances peaked in area 3b, but ipsilateral hemisphere showed lower distances in 3b than in areas 1 and 2. To quantify this effect, we performed a hemisphere x ROI ANOVA on the distance estimates in the active condition. Both main effects were significant (hemisphere: $F_{(1,6)}$=35.827, p=0.001, ROI: $F_{(6,36)}$=20.272, p=3.33e^{-10}), but importantly the interaction between them was significant as well ($F_{(6,36)}$=17.236, p=2.83e^{-9}). This suggests that the ipsilateral hemisphere has a unique profile across areas, with relatively stronger finger-specific representations in premotor and parietal areas.

2.3.4 Correlation of activity patterns during active and passive conditions

Finally, we examined to what degree active and passive conditions activate the same or different finger-specific circuits. On one extreme, individual finger presses and individual finger stimulation could evoke the same responses in the same voxels. On the other extreme, the two conditions could activate completely different voxels or the same voxels to a different extent. Using PCM, we can determine the degree to which finger-specific patterns of activity were shared across the two conditions. When estimating the correlation between active and passive conditions (corrected for the measurement noise, see section 2.2.9 Pattern component analysis) on the contralateral hemisphere, we obtained an average value of 0.84 between across all areas of interest (**Figure 2.5a** – solid line). Also in the ipsilateral hemisphere, consistently positive correlations (average r =0.66) were found (**Figure 2.5a** – dashed line).

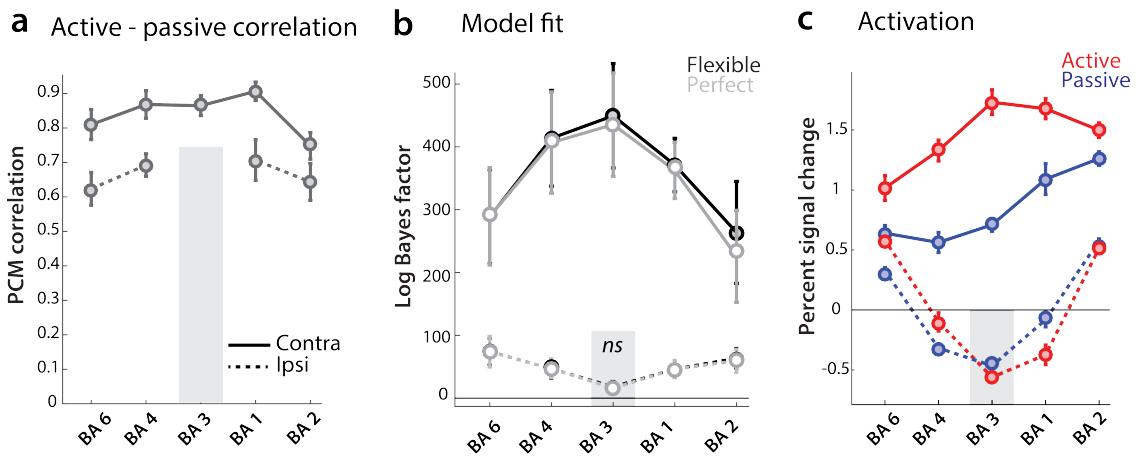

Figure 2.5. Correlation between finger-specific activity patterns in the active and passive conditions.

a) Correlations coefficient estimated using pattern-component modelling (PCM) for contralateral (solid line) and ipsilateral hemisphere (dash line). Note that for ipsilateral area BA3, there was not enough evidence for a finger-specific representation in the passive condition to reliably estimate a correlation coefficient. **b)** Performance of the model with correlation between active and passive patterns unconstrained ('flexible correlation' model) and the model where the correlation is constrained to be one ('perfect correlation' model) – both expressed relative to a 'null' model (no correlation between active and passive patterns). While a log-Bayes factor of 1 is considered positive evidence, and a log-Bayes factor of 3 as strong model evidence (Kass and Raftery, 1995), our log-Bayes factors are likely inflated due to residual dependence between voxels after pre-whitening. Therefore, the critical test is whether the group log-Bayes factors are significantly different than zero in a frequentist (t) test. **c)** Percent signal change in active and passive conditions for contralateral (solid) and ipsilateral (dashed) hemispheres. Error bars reflect standard error of the group mean.

These results clearly show that the passive and active conditions engage overlapping finger-specific circuits on the contralateral side, and to a lesser extent on the ipsilateral side. However, the problem is that correlation coefficients underestimate the true correlation (Diedrichsen et al., 2017), such that the lower correlation coefficient on the ipsilateral side likely reflects a lower signal-to-noise ratio. To test whether the data could be explained by a true correlation of r =1 between active and passive patterns, we compared two PCM models: a *'perfect correlation' model* which constrained the correlation between passive and active patterns to 1, and a *'flexible correlation' model* in which the correlation was estimated in a cross-validated fashion across subjects. Evidence for these two models was expressed relative to a *'null' model* which assumes that the correlation between active and passive patterns is 0. On the contralateral side, both flexible and perfect correlation models were a better descriptor of our data than the null model (**Figure 2.5b**) – the *flexible correlation model* had a log-Bayes factor of 357 (one-sample t-test against zero: $t_{(6)}$=10.684, p=3.41e^{-16}), whereas the *perfect correlation model* had a log-Bayes factor of 344 ($t_{(6)}$=10.188, p=2.53e^{-16}). The two models performed indistinguishably in all contralateral ROIs (all $t_{(6)}$<2.12, p>0.078).

On the ipsilateral hemisphere both models had lower log-Bayes factors; the flexible correlation model had an average log-Bayes factor of 54.2 across regions, whereas the perfect correlation model average log-Bayes factor was 52.9. Specifically in area BA3, where evidence for both models was the highest in the contralateral hemisphere, the two models on the ipsilateral hemisphere did not perform better than the null model (flexible model: $t_{(6)}$=1.45, p=0.098; perfect correlation model: $t_{(6)}$=1.54, p=0.086). This is caused by the absence of a significant finger representation in this area in the passive condition (see **Figure 2.3d**), which makes the estimation of a correlation impossible. Additionally, this area displayed the lowest elicited activation during the passive and active conditions (**Figure 2.5c**). Together, our results demonstrate that in all areas, in which both active and passive conditions elicit reliable finger-specific activity patterns, these representations are highly related.

2.4 Discussion

In this study, we used active finger presses and passive finger stimulation to investigate the origin of finger representations in the ipsilateral sensorimotor cortex. We first provided a detailed characterization of the nature of contralateral representations. We found that finger-specific representations were equally strong across active and passive conditions despite BOLD activations being larger for the active condition. We expanded upon these results in two ways. First, we quantified finger representations across the subfields of the sensorimotor cortex, and report that representations were most pronounced in BA3a, 3b and BA1. Second, we demonstrate that finger-specific activity patterns were highly correlated between active and passive conditions. Altogether, our results demonstrate that passive finger stimulation drives contralateral finger-specific motor circuits as strongly as active finger presses. While this may be surprising in some ways, it aligns with the importance of sensory inputs in dexterous manipulation (Pruszynski et al., 2016). These findings are therefore expected under the hypothesis that the main function of the primary motor cortex is feedback control (Scott, 2004).

Having established the nature of contralateral sensorimotor finger representations, we then examined the extent to which the ipsilateral motor areas are recruited during active and passive conditions. Overall, ipsilateral representations were weaker than those in the contralateral hemisphere. Critically, however, while contralateral representations were equally strong for both active and passive conditions, ipsilateral sensorimotor representations were significantly stronger for the active condition. There was no reliable finger representation during passive stimulation in ipsilateral areas 4p, 3a and 3b. The difference between hemispheres became also clear when investigating the spatial distribution of finger representations – in the contralateral hemisphere, finger representations were strongest along the central sulcus, whereas on the ipsilateral side, they were strongest in premotor and parietal areas. These data provide clear evidence that finger-specific representation in contralateral and ipsilateral hemispheres differ qualitatively, likely reflecting the difference in the functional role of these representations.

Our data therefore clearly argue against the idea that ipsilateral representations are caused by a passive spill-over from the homologous areas though transcallosal connections

(e.g. M1-M1; Asanuma and Osamu, 1962), as such a fixed information transmission should have resulted in the same active / passive ratio of information in both hemispheres. At the very least, our results indicate that the information transmission between hemisphere is strongly modulated by the behavioural context (active vs. passive). Similarly, our results confirm that the process that leads to global suppression of the BOLD signal in the ipsilateral hemisphere (supposedly through inter-hemispheric inhibition, Gerloff et al., 2004), is qualitatively different from the mechanism that causes the finger-specific ipsilateral activity patterns. While the overall ipsilateral suppression in BA 3 and 4 was equivalent across active and passive conditions, the strength of the finger representations showed substantial differences. Furthermore, we have shown in previous papers that the ipsilateral patterns are caused by an activation of the corresponding finger representations for the other hand, not by a suppression of these circuits (Diedrichsen et al., 2013). Together, evidence suggests that ipsilateral representations are not passive copies of their contralateral homologous counterparts.

While other possible explanations exist, the most likely interpretation of the whole pattern of results is that ipsilateral representations are more related to the planning and initiation of actions, and less to the ongoing feedback control of movements. In favour of this interpretation, there was very little ipsilateral finger-specific information in the passive condition in the ipsilateral primary somatosensory areas. If the ipsilateral hemisphere had a direct role in feedback control of the movement, we would have expected a clear representation of sensory information here, as observed for the contralateral hemisphere. Additionally, the finger-specific representations in the ipsilateral hemisphere was most pronounced in premotor and parietal areas, which are thought to be involved in motor planning (this pattern of results was observed also in the ipsilateral superior parietal lobule and supplementary motor areas, not shown in the results section). The function of the ipsilateral representations to movement planning (rather than control) is also more consistent with research in non-human primates demonstrating that the ipsilateral hemisphere has limited capacity to cause upper-limb movements (Kuypers et al., 1962), and therefore most likely plays a modulatory or indirect role in active control (Soteropoulos et al., 2011).

Interestingly, however, ipsilateral premotor and parietal areas also displayed significant finger representations in the passive conditions. This raises the alternative hypothesis that the ipsilateral finger representations may reflect attentional signals. Given that participants knew which finger would be stimulated, they may have allocated spatial attention to the specific finger, causing finger-specific activity patterns to occur. Alternatively, participants may have internally prepared an action with the corresponding finger.

Is it possible that the differences in finger representations across active and passive conditions are caused by participants allocating more attention to the finger in the active condition? We think that this explanation is unlikely, as the biggest relative difference between conditions was found in the ipsilateral M1 / S1, whereas the difference in contra- and ipsilateral premotor areas was much less pronounced. If anything, attentional effects should be expressed more in these higher-order areas and should also be found in the contralateral sensorimotor cortex (Johansen-Berg and Matthews, 2002; Rushworth et al., 2003).

One possibility is that the finger representations in ipsilateral primary sensorimotor areas are a pure epiphenomenon without any functional relevance. Namely, the presence of a detailed representation during the active condition (as observed with fMRI or electrophysiology) does not automatically imply that the activity plays any causal role. For example, bilateral representations in primary sensorimotor regions could arise from covert planning of candidate responses with either hand (Cisek & Kalaska, 2010). The ipsilateral representations would then be suppressed when the choice of hand is made, without contributing in any way to motor performance. While there is some evidence that disruption of ipsilateral motor circuits impedes the quality and skill of motor execution (Chen et al., 1997; Johansen-Berg et al., 2002), the observed deficits are rather subtle (Noskin et al., 2008; Xu et al., 2017). Even if it turns out that ipsilateral representation is not essential to ensure normal motor control, it is still possible that this activity subserves other functions. For example, it has been suggested that bilateral representations of motor plans may promote transfer of motor learning across hands (Wiestler et al., 2014). Furthermore, the representation could provide a redundant code that could obtain a

functional role when the corresponding regions in the opposite hemispheres are disrupted (Li et al., 2016). Thus, in the case of case of brain injury, the ipsilateral hemisphere may play a compensatory role.

In conclusion, we have provided a detailed characterization of the nature of ipsilateral sensorimotor representations during active presses and passive finger stimulation. Our results suggest that the ipsilateral hemisphere does not receive the sensory input critical for dexterous feedback control; instead, it may be primarily involved in planning-related processes. Therefore, our study provides important constrains on the role that the ipsilateral hemisphere can play in the control of movement in health and disease.

2.5 References

Asanuma, H., Osamu, O., 1962. Effects of transcallosal volleys on pyramidal tract cell activity of cat. J. Neruophysiology 25, 198–208.

Augurelle, A.-S., Smith, A.., Lejeune, T., Thonnard, J.-L., 2003. Importance of Cutaneous Feedback in Maintaining a Secure Grip During Manipulation of Hand-Held Objects. J. Neurophysiol. 89, 665–671.

Blakemore, S.J., Frith, C.D., Wolpert, D.M., 1999. Spatio-temporal prediction modulates the perception of self-produced stimuli. J. Cogn. Neurosci. 11, 551–559.

Brinkman, J., Kuypers, H.G.J.M., 1973. Cerebral control of contralateral and ipsilateral arm, hand and finger movements in the split-brain rhesus monkey. Brain 96, 653–674.

Chen, R., Gerloff, C., Hallett, M., Cohen, L.G., 1997. Involvement of the ipsilateral motor cortex in finger movements of different complexities. Ann. Neurol. 41, 247–254.

Cisek, P., Crammond, D.J., Kalaska, J.F., 2003. Neural Activity in Primary Motor and Dorsal Premotor Cortex In Reaching Tasks With the Contralateral Versus Ipsilateral Arm. J. Neurophysiol. 89, 922–942.

Cisek, P., Kalaska, J.F., 2010. Neural mechanisms for interacting with a world full of action choices. Annu. Rev. Neurosci. 33, 269–298.

Cramer, S.C., Finklestein, S.P., Schaechter, J.D., Bush, G., Rosen, B.R., Hinder, M.R., Schmidt, M.W., Garry, M.I., Carroll, T.J., Jeffery, J., Wu, C.C., Fairhall, S.L., Mcnair, N.A., Hamm, J.P., Kirk, I.J., Cunnington, R., Anderson, T., Lim, V.K., Lee, M., Hinder, M.R., Gandevia, S.C., Carroll, T.J., Cramer, S.C., Finklestein, S.P., Schaechter, J.D., Bush, G., 2011. Activation of Distinct Motor Cortex Regions During Ipsilateral and Contralateral Finger Movements older adults Activation of Distinct Motor Cortex Regions During Ipsilateral and Contralateral Finger Movements. J. Neruophysiology 81, 383–387.

Dale, A.M., Fischl, B., Sereno, M.I., Dale, A.M., 1999. Cortical Surface-Based Analysis. Neuroimage 9, 179–194.

Diedrichsen, J., Provost, S., Zareamoghaddam, H., 2016. On the distribution of cross-validated Mahalanobis distances. arXiv Prepr. arXiv 1607.01371.

Diedrichsen, J., Wiestler, T., Krakauer, J.W., 2013. Two distinct ipsilateral cortical representations for individuated finger movements. Cereb. Cortex 23, 1362–1377.

Diedrichsen, J., Yokoi, A., Arbuckle, S.A., 2017. Pattern component modeling: A flexible approach for understanding the representational structure of brain activity patterns. Neuroimage. 180, 119–133.

Diedrichsen, J.J., Kriegeskorte, N., 2017. Representational models: A common framework for understanding encoding, pattern-component, and representational-similarity analysis. PLoS Comput. Biol. 13, e1005508.

Ejaz, N., Hamada, M., Diedrichsen, J., 2015. Hand use predicts the structure of representations in sensorimotor cortex. Nat. Neurosci. 18, 1034–1040.

Fischl, B., Rajendran, N., Busa, E., Augustinack, J., Hinds, O., Yeo, B.T.T., Mohlberg, H., Amunts, K., Zilles, K., 2008. Cortical folding patterns and predicting cytoarchitecture. Cereb. Cortex 18, 1973–1980.

Fujiwara, Y., Matsumoto, R., Nakae, T., Usami, K., Matsuhashi, M., Kikuchi, T., Yoshida, K., Kunieda, T., Miyamoto, S., Mima, T., Ikeda, A., Osu, R., 2017. Neural pattern similarity between contra- and ipsilateral movements in high-frequency band of human electrocorticograms. Neuroimage 147, 302–313.

Hutton, C., Bork, A., Josephs, O., Deichmann, R., Ashburner, J., Turner, R., 2002. Image distortion correction in fMRI: A quantitative evaluation. Neuroimage 16, 217–240.

Indovina, I., Sanes, J.N., 2001. On somatotopic representation centers for finger movements in human primary motor cortex and supplementary motor area. Neuroimage 13, 1027–1034.

Johansen-Berg, H., Matthews, P.M., 2002. Attention to movement modulates activity in sensori-motor areas, including primary motor cortex. Exp. Brain Res. 142, 13–24.

Johansen-Berg, H., Rushworth, M.F.S., Bogdanovic, M.D., Kischka, U., Wimalaratna, S., Matthews, P.M., 2002. The role of ipsilateral premotor cortex in hand movement after stroke. Proc. Natl. Acad. Sci. 99, 14518–14523.

Kass, R.E., Raftery, A.., 1995. Bayes Factors. J. Am. Stat. Assoc. 90, 773–795.

Kuypers, H.G.J.M., Fleming, W.R., Farinoholt, J.W., 1962. Subcorticospinal projections in the Rhesus monkey. J. Comp. Neurol. 118, 107–137.

Li, N., Daie, K., Svoboda, K., Druckmann, S., 2016. Robust neuronal dynamics in premotor cortex during motor planning. Nature 532, 459–64.

Nili, H., Wingfield, C., Walther, A., Su, L., Marslen-Wilson, W., Kriegeskorte, N., 2014. A Toolbox for Representational Similarity Analysis. PLoS Comput. Biol. 10, e1003553.

Noskin, O., Krakauer, J.W., Lazar, R.M., Festa, J.R., Handy, C., O'Brien, K.A., Marshall, R.S., 2008. Ipsilateral motor dysfunction from unilateral stroke: Implications for the functional neuroanatomy of hemiparesis. J. Neurol. Neurosurg. Psychiatry 79, 401–406.

Oosterhof, N.N., Wiestler, T., Downing, P.E., Diedrichsen, J., 2011. A comparison of volume-based and surface-based multi-voxel pattern analysis. Neuroimage 56, 593–600.

Pruszynski, J.A., Johansson, R.S., Flanagan, J.R., 2016. A rapid tactile-motor reflex automatically guides reaching toward handheld objects. Curr. Biol. 26, 788–792.

Rushworth, M.F.S., Johansen-Berg, H., Göbel, S.M., Devlin, J.T., 2003. The left parietal and premotor cortices: Motor attention and selection. Neuroimage 20, S89–S100.

Scherer, R., Zanos, S.P., Miller, K.J., Rao, R.P.N., Ojemann, J.G., 2009. Classification of contralateral and ipsilateral finger movements for electrocorticographic brain-computer interfaces. Neurosurg. Focus 27, E12.

Scott, S.H., 2004. Optimal feedback control and the neural basis of volitional motor control. Nat. Rev. Neurosci. 5, 534–546.

Soteropoulos, D.S., Edgley, S.A., Baker, S.N., 2011. Lack of Evidence for Direct Corticospinal Contributions to Control of the Ipsilateral Forelimb in Monkey. J. Neurosci. 31, 11208–11219.

Verstynen, T., Diedrichsen, J., Albert, N., Aparicio, P., Ivry, R.B., 2005. Ipsilateral Motor Cortex Activity During Unimanual Hand Movements Relates to Task Complexity. J. Neurophysiol. 93, 1209–1222.

Walther, A., Nili, H., Ejaz, N., Alink, A., Kriegeskorte, N., Diedrichsen, J., 2016. Reliability of dissimilarity measures for multi-voxel pattern analysis. Neuroimage 137, 188–200.

Wiestler, T., McGonigle, D.J., Diedrichsen, J., 2011. Integration of sensory and motor representations of single fingers in the human cerebellum. J. Neurophysiol. 105, 3042–3053.

Wiestler, T., Waters-Metenier, S., Diedrichsen, J., 2014. Effector-Independent Motor Sequence Representations Exist in Extrinsic and Intrinsic Reference Frames. J. Neurosci. 34, 5054–5064.

Xu, J., Ejaz, N., Hertler, B., Branscheidt, M., Widmer, M., Faria, A. V., Harran, M.D., Cortes, J.C., Kim, N., Celnik, P.A., Kitago, T., Luft, A.R., Krakauer, J.W., Diedrichsen, J., 2017. Separable systems for recovery of finger strength and control after stroke. J. Neurophysiol. 118, 1151–1163.

Yousry, T.A., Schmid, U.D., Alkadhi, H., Schmidt, D., Peraud, A., Buettner, A., Winkler, P., 1997. Localization of the motor hand area to a knob on the precentral gyrus. A new landmark. Brain 120, 141–157.

CHAPTER 3

3 A critical re-evaluation of fMRI signatures of motor sequence learning

3.1 Introduction

Humans have the remarkable ability to learn complex sequences of movements. While behavioural improvements in sequence learning tasks are easily observable, the underlying neural processes remain elusive. Understanding the neural underpinnings of motor sequence learning could provide clues about more general mechanisms of plasticity in the brain. This motivation has led numerous functional magnetic resonance imaging (fMRI) studies to investigate the brain changes related to motor sequence learning. However, there is little agreement about how and where in the brain learning-related changes are observable. Previous studies include reports of signal increases across various brain regions (Floyer-Lea & Matthews, 2005; Grafton, Hazeltine, & Ivry, 1995; Hazeltine, Grafton, & Ivry, 1997; Karni et al., 1995; Lehéricy et al., 2005; Penhune & Doyon, 2002), as well as signal decreases (Jenkins, Brooks, Nixon, Frackowiak, & Passingham, 1994; Peters, Lee, Hedrick, Neil, & Komiyama, 2017; Toni, Krams, Turner, & Passingham, 1998; Ungerleider, Doyon, & Karni, 2002; Wiestler & Diedrichsen, 2013), nonlinear changes in activation (Ma et al., 2010; Xiong et al., 2009), spatial shifts in activity (Lehéricy et al., 2006; Steele & Penhune, 2010), changes in multivariate patterns (Wiestler and Diedrichsen, 2013; Wymbs and Grafton, 2015), and changes in inter-regional functional connectivity (Bassett, Yang, Wymbs, & Grafton, 2015; Bassett et al., 2010; Doyon et al., 2002; Mattar et al., 2016). Additionally, some experiments have matched the speed of performance (Karni et al., 1995; Penhune & Doyon, 2002; Steele & Penhune, 2010; Lehéricy et al., 2005; Seidler et al., 2002, 2005), while others have not (Bassett et al., 2015; Lutz, Koeneke, Wüstenberg, & Jäncke, 2004; Wiestler & Diedrichsen, 2013; Wymbs & Grafton, 2015). Given that fMRI analysis has many degrees of freedom, these

inconsistencies may not be too surprising. However, the implicit pressure in the publication system to report findings may also have contributed to a lack of coherency. To address this issue, we designed a comprehensive longitudinal study of motor sequence learning that allowed us to systematically reinvestigate previous findings. In order to increase transparency, we pre-registered the design, as well as all tested hypotheses on the Open Science Framework (Berlot, Popp, & Diedrichsen, 2017; https://osf.io/etnqc), and make the full dataset available to the research community.

The main aim of our study was to systematically evaluate different ideas of how learning-related changes are reflected in the fMRI signal. In the context of motor sequence learning, the most commonly examined brain region is the primary motor cortex (M1). Previous reports of increased M1 activation after long-term learning have been interpreted as additional recruitment of neuronal resources for trained behaviour, taken to suggest the skill is represented in M1 (Floyer-Lea & Matthews, 2005; Karni et al., 1995, 1998; Lehéricy et al., 2005; Penhune & Doyon, 2002; for a review see Dayan & Cohen, 2011; **Figure 3.1a**). Since then, several pieces of evidence have suggested that sequence-specific memory may not reside in M1 (Beukema et al., 2019; Wiestler and Diedrichsen, 2013; Yokoi and Diedrichsen, 2019). However, some of these reports studied skill acquisition over a course of a few days, while human skill typically evolves over weeks (and months) of practice. Therefore, including several weeks of practice might be more suitable to test whether, and at what time point, M1 develops skill-specific representations.

Outside of M1, learning-related activation changes have been reported in premotor and parietal areas (Grafton et al., 2002; Hardwick et al., 2013; Honda et al., 1998; Penhune and Doyon, 2002; Tamás Kincses et al., 2008; Vahdat et al., 2015), with activation increases commonly interpreted as increased involvement of these areas in the skilled behaviour. Yet, recent studies have mostly found that, as the motor skill develops, activation in these areas predominantly decreases (Penhune and Steele, 2012; Wiestler and Diedrichsen, 2013; Wu et al., 2004). Such reductions are harder to interpret as they could reflect a reduced areal involvement in skilled performance or, alternatively, more energy efficient implementation of the same function (**Figure 3.1b**) (Picard et al., 2013; Poldrack et al., 2005). To complicate things further, regional activity increases and decreases could

occur simultaneously in the same area (**Figure 3.1c**; Steele & Penhune, 2010). In such a scenario, the net activation in the region would not change, yet, the trained sequences would engage slightly different subpopulations of the region than untrained sequences.

A variant of this idea is that each specific sequence becomes associated with dedicated neuronal subpopulation (and hence fMRI activity pattern). Such a representation would form the neural correlate of sequence-specific learning – the part of the skill that does not generalize to novel, untrained motor sequences (Karni et al., 1995). Sequence-specific activation patterns should change early in learning (**Figure 3.1d**), when behaviour improves most rapidly, and stabilize later, once the skill has consolidated and an optimal pattern is established (Peters et al., 2017). One possible way in which sequence-specific patterns could reorganize is by becoming more distinct from one another (**Figure 3.1e**; Wiestler & Diedrichsen, 2013). Having a distinctive code for each sequence might be of particular importance to the system in a trained state, allowing it to produce different dynamical sequences, while avoiding confusion or "tangling" of the different neural trajectories (Russo et al., 2018).

To systematically examine the cortical changes associated with motor sequence learning, we carried out a longitudinal study over five weeks of training with four sessions of high-field (7 T) fMRI scans. Behavioural performance in the first three scanning sessions was imposed to the same speed of performance. This allowed us to inspect whether examined fMRI metrics reflect brain reorganization, independent of behavioural change. However, controlling for speed incurs the danger of not tapping into neural resources that are necessary for skilled performance (Orban et al., 2010; Poldrack, 2000). We therefore compared the fMRI session with paced performance at the end of behavioural training with one acquired with full speed performance. This manipulation allowed us to systematically assess the role of speed on the fMRI metrics of learning, thereby addressing an important methodological problem faced by virtually every study on motor learning.

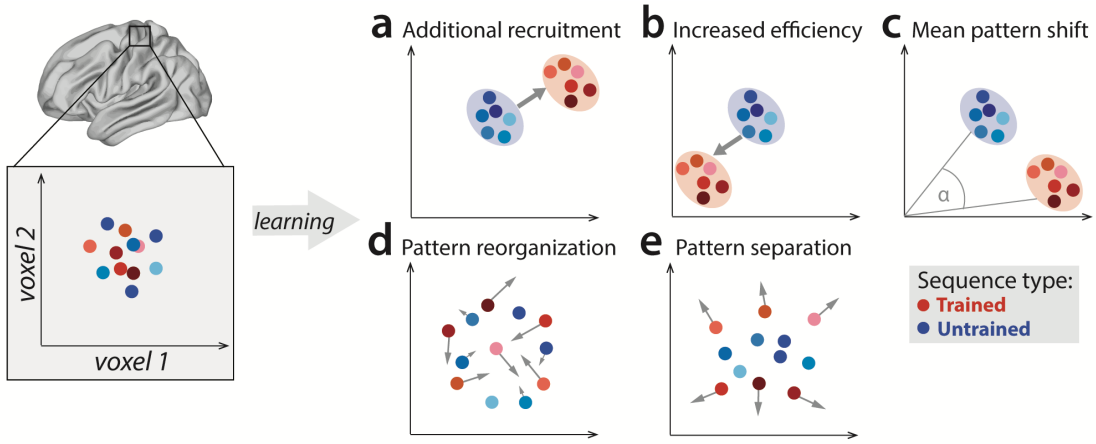

Figure 3.1. Potential fMRI signatures of learning in a specific brain area.

Each panel shows hypothetical activation for the six trained sequences (red) and the six untrained sequences (blue) in the space of two example voxels. **a)** Activation could increase during learning across voxels, indicating additional recruitment of resources involved in skilled behaviour. **b)** Activation could decrease across voxels, implying that the region performs its function more efficiently. **c)** Some voxels (x-axis) could increase activation with training, while others (y-axis) could decrease. This would lead to a shift of the overall activity pattern in the region without an overall net change in activation. **d)** Activation patterns specific to each trained sequence could undergo more change than activation patterns for untrained sequences, reflective of plastic reorganization of the sequence representation. Arrow length in the figure indicates the amount of reorganization. **e)** One specific form of such reorganization would be increasing dissimilarities (pattern separation) between activity patterns for individual trained sequences.

3.2 Methods

3.2.1 Participants

Twenty-seven volunteers participated in the experiment. One of them was excluded because field map acquisition was distorted in one of the four scans. The average age of the remaining 26 participants was 22.2 years (SD = 3.3 years), and the sample included 17 women and 9 men. All participants were right-handed and had no prior history of psychiatric or neurological disorders. They provided written informed consent to all procedures and data usage before the study started. The experimental procedures were approved by the Ethics Committee at Western University.

3.2.2 Apparatus

Participants performed finger sequences with their right hand on an MRI-compatible keyboard (**Figure 3.2a**), with keys numbered 1-5 for thumb-little finger. The keys had a groove for each fingertip and were not depressible. The force of isometric finger presses was measured by the force transducers (FSG-15N1A, Sensing and Control, Honeywell; dynamic range 0-25 N) mounted underneath each key with an update rate of 2 ms. A key press was recognized when the sensor force exceeded 1 N. The measured signal was amplified and sampled at 200 Hz.

Figure 3.2. Experimental design and paradigm.

a) Apparatus and task. Participants were trained to perform six 9-item sequences on a keyboard device. For each finger press, the corresponding digit on the screen turned green (correct) or red (incorrect). During fMRI scans 1-3, an expanding pink line under the numbers indicated the pace at which participants had to press the keys. **b)** Training protocol lasted for five weeks, and included four behavioural test sessions (yellow underlay) and four scans (grey underlay). Scans 1-3 were performed at a paced speed, while performance in scan 4 was at full speed *(fs)*. **c)** Average group performance executing trained sequences across the training sessions, measured in seconds. The average movement time (MT) decreased with learning. Shaded area denotes standard error of the group mean. **d)** Performance during scanning sessions and behavioural tests, measured in seconds. Performance of trained sequences improved across all subsequent behavioural test sessions. Performance improved also for untrained sequences from week 2 onwards, suggesting some transfer in learning, but execution was faster for trained sequences, indicating sequence-specific learning. Error bars indicate standard error of the group mean. Stars denote significance levels lower than $p<.001$.

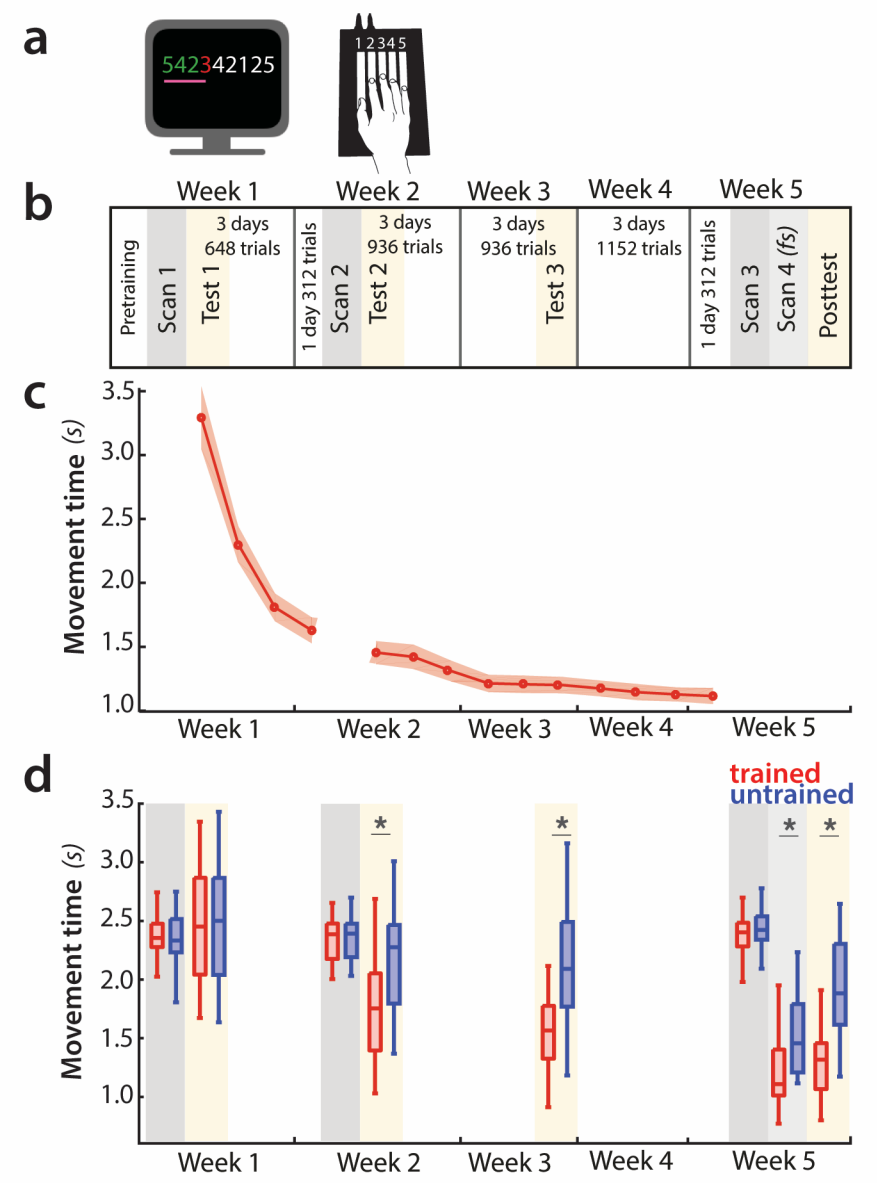
a
54234 2125
1 2 3 4 5
b
Week 1
Week 2
Week 3
Week 4
Week 5
Pretraining
Scan 1
Test 1
3 days
648 trials
1 day 312 trials
Scan 2
Test 2
3 days
936 trials
3 days
936 trials
Test 3
3 days
1152 trials
1 day 312 trials
Scan 3
Scan 4 (fs)
Posttest
c
Movement time (s)
3.5
3.0
2.5
2.0
1.5
1.0
Week 1
Week 2
Week 3
Week 4
Week 5
d
trained
untrained
Movement time (s)
3.5
3.0
2.5
2.0
1.5
1.0
*
*
*
*
Week 1
Week 2
Week 3
Week 4
Week 5

3.2.3 Learning paradigm

Participants were trained to execute six 9-digit finger sequences over a period of five weeks (**Figure 3.2a**). They were randomly split into two groups, with trained sequences of one group constituting the untrained sequences for the other group and vice versa. Finger sequences of both groups were matched as closely as possible in terms of the starting finger, number of finger repetitions in a sequence and first-order finger transitions. This counterbalancing between the groups ensured that any of the observed results were not specific to a set of chosen trained sequences.

In the pre-training session prior to the first scan (**Figure 3.2b**), participants were acquainted with the apparatus and task performed during scanning. Sequences executed during this pre-training session were not encountered later on in the experiment.

During the training sessions, participants were trained to perform the six sequences as fast as possible. They received visual feedback for the correctness of their presses with digits turning green for a correct finger press and red for an incorrect one. After each trial, participants received points based on the accuracy and their movement time (MT – time from the first press until the last finger release in the sequence; **Figure 3.2c**). Trials executed correctly and faster than participant's median MT from the previous blocks were rewarded with 1 point. If participants performed correctly and 20% faster than the median MT from previous blocks, they received 3 points. If they made a mistake or performed below their median MT, they received 0 points. Participants performed each sequence twice in a row: digits were written on the screen for the first execution, but removed for the second execution so that participants had to perform the finger sequence from memory. Training sessions were broken into several blocks, each consisting of 24 trials (four trials per trained sequence), with time between blocks to rest. At the end of each block, participants received feedback on their error rate, median MT and points obtained during the block. If participants performed with an error of <15% and faster than the previous median MT, the MT threshold was updated. This design feature was chosen to maintain participants' motivation to execute the sequences as fast as possible, within the allowed error range.

During the behavioural test sessions (**Figure 3.2d**), participants executed both the sequences they were trained on, as well as matched untrained sequences, with all sequences randomly interspersed. As in training, each sequence was performed twice in a row – however, the 9-digit sequence numbers were presented on the screen present on both executions. Therefore, the requirement to remember the sequences from the first to second execution, which was present in training sessions, was omitted for test sessions. For this reason, performance between training and test sessions (**Figure 3.2c-d**) cannot be directly compared.

As an additional feature of the four behavioural test sessions, we examined participants' performance with their left hand. Specifically, we tested them on execution of intrinsically-matched trained sequences (i.e. producing the same finger combinations), extrinsically-matched trained sequences (i.e. producing the same external consequences using mirrored fingers) and random sequences. This was added to probe to what extent learning generalized to the other effector in intrinsic or extrinsic coordinate frames, at different stages of learning. Per session, participants performed four repetitions of each trained sequence in intrinsically-matched space and four repetitions in extrinsically-matched space.

3.2.4 Experimental design during scanning

Participants underwent four scanning sessions (**Figure 3.2d**) – with the first one before learning regime started, the second after a week and two more scans after completion of the five training weeks. Each scanning session consisted of eight functional runs. We employed an event-related design, randomly intermixing execution of trained and untrained sequences. Each sequence was repeated twice in a row with digits present on the screen during both executions. Thus, there was no need to memorize either trained or untrained sequences from first to second execution in the scanner. Each sequence was repeated for a total of six times in every run. Each trial started with 1 second preparation time, during which the sequence was presented on the screen. After that time, a 'go' signal was displayed as short pink line underneath the sequence numbers. In scanning sessions 1-3, this line started expanding below the written numbers, indicating the speed at which

participants were required to press along. In scanning session 4, only a short line was presented in front and underneath the sequences. When the line disappeared, this signaled a ‘go’ cue for participants to execute the presented sequence as fast as possible. The execution phase including the feedback on overall performance lasted for 3.5 seconds, and the inter-trial interval was 0.5 seconds (**Figure 3.3**). Each trial lasted for 5 seconds. Participants always received 3 points upon correct execution of the sequence, and 0 points otherwise. Five periods of rest, each 10 seconds long, were added randomly between trials in each run to provide a better estimate of baseline activation. Participants performed the task inside the scanner for approximately 75 minutes. After each scanning session, they filled out a recall and recognition questionnaires on trained and untrained sequences performed inside the scanner.

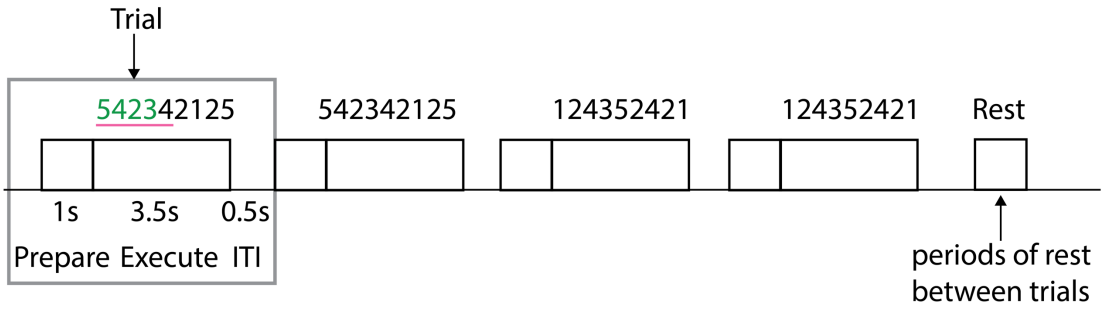

Figure 3.3. Experimental trial structure during scanning sessions.

Each trial consisted of a preparation period, execution period and inter-trial-interval (ITI), during which the feedback was presented on correctness of the trial. Each sequence was presented twice in a row. Periods of rest were added in-between the trials.

3.2.5 Image acquisition

Data was acquired on a 7-T Siemens Magnetom scanner with a 32-receive channel head coil (8-channel parallel transmit). Anatomical T1-weighted scan was acquired at the beginning of the first scanning session, using a magnetization-prepared rapid gradient echo sequence (MPRAGE) with voxel size of 0.75x0.75x0.75 mm isotropic (field of view = 208 x 157 x 110 mm [A-P; R-L; F-H], encoding direction coronal). Functional data were acquired using a sequence (GRAPPA 3, multi-band acceleration factor 2, repetition time [TR] = 1.0 s, echo time [TE] = 20 ms, flip angle [FA] = 30 deg). We acquired 44 slices with isotropic voxel size of 2x2x2 mm. For estimating magnetic field inhomogeneities, we additionally acquired a gradient echo field map. Acquisition was in the transversal orientation with field of view 210 x 210 x 160 mm and 64 slices with 2.5 mm thickness (TR = 475 ms, TE = 4.08 ms, FA = 35 deg). To monitor the use of 7T for human research, participants filled out a questionnaire rating their levels of dizziness, wellbeing, alertness and focus after each imaging session.

3.2.6 First-level analysis

Functional data were analyzed using SPM12 and custom written code in MATLAB (The MathWorks). Functional runs were corrected for geometric distortions using field map data (Hutton et al., 2002), and head movements during the scan (three translations: x, y, z; three rotations: pitch, roll, yaw), and aligned across sessions to the first run of the first session. The functional data were then co-registered to the anatomical scan. No smoothing or normalization to an atlas template was performed.

Preprocessed data were analyzed using a general linear model (GLM; Friston et al., 1994). Each of the performed sequences was defined as a separate regressor per imaging run, resulting in 12 regressors per run (six trained, six untrained sequences), together with intercept for each of the functional runs. All instances of sequence execution were included into estimating regressors, regardless of whether the execution was correct or erroneous (see section 3.2.11 Treatment of error trials). The regressor was a boxcar function starting at the beginning of the trial and lasting for trial duration. The boxcar function was

convolved with a hemodynamic response function, with a time to peak of 5.5 seconds, and time to undershoot of 12.5 seconds. We adjusted the hrf onset individually per participant. For that, we defined a combined region of interest between PMd and M1, and averaged the response across all voxels in the combined ROI for all performed sequences (i.e. trained and untrained sequences together) in session 1. We then performed a grid-search with delay values of 0, 0.5 and 1 second, and chose the one that maximally fit the evoked response for each subject. The same delay was used across all sessions. Ultimately, this analysis resulted in one activation estimate (beta image) for each of the 12 conditions per run, for each scanning session.

3.2.7 Surface reconstruction and regions of interest

We reconstructed individual subjects' cortical surfaces using FreeSurfer (Dale et al., 1999). All individual surfaces were aligned to the FreeSurfer's Left-Right symmetric template (workbench, 164k nodes) via spherical registration. To detect sequence representation across the cortical surface, we used a surface-based searchlight approach (Oosterhof et al., 2011), where for each node we selected a circular region of 120 voxels in the grey matter. The resulting analyses (dissimilarities between sequence-specific activity patterns, see below) was assigned to the center node. As a slightly coarser alternative to searchlights, we performed regular tessellation of cortical surface into 162 tessels per hemisphere. This allowed us to fit correlation models (see below) across the cortical surface, while not being as computationally intensive as searchlight analyses.

We defined four regions of interest to cover primary somato-motor regions as well as secondary associative regions. M1 was defined using probabilistic cytoarchitectonic map (Fischl et al., 2008) by including nodes with the highest probability of belonging to Brodmann area (BA) 4, while excluding nodes more than 2.5 cm from the hand knob (Yousry et al., 1997). Similarly, S1 was defined as nodes related to hand representation in BA 1, 2 and 3. Additionally, we included dorsal premotor cortex (PMd) as the lateral part of the middle frontal gyrus. The anterior part of the superior parietal lobule (SPLa) was defined to include anterior, medial and ventral intraparietal sulcus. We also defined caudate

nucleus and putamen as striatal regions of interest. The definition was carried out in each subject using FSL's subcortical segmentation.

3.2.8 Changes in overall activation

We calculated the average percent signal change for trained and untrained sequences (averaged across the six trained and six untrained sequences) relative to the baseline for each voxel. The resulting volume map was projected to the surface for each subject, and a group statistical *t*-map was generated across subjects. Statistical maps were thresholded at $p<.01$, uncorrected, and the family-wise error corrected *p*-value for the size of the peak activation and activation cluster size was determined using a permutation test. Specifically, we ran 1000 simulations where we randomly flipped the sign of the contrast for subjects (chosen at random out of 2^{26} possible permutations). The rationale behind this is that under the null hypothesis, there should be no difference between the two conditions, and the sign of each contrast should be interchangeable. As for the data, we thresholded the statistical map from each permutation, and recorded the peak *t*-value (across the map) and the size of the largest cluster. The real data was then compared against this distribution to assess the probability of the observed *t*-value and cluster-size under the null hypothesis.

Additionally, we assessed changes in percent signal in predefined regions of interest (M1, S1, PMd, SPLa). This was performed in the native volume space of each subject. To do so, we averaged the percent signal change of voxels belonging to a defined region per subject and quantified activation changes across subjects using ANOVAs and t-tests across subjects.

Besides overall activation, we also examined *relative* changes in elicited activation for trained sequences across sessions. This was done by normalizing (z-scoring) the percent signal change surface maps across voxels, separately for each subject. Normalization was applied both map-wise (for **Figure 3.8b**), as well as for each of the pre-defined ROIs separately (for cross-sections in **Figure 3.8c**). Statistical assessment of the difference between relative evoked activation pattern for trained vs. untrained sequence was carried

out by calculating cosine angle dissimilarities between the mean evoked patterns. Cosine angle dissimilarity was chosen because it is not sensitive to overall magnitude in activation, and therefore assesses the difference in the relative activation distribution.

3.2.9 Dissimilarities between sequence-specific activity patterns

To evaluate which cortical areas display sequence-specific encoding, we performed a searchlight analysis calculating the dissimilarities between evoked beta patterns of individual sequences. Beta patterns were first multivariately prewhitened (standardized by voxels' residuals and weighted by the voxel covariance matrix), which has been found to increase the reliability of dissimilarity estimates (Walther et al., 2016). We then calculated the cross-validated squared Mahalanobis dissimilarities (i.e. crossnobis dissimilarities) between evoked sequence patterns (66 dissimilarity pairs for the six trained and six untrained sequences). These dissimilarities were then averaged overall, as well as separately for pairs within trained sequences, and within untrained sequences. This metric was used both for searchlight analysis and calculation of metric within predefined regions (cortical and striatal). The cortex surface maps contrasting dissimilarities between trained and untrained sequences were corrected for multiple comparisons using permutations, as described above for percent signal change surface maps.

3.2.10 Pattern component analysis: modelling sequence-specific correlation across sessions

Correspondence of sequence-specific patterns across sessions was quantified using pattern component modelling (PCM; Diedrichsen et al., 2017). This framework is superior at estimating correlations than simply performing Pearson's correlation on raw activity patterns, or even in a crossvalidated fashion. The main problem with estimating correlations on data is that activation patterns are biased by noise, which varies across scanning sessions, and would therefore underestimate the true correlation. PCM separately models the noise and signal component, and can in this way combat the issue more than

simply performing crossvalidation would. We designed 30 correlation models with correlations between 0 and 1 in equal step sizes and assessed the group likelihood of the observed data under each model.

Subsequent group inferences were performed using crossvalidated approach on assessing individual log-Bayes factors (model evidence). A crossvalidated approach was used to ensure that our choice of 'best-fitting models' and the evidence associated was independent and did not involve double-dipping. Specifically, we used n-1 subjects to determine the best-fitting models for trained and untrained patterns and recorded the log-Bayes factors for those two correlation models on the left-out subject. This was repeated across all subjects and a t-test was performed on the recorded log-Bayes factors (i.e. out-of-sample model evidences). The same evaluation was performed for pre-defined regions of interest (**Figure 3.9b**), as well as a regular tessellation across the cortical surface (**Figure 3.9c**).

3.2.11 Treatment of error trials

As in behavioural sessions, participants were instructed to keep their error rate below 15% also inside the scanner. This was on average achieved, with the following error rate for trained vs. untrained sequences across the four scanning sessions: week 1: 0.14±0.02 vs. 0.15±0.02, week 2: 0.08±0.01 vs. 0.14±0.02, week 5: 0.06±0.01 vs. 0.09±0.01, speeded scan week 5: 0.14±0.01 vs. 0.13±0.01. The number of errors varied significantly across sessions, and between sequence types. A session x sequence type ANOVA was significant for week ($F_{(3,75)}$=9.19, p=2.97e^{-5}), sequence type ($F_{(1,25)}$=11.16, p=2.63e^{-3}), as well as for their interaction ($F_{(3,75)}$=8.39, p=7.00e^{-5}). Post-hoc t-tests revealed that the error rate differed between trained and untrained sequences in paced sessions of week 2 ($t_{(25)}$=4.20, p=2.95e^{-4}) and 5 ($t_{(25)}$=4.81, p=6.1e^{-5}), but not in week 1 and for the speeded session of week 5. To control for difference in error rate, we performed an additional first-level analysis with error trials excluded to ensure that our results were not due to inclusion of errors. Indeed, our results did not differ qualitatively when excluding errors, therefore we here report only the analyses with all trials included.

3.3 Results

3.3.1 Speed of sequence execution increases with learning

We trained 26 participants to perform six 9-digit sequences with their right hand on a keyboard device (**Figure 3.2a**). During training, they received visual feedback (green for correct and red for incorrect presses) and were rewarded for both accuracy and speed (see section 3.2.3 Learning paradigm). Over the course of five weeks, participants practiced ~4000 trials (**Figure 3.2b**). This led to substantial performance improvement, with the average movement time (MT) to complete a sequence decreasing from an initial 3.2 seconds to 1.2 seconds at the end of the training (**Figure 3.2c**). The training regime was complemented with behavioural assessments on four occasions designed to specifically assess participants' performance on trained sequences relative to untrained sequences (**Figure 3.2d**, yellow underlay). Prior to training (test day 1), the speed of sequence execution did not differ between trained and untrained sequences. For all subsequent sessions, MTs were significantly faster for trained than untrained sequences ($p<.001$), implying sequence-specific learning. Additionally, performance of trained sequences improved between all subsequent sessions, even after week 3 (week 3-5: $t_{(25)}=5.49$, $p=1.1e^{-5}$). Thus, participants' performance of trained sequences improved across the five weeks.

To assess fMRI changes with learning, participants underwent four fMRI scans (1st scan: before the main training; 2nd scan: week 2; 3rd & 4th scan: week 5), performing both trained and untrained sequences (**Figure 3.2d** – grey underlay). Both trained and untrained sequences were always cued by presenting the corresponding digits on the screen (**Figure 3.2a**). During the first three sessions, participants were paced with a metronome so that all sequences, trained and untrained, were performed at the same speed as in the first scan. Performance in the fourth session was at maximum speed, resulting in significantly lower MTs for trained compared to untrained sequences (**Figure 3.2d**). To assess different neural signatures of observed behavioural learning, we first examined how the overall evoked activation changed over weeks of training for the same speed of movement.

3.3.2 Overall activation does not change in M1

First, we re-investigated the classical finding that activity, measured as the percent BOLD signal change relative to rest, increased in M1 for matched performance after long-term training (Karni et al., 1995; **Figure 3.1a**). Our task elicited activation in a range of cortical areas (**Figure 3.4a** for session 1 – i.e., prior to learning). A region of interest (ROI) analysis of the hand area of M1, contralateral to the performing hand, however, showed no significant change across weeks ($F_{(2,50)}$=0.44, p=.85). There was a significant main effect of sequence type ($F_{(1,25)}$=6.32, p=.019), but none of the post-hoc t-tests revealed a significant difference. Additionally, the interaction between the two factors was also not significant ($F_{(2,50)}$=0.17, p=.84).

The absence of overall activity changes, however, should not be taken as evidence for an absence of plasticity in the region. It is possible that some subregions of M1 increased in activation for learned sequences, while other decreased, as suggested by Steele and Penhune (2010). Such mixed changes would result in a shift of the overall pattern, which would lead to an increase in the angle between the mean activity pattern for trained and untrained sequences (**Figure 3.1c**). Because we calculated the angle between activity patterns for each participant separately, this criterion does not assume that the observed shift is spatially consistent across individuals – any idiosyncratic shift could be detected. Therefore it serves as a sensitive statistical criterion to detect shifts in spatial location of activation, which were previously reported only descriptively (Steele and Penhune, 2010).

However, in M1, the averaged cosine angle (**Figure 3.4c**) remained unchanged across the weeks ($F_{(2,50)}$=1.71, p=.19), indicating that the average activity pattern remained comparable across trained and untrained sequences. In sum, we found no evidence for activation increases (Karni et al., 1995), decreases, or relative shifts in activation patterns (Steele and Penhune, 2010) in M1.

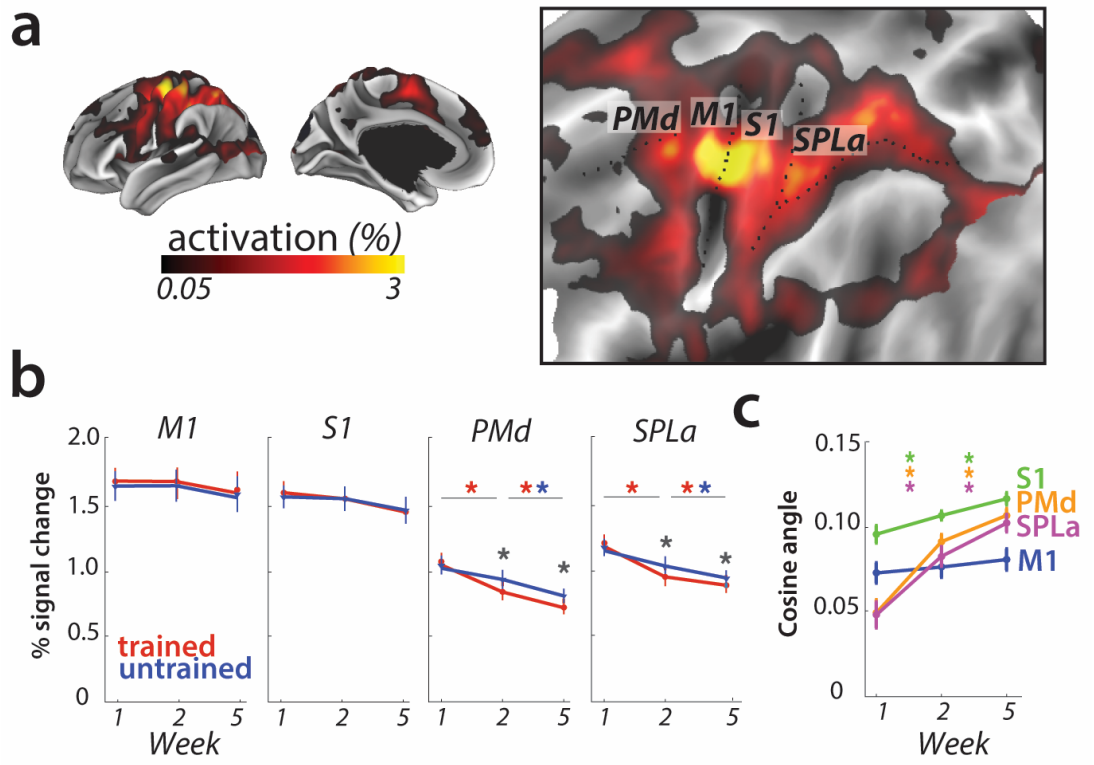

Figure 3.4. Overall activation and changes with learning in defined regions of interest. **a)** Average activation during production of any sequence in scanning session 1 (prior to learning) in the left hemisphere, i.e. contralateral to the performing hand. Activation was contrasted against resting baseline. On the right, activation map is presented on a flattened surface, corresponding to surface maps in other figures. **b)** Changes in activation across predefined areas – primary motor cortex (M1), primary somatosensory cortex (S1), dorsal premotor cortex (PMd) and superior parietal lobule – anterior (SPLa). No significant changes in activation were observed in M1 or S1 across weeks or between trained and untrained sequences (* indicates $p<.01$). Error bars indicate standard error of the group mean. See **Figure 3.5** for results with error trials excluded. **c)** The cosine angle dissimilarity between average trained and untrained sequence across scanning weeks. The cosine angle increased significantly across weeks in PMd, SPLa and S1, but not M1 (* indicates $p<.05$). Error bars indicate standard error of the group mean.

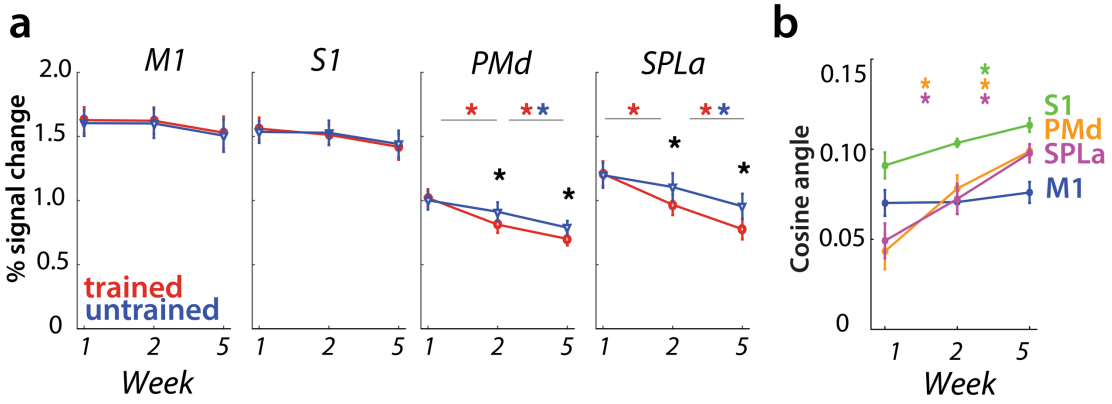

Figure 3.5. Changes in activation and mean pattern dissimilarity across predefined areas, estimated only on correct trials.

a) Changes in activation across predefined areas – primary motor cortex (M1), primary somatosensory cortex (S1), dorsal premotor cortex (PMd) and superior parietal lobule – anterior (SPLa). As in the analysis with all trials included, no significant changes in activation were observed in M1 or S1 across weeks or between trained and untrained sequences (* indicates $p<.01$). Error bars indicate standard error of the group mean. **b)** The cosine angle dissimilarity between average trained and untrained sequence across scanning weeks. The cosine angle increased significantly across weeks in PMd, and SPLa, but not M1. In S1, average dissimilarity estimated on correct trials only increased significantly across weeks 2-5, but not 1-2 (* indicates $p<.05$). Error bars indicate standard error of the group mean.

3.3.3 Learning-related activation changes in premotor and parietal areas

To investigate activation changes in areas outside of M1, we calculated changes in activity between the weeks in a map-wise approach (**Figure 3.6a**). Over the three measurement time points, we found no reliable activation increases in any cortical area that was activated by the task in week 1. Instead, we observed widespread learning-related reductions in activity in premotor and parietal areas (**Figure 3.6a**), in line with our pre-registered prediction. These activation reductions were observed across both subsequent sessions (i.e. weeks 1-2, weeks 2-5) for trained and untrained sequences, with bigger reductions for trained sequences. In weeks 2 and 5, trained sequences elicited overall lower activity than untrained sequences (**Figure 3.6b**; see **Figure 3.7** for statistical maps). These learning-related reductions in activity were also statistically significant in our predefined ROIs in premotor (dorsal premotor cortex – PMd) and parietal cortices (anterior superior parietal lobule – SPLa) (**Figure 3.4b**): In a 3 (week) x 2 (sequence type) ANOVA on observed activation both main effects and interaction were highly significant in PMd (week: $F_{(2,50)}$=17.47, p=1.77e^{-6}; sequence type: $F_{(1,25)}$=11.86, p=2.03e^{-3}; interaction: $F_{(2,50)}$=13.22, p=2.46e^{-5}) as well as in SPLa (week: $F_{(2,50)}$=19.14, p=6.73e-7; sequence type: $F_{(1,25)}$=19.36, p=1.77e^{-4}; interaction: $F_{(2,50)}$=21.59, p=1.74e^{-7}). In contrast, no main effect of week was observed in S1 ($F_{(2,50)}$=1.82, p=.17). Neither was there a significant effect of sequence type ($F_{(1,25)}$=0.19, p=.66), or interaction between the two factors ($F_{(2,50)}$=2.01, p=0.14). This pattern of results on changes in overall activation remained unchanged after excluding error trials from the analyses (see **Figure 3.5a**). Thus, we observed widespread activation decreases with learning across secondary and association cortical areas.

In a few smaller areas, activation increased with learning (red patches in **Figure 3.6a-b**). This was observed uniformly in areas with activity at or below baseline – thus these changes reflect decreased suppression of activity rather than increases. It is likely that these activity increases are not task relevant, but instead reflect the increasing automaticity and lower need for central attentional resources with learning (see section 3.4 Discussion).

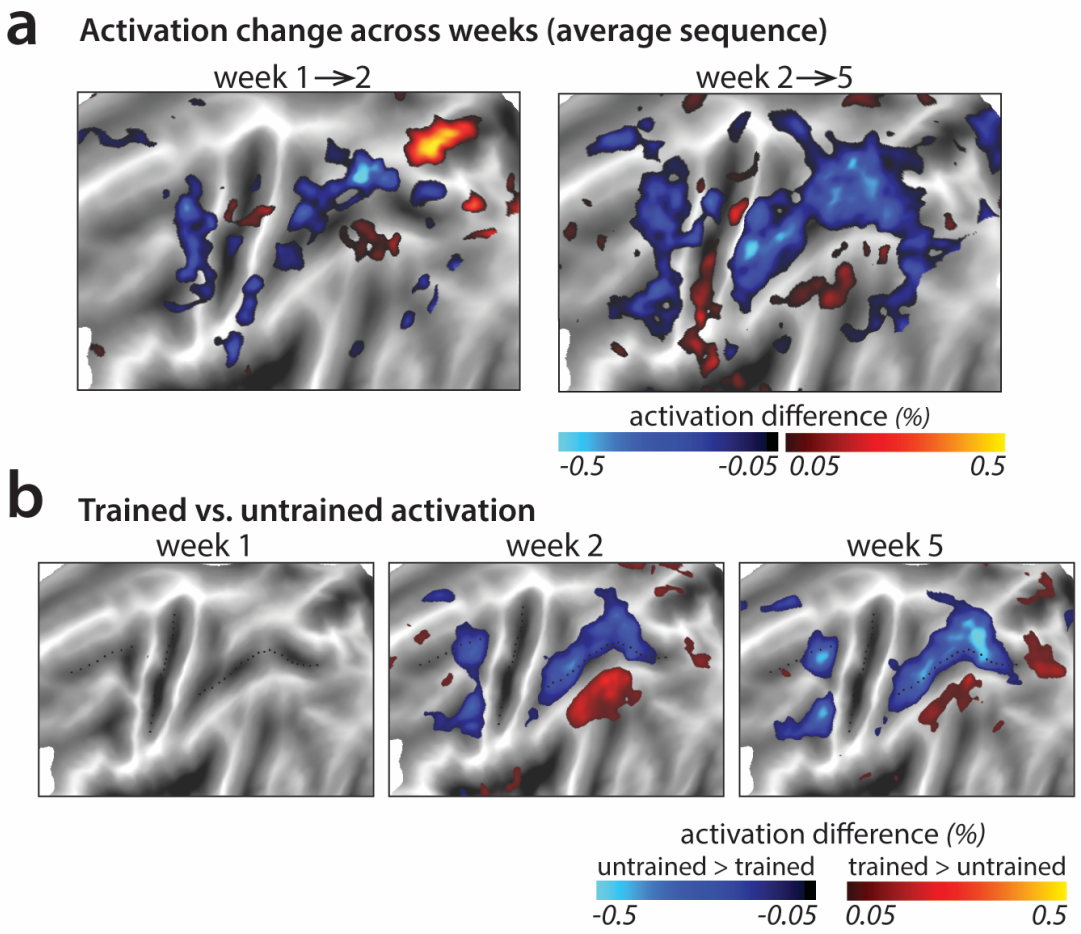

Figure 3.6. Changes in average activation across the cortical surface.

a) Average change in activation across subsequent sessions. Activation was measured as the difference in percent signal change relative to the resting baseline. Activation decreased (blue shades) in motor-related regions across sessions during sequence execution. **b)** Contrast of activation for trained vs. untrained sequences per scanning session. In weeks 2 and 5, trained sequences elicited lower activation in motor-related regions than untrained sequences (blue shades; see **Figure 3.7** for *t*-maps and statistical quantification of activation clusters). Areas with observed increases in activation for trained sequences (red shades) lie in the default mode network that showed on average lower activity during task than rest.

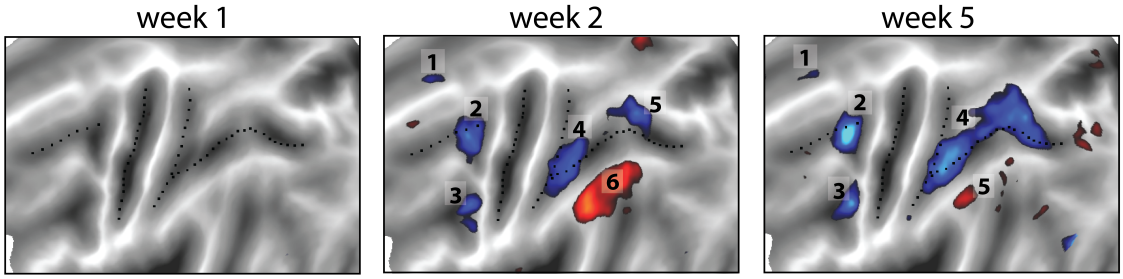

#	peak t_{25}	p_{t_unc}	p_{t_corr}	cm^2	$p_{cluster}$
1	2.85	.010	.34	0.5	.073
2	4.28	3.13e^{-4}	.003	3.4	.003
3	4.03	5.88e^{-4}	.010	2.3	.008
4	3.95	7.16e^{-4}	.012	3.9	<.001
5	4.13	4.59e^{-4}	.006	2.5	.003
6	4.23	3.50e^{-4}	.004	7.1	<.001

#	peak t_{25}	p_{t_unc}	p_{t_corr}	cm^2	$p_{cluster}$
1	2.85	.0122	.34	0.3	.072
2	5.61	1.00e^{-5}	0	3.1	<.001
3	4.49	1.83e^{-4}	.004	2.4	<.001
4	4.50	1.77e^{-4}	.003	12.7	<.001
5	3.39	.0029	.059	0.8	.032

Figure 3.7. Statistical maps for the trained vs. untrained contrasts on elicited activation in each session.

Trained>untrained is shown in red, untrained>trained in blue. Maps were thresholded at a $t_{(25)}$=±2.5, p<.01 uncorrected for a two-tailed t-test. Tables show peak t-value and size (in cm^2) for each super-threshold cluster (indicated by numbers) for maps of week 2 and 5. p_{t_unc} is the uncorrected p-value for the peak of each cluster. Family-wise error corrected p-values were determined using permutation testing for the peak t-value (p_{t_corr}) and cluster size ($p_{cluster}$).

We also examined whether there were, in addition to the overall activity decreases, shifts in the average activity patterns in the predefined regions of interest (**Figure 3.1c**). As for M1, we calculated the cosine angle dissimilarity (see section 3.2.8 Changes in overall activation) between the average activity patterns for trained and untrained sequences, separately for each scanning session. Figure **3.8a** shows cosine angle dissimilarities between trained and untrained sequences in PMd, displayed using multidimensional scaling (MDS). Patterns for trained sequences moved away from the starting point over weeks, and became more different from untrained patterns. Both in parietal and premotor areas there was clear evidence for a shift – cosine angular dissimilarity between the average trained and untrained sequence activation increased significantly across weeks (PMd: $F_{(2,50)}$=23.63, p=5.98e^{-8}; SPLa: $F_{(2,50)}$=23.19, p=7.49e^{-8}) (**Figure 3.4c**). S1 also showed a significant increase in cosine dissimilarity between trained and untrained patterns with learning ($F_{(2,50)}$=8.68, p=5.79e^{-4}). These changes, however, were much less pronounced than those observed in premotor and parietal areas. This observed increase in dissimilarity between average trained and untrained pattern in PMd and SPLa, and to a lesser extent in S1, was also observed when analyzing only trials with correct performance (see **Figure 3.5b**).

To investigate whether the observed changes in the overall activity patterns in premotor and parietal areas were spatially consistent across individuals, we normalized (z-scored) activation maps in each region and assessed the relative contribution of subregions to overall activation in weeks 1 and 5 (**Figure 3.8b**). Comparing the pattern of activation revealed that before training (week 1, blue) sequences elicit relatively more activation in rostral parts of the premotor and supplementary motor areas, and that activity was more caudal after training (week 5, red; **Figure 3.8c** displays the cross-section of relative activation changes). Some differences were also observed in the posterior parietal cortex, with activation shifting from more posterior to anterior subregions after learning (**Figure 3.8c**). Altogether, these results show that with learning, the execution of sequences relies on slightly different subareas within premotor and parietal regions.

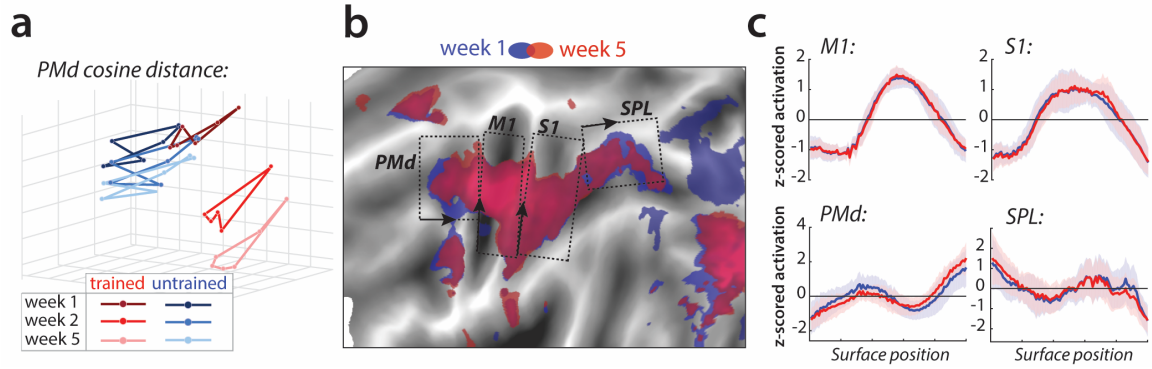

Figure 3.8. Relative change in evoked activation.

a) Multidimensional scaling plot of cosine angle dissimilarities for trained and untrained sequences in dorsal premotor cortex (PMd) across weeks 1-5. Each dot represents a single sequence, and dots are connected for each session and sequence type separately. Trained sequences on average become more distant from untrained sequences with learning. Untrained sequences on average also progress across weeks, but less than trained sequences. **b)** Normalized activation plots for trained sequences in week 1 (blue) and 5 (red). The arrows and brackets indicate the direction and range of activation cross-sections presented in c). Areas: dorsal premotor cortex (PMd), primary motor cortex (M1), primary somatosensory cortex (S1), superior parietal lobule (SPL). **c)** Cross-section of elicited activation for trained sequences in defined areas, in weeks 1 (blue) and 5 (red). Shaded error bars indicate standard error of the group mean.

3.3.4 Sequence-specific activity patterns reorganize early in learning

Our analyses so far have been concerned with changes in the overall pattern of trained vs. untrained sequences, and showed widespread reductions in activation and some more subtle changes in relative location. The sequence-specific performance advantage, however, indicates that the brain must represent specific sequences – i.e. there should be activity patterns that are unique to each individual sequence. Sequence-specific learning should then be reflected in changes of these sequence-specific activity patterns with learning (**Figure 3.1d**). Consistent with previous results (Wiestler and Diedrichsen, 2013; Yokoi and Diedrichsen, 2019), we detected sequence-specific activity patterns, i.e. activity patterns that differentiate between the tested motor sequences, in various cortical regions, even in session 1 (**Figure 3.9a**). This allowed us to assess their reorganization across sessions.

Our pre-registered hypothesis (https://osf.io/etnqc) was that earlier in learning sequence-specific activity patterns would change more for trained than untrained sequences, and would stabilize later in learning. In contrast to the other ideas tested in this paper, this was a novel hypothesis and not based on previous reports. Specifically, we predicted that the correlation of each sequence-specific pattern between weeks 1 and 2 should be lower for trained as compared to untrained sequences. The problem with performing a simple correlation analysis on the patterns, however, is that the estimated correlation will be biased by noise – i.e., more within-session variability for one set of sequences will result in a lower correlation (Diedrichsen et al., 2017). To address this problem, we used the pattern component modelling (PCM) framework which explicitly models and estimates the signal and noise for each session. Using this approach, we estimated the likelihood of participants' data under a series of models, each assuming a true correlation in the range between *0* (uncorrelated patterns) and *1* (perfect positive correlation; see section 3.2.10 Pattern component modelling for details). Figure **3.9b** shows the log-likelihood for each specific correlation model relative to the mean across all models. In SPLa, the most likely correlation of the activity patterns for the trained sequences between weeks 1 and 2 was r =0.37. For week 2-5, the likelihood peaked at r =0.6. In contrast, the likelihood functions for untrained sequences indicated that the most

likely model was between r =0.6-0.7 for both week transition 1-2 and 2-5. The advantage of this analysis is that we can be sure that the observed low correlation across weeks 1-2 for trained sequence was not due to increased noise. In fact, if the noise in one or both sessions was too high, then the model would be unable to distinguish between any of the correlation models – i.e. the likelihood curve would be a flat line.

To statistically assess the difference in correlations across trained and untrained sequences, we compared the likelihood of the data of trained sequences between two models: the best-fitting model for the trained sequences (r =0.37 in SPLa) and the correlation model best fitting the data of untrained sequences (r =0.6) (black dots and projections onto y-axis in **Figure 3.9b**). To avoid double-dipping, the 'best-fitting' model was chosen on 25 participants (n-1) and the likelihood assessed on the left-out subject (see section 3.2.10 Pattern component modelling). The difference in model evidence was significant for correlation between weeks 1-2 in SPLa ($t_{(25)}$=2.88, p=4.0e^{-3}). In contrast, no difference in correlation was observed later in learning, between weeks 2 and 5 ($t_{(25)}$=1.21, p=0.24). A similar pattern of results was observed in PMd**,** with correlation of trained sequences significantly lower than that of untrained sequences between weeks 1 and 2 ($t_{(25)}$=2.93, p=3.6e^{-3}), but not between weeks 2 and 5 ($t_{(25)}$=0.88, p=.39). No such change in correlation across weeks 1-2 was observed in M1 ($t_{(25)}$=0.43, p=.34). In S1, the effect was just significant ($t_{(25)}$=1.72, p=0.049). To ensure that the observed lower correlation for trained patterns was not due to larger difference in error rate between weeks 1 and 2 for trained than for untrained sequences, we repeated the analysis excluding error trials. The pattern of results remained unchanged in PMd and SPLa (**Figure 3.10a**), with lower correlation for trained than untrained patterns across weeks 1-2. In S1, after accounting for error trials, the correlation across weeks 1-2 did no longer differ between trained and untrained patterns. Overall, we found significant evidence that sequence-specific trained patterns in SPLa and PMd reorganize more in weeks 1-2 as compared to the untrained sequences, and stabilize later on with learning, in line with our new pre-registered prediction.

Figure 3.9. Sequence-specific activity patterns reorganize across sessions.

a) Cortical surface map of crossnobis dissimilarities between activity patterns for different sequences in session 1. These regions encode which sequence is executed by the participant. **b)** Evidence of models of correlation values between r =0 and r =1 for sequence-specific patterns across weeks 1-2 (solid) and 2-5 (dashed), separately for trained (red) and untrained (blue) sequences. Evidence was assessed with a type-II log-likelihood, relative to the average log-likelihood across models. Shaded areas indicate standard error of the group mean. Difference between log-likelihoods can be interpreted as log-Bayes factor, with a difference of 1 indicating positive evidence. Vertical lines indicate the winning correlation model for trained (red) and untrained (blue) patterns across weeks 1-2. Black dots are projections of the two winning models onto the correlation function of trained sequences across weeks 1-2. The horizontal lines from the two black dots indicate the likelihood of the trained data under the two models, which was tested in a crossvalidated t-test. See **Figure 3.10a** for the same analysis with error trials excluded. **c)** Map displaying the correlation of the winning model for trained and untrained sequences across weeks 1-2 and 2-5. The correlation of the winning correlation model is shown in all tessels where the difference between evidence for winning model vs. worst-fitting model exceeds log-Bayes factor of 1 (averaged across participants). See **Figure 3.10b** for the difference in best model correlation between trained and untrained sequences, and an indication of tessels where the difference is significant, as based on the crossvalidated t-test. **d)** Crossnobis dissimilarities between trained and untrained sequence pairs across weeks. No significant effect of week, sequence type or their interaction was observed in any of the regions. Error bars indicate standard error of the group mean.

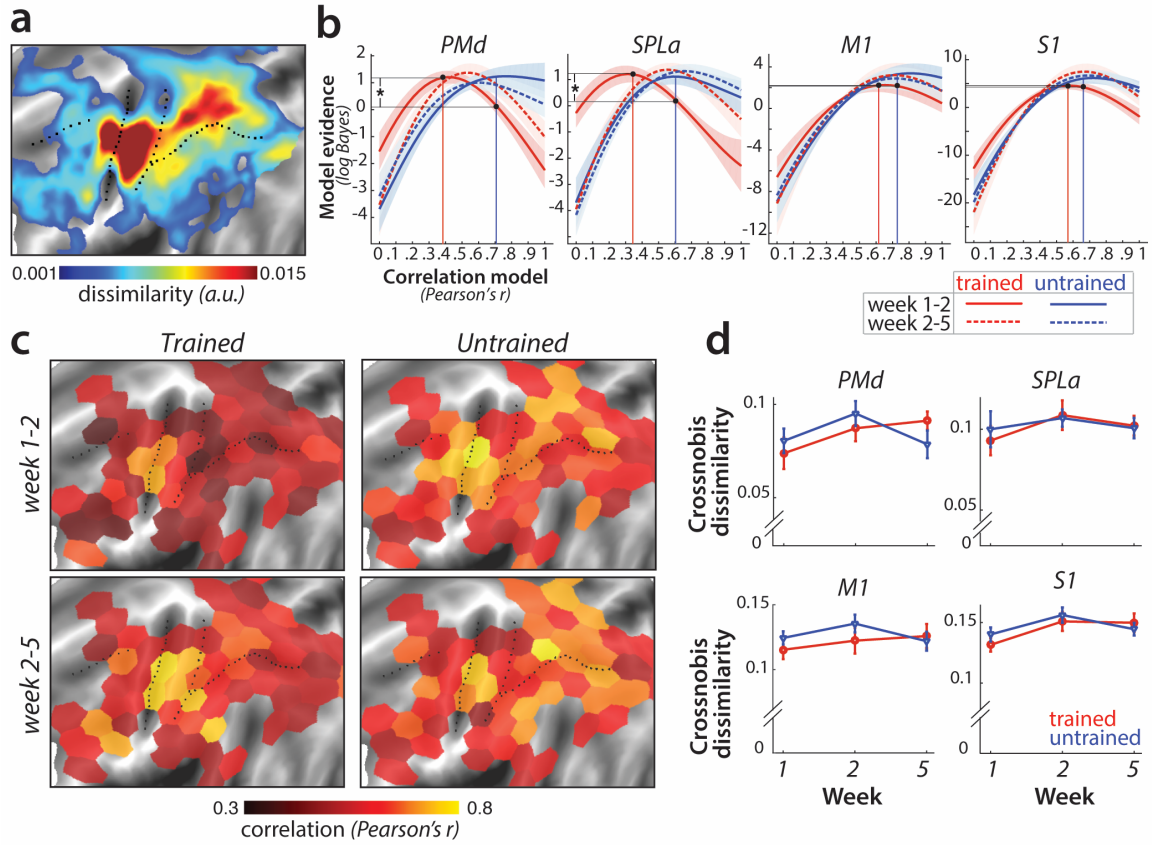
a
0.001
0.015
dissimilarity (a.u.)
b
PMd
SPLa
M1
S1
Model evidence (log Bayes)
Correlation model
(Pearson's r)
trained untrained
week 1-2
week 2-5
c
Trained
Untrained
week 1-2
week 2-5
0.3
0.8
correlation (Pearson's r)
d
PMd
SPLa
M1
S1
Crossnobis dissimilarity
trained
untrained
Week

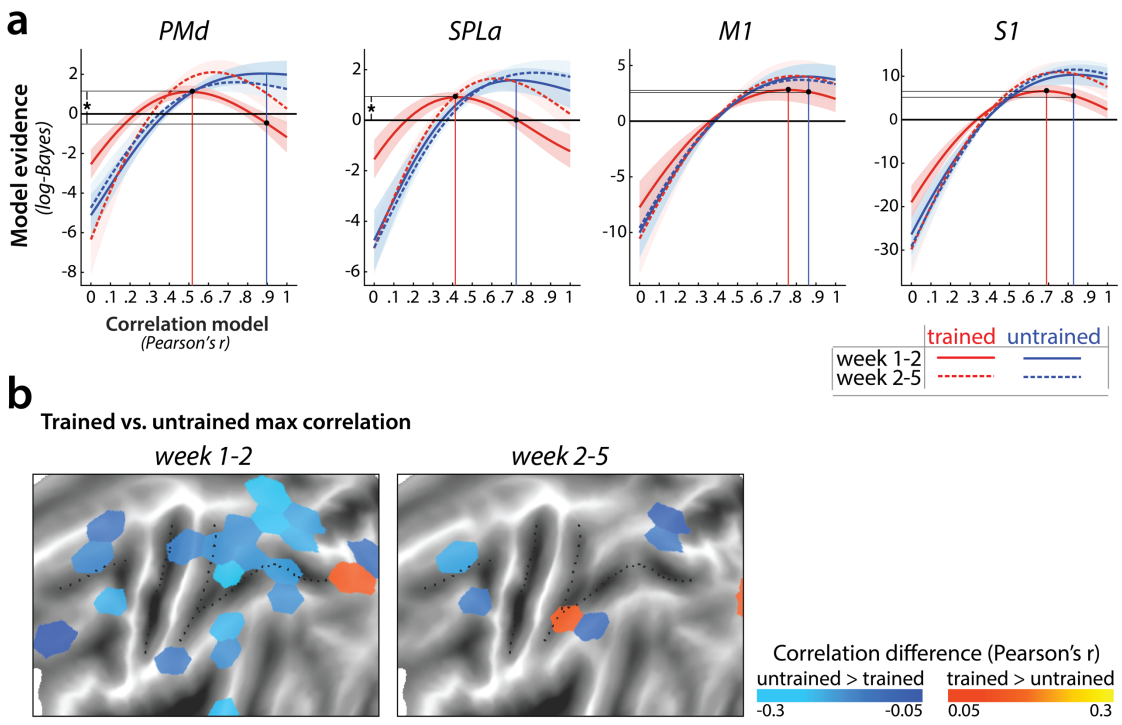

Figure 3.10. Pattern correlation analyses across sessions, estimated only on correct trials.

a) Evidence for models of correlation values between r =0 and r =1 for sequence-specific patterns across weeks 1-2 (solid) and 2-5 (dashed), estimated only on trials with correct performance. Correlations of trained patterns are in red, untrained in blue. Evidence was assessed with a type-II log-likelihood, relative to the average log-likelihood across models. Shaded areas indicate standard error of the group mean. Vertical lines indicate the winning correlation model for trained (red) and untrained (blue) patterns across weeks 1-2. Black dots mark the log-likelihood of the trained sequence across weeks 1-2 under the winning models. Horizontal lines from the two black dots indicate the difference in likelihood of the trained data under the two models, tested in a crossvalidated t-test (* indicates p<0.05 for one-tailed t-statistics). **b)** Difference between correlation of the winner models for trained and untrained sequences, as presented in **Figure 3.9c**. Blue indicates a lower correlation across weeks for trained than untrained patterns of activity. The correlation difference values are plotted in tessels where the difference in model evidence was significant, as based on the cross-validated t-test (for two-tailed p<.05).

To determine more generally where in the neocortex sequence-specific plasticity could be detected, we fit PCM correlation models to regularly tessellated regions spanning the cortical surface. Figure **3.9c** displays the correlation with the highest evidence for activity patterns across weeks 1-2 and 2-5; separately for trained and untrained sequences. In general, the highest correlations were found in core sensory-motor areas. Across weeks 1-2 for trained sequences, correlations were significantly lower in a number of dorsal premotor, inferior frontal, and parietal regions (**Figure 3.9c**). Across the cortex, correlation for trained patterns increased for weeks 2-5, resulting in similar values which did not differ significantly between trained and untrained sequences for most tessels (see **Figure 3.10b**). Together, these results confirmed that sequence-specific activation patterns in secondary association areas show less stability early in learning, but stabilize later on.

Can we obtain further insight into *how* the sequence-specific patterns change in these areas? One specific preregistered prediction was that there would be an increase in distinctiveness (dissimilarity) between fMRI patterns underlying each trained sequence (Wiestler & Diedrichsen, 2013; **Figure 3.1e**). To test this hypothesis, we calculated crossnobis dissimilarities (Walther et al., 2016) between sequence-specific activations, separately for trained and untrained sequences. In contrast to our prediction, no significant change in dissimilarity across weeks was observed in any of the predefined regions (**Figure 3.9d**). This suggests that the reorganization observed for trained sequences early in learning did not increase the average distinctiveness of the sequence-specific patterns.

3.3.5 Trained sequences elicit distinct patterns during full speed performance

In the last part of the experiment, we asked whether some of the negative findings (e.g. no changes in M1, no increase in dissimilarities for trained sequences) might have been due to the fact that participants were paced at a relatively slow speed. Matching the speed across sessions allows for the comparisons of changes in neural activity for exactly the same behavioural output (Karni et al., 1995; Lehéricy et al., 2005). However, it could be that controlling for speed impairs our ability to study brain representations of motor skill;

simply because after learning, the system is not challenged enough to activate the neuronal representations supporting skilled performance. Consequently, several studies have not (Bassett et al., 2010; Wymbs & Grafton, 2015), or not strictly (Wiestler and Diedrichsen, 2013), matched performance across sessions or levels of training. To examine the effect of performance speed, we added a fourth scanning session *(fs)*, just a day after from the third session in week 5, in which participants were instructed to perform the sequence as fast as possible.

Performance during the 4th scan was 1010 ms faster than in the first session ($t_{(25)}$=15.7, p=1.82e^{-14}) and also 338 ms ($t_{(25)}$=9.92, p=4.58e^{-10}) faster for trained than for untrained sequences. Averaged over trained and untrained sequences, we found that the faster performance in this session led to an increase in activity across premotor and parietal areas (**Figure 3.11a, b**). Although trained sequences were executed faster than untrained sequences, activation was still lower for trained compared to untrained sequences, similar to what we observed for paced performance (**Figure 3.11c;** see **Figure 3.12a** for statistical maps). In M1 and S1, we found no difference in activation between trained and untrained sequences (**Figure 3.11a**; M1: $t_{(25)}$=1.78, p=.09; S1: $t_{(25)}$=1.69, p=.10). Overall, the pattern of results for evoked activation did not change qualitatively when participants performed at full speed.

Next, we examined whether the brain representations of individual sequences are similarly engaged at slow and fast speeds. The correlation between sequence-specific patterns was relatively high (r =0.62) across our regions of interest. We found no differences between the different regions ($F_{(3,75)}$=1.47, p=.23), or sequence types (trained vs. untrained: $F_{(1,25)}$=0.25, p=.62). Thus, the sequence-specific representations activated during performance at high skill level (full speed) are at least partly activated even when performance slowed down.

Figure 3.11. Speed-related changes in activation and dissimilarities.

a) Overall activation in week 5 in paced and full speed sessions for trained (red) and untrained (blue) sequences. Activation was measured as percent signal change over resting baseline (* indicates $p<.05$). Error bars indicate standard error of the group mean. **b)** Increase in activation for full speed compared to paced speed in percent signal change, averaged across trained and untrained sequences. Red colors indicate an increase in activity during full speed performance compared to paced performance. Blue colors indicate higher activation during paced compared to full speed performance. **c)** Difference in activation elicited for trained relative to untrained sequences, during the paced and full speed sessions (see **Figure 3.12a** for statistical maps). Trained>untrained is shown in red, untrained>trained in blue. **d)** Average crossnobis dissimilarity between sequence-specific patterns in paced and full speed sessions for trained and untrained sequences. Dissimilarities are significantly larger for trained (red), as compared to untrained (blue) patterns, in PMd for full-speed session (* indicates $p<.05$). Error bars indicate standard error of the group mean. **e)** Difference between crossnobis dissimilarities across full speed and paced sessions, averaged across trained and untrained sequences. Higher dissimilarities for full speed than paced session are shown in red, whereas blue / green hues indicate higher dissimilarities during paced than full speed session. **f)** Difference in dissimilarities for trained relative to untrained sequences, during the paced and full speed sessions. Trained>untrained is shown in red, untrained>trained in blue / green. Trained sequences elicited higher dissimilarities than untrained in full speed, but not paced session (see **Figure 3.12b** for statistical *t*-maps).

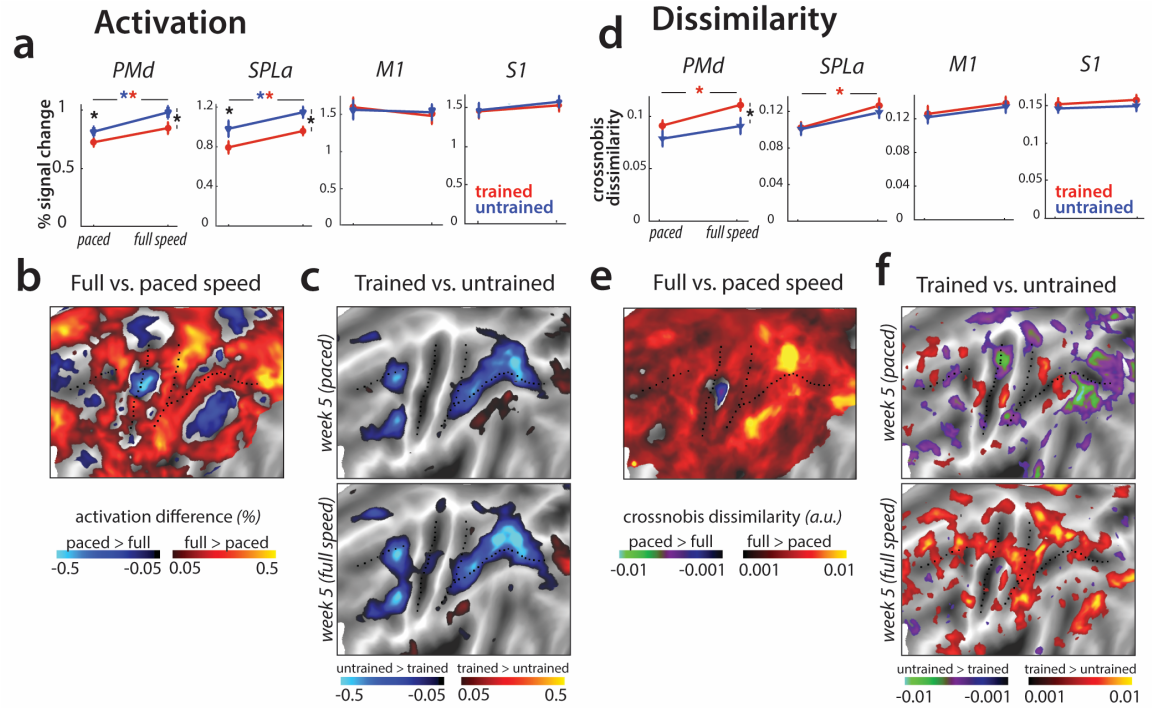
a
Activation
PMd
SPLa
M1
S1
% signal change
paced
full speed
trained
untrained
d
Dissimilarity
crossnobis dissimilarity
b
Full vs. paced speed
activation difference (%)
paced > full
full > paced
-0.5
-0.05
0.05
0.5
c
Trained vs. untrained
week 5 (paced)
week 5 (full speed)
untrained > trained
trained > untrained
e
Full vs. paced speed
crossnobis dissimilarity (a.u.)
-0.01
-0.001
0.001
0.01
f
Trained vs. untrained

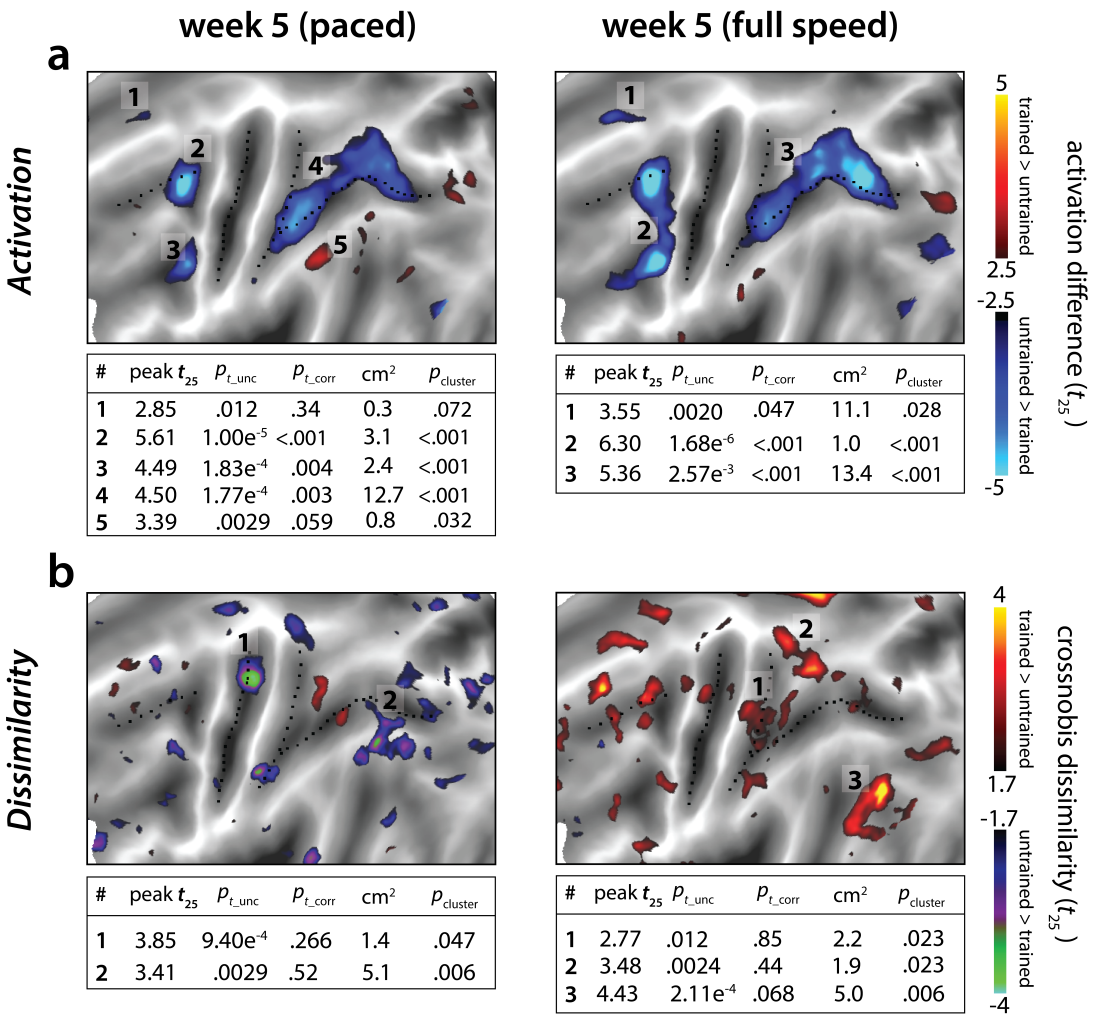

Figure 3.12. Statistical maps for trained vs. untrained contrasts in week 5 (paced) and 5* (full speed) sessions.

Trained>untrained contrast is shown in red, untrained>trained in blue. **a)** Statistical contrast for average activation. Maps were thresholded at a $t_{(25)}$=± 2.5, p<.01 uncorrected for a two-tailed t-test. Tables show peak t-value and size (in cm^2) for each super-threshold cluster. p_{t_unc} is the uncorrected p-value for the peak of each cluster. Family-wise error corrected p-values were determined using permutation testing for the peak t-value (p_{t_corr}) and cluster size ($p_{cluster}$). **b)** Statistical contrast for average dissimilarity of sequence-specific activity pattern. Map was thresholded at $t_{(25)}$=± 1.7, p<.05, uncorrected. Statistical quantification using permutation tests is in the table below each map.

Having established that the mean activation results are replicated across paced and full-speed performance, and that similar sequence-specific representations are activated in both cases, we tested whether activation patterns for different trained sequences are more distinct during full speed performance, as reported in Wiestler & Diedrichsen (2013). Overall, crossnobis dissimilarities increased at full speed for trained sequences in PMd and SPLa (**Figure 3.11e**). No such changes were found in M1 or S1. Moreover, trained sequences showed larger dissimilarities than untrained at full-speed performance across premotor and parietal cortices (**Figure 3.11f**), which was not the case for the last paced session. In our predefined ROIs, this difference was significant for PMd (**Figure 3.11d**), but also parietal areas showed significantly higher dissimilarities between trained sequences at full speed (**Figure 3.12b**). This suggests that while activity patterns at full speed are correlated to those during paced performance, they are more distinguishable for trained sequences.

Could this effect be driven by behavioural performance, with trained sequences performed more differently at full speed (i.e. different speeds across trained sequences), while untrained sequences were performed at a more equal speed? To test for this, we calculated crossnobis dissimilarities between movement times associated with different trained and untrained sequences. The dissimilarities based on speed of performance did not differ significantly across trained and untrained sequences ($t_{(25)}$=0.57, p=.57). Therefore, increased dissimilarity of trained compared to untrained patterns in premotor and parietal areas could not be explained by a difference in execution speed. Instead, this effect likely reflects changes in activity patterns underlying full speed skilled performance.

3.3.6 Striatal activity patterns for trained sequences manifest at full speed performance

We observed learning-related changes in cortical association areas, but not in the primary motor cortex. Of course, learning could also be driven by neuronal changes in subcortical brain regions (Ashby et al., 2010; Graybiel, 2016; Graybiel and Grafton, 2015; Hikosaka et al., 1999; Yin et al., 2009). The striatum in particular has been proposed as a structure

where motor skills are stored (Kawai et al., 2015; Lehéricy et al., 2006). Inspecting changes in overall activity across sessions, we observed no difference in activity between trained and untrained sequences in either putamen or caudate nucleus (**Figure 3.13a**).

Previous experiments have reported that with learning, activation moves from more 'cognitive' areas of the striatum (i.e. caudate nucleus) to more 'motor' areas (i.e. putamen) (Coynel et al., 2010; Lehéricy et al., 2005; Reithler, van Mier, & Goebel, 2010). Our data fail to replicate this result: both the visual inspection (**Figure 3.13b**), and statistical quantification of the mean pattern difference for trained and untrained sequences across sessions revealed no such learning-specific shift of mean striatal activation pattern with learning.

Lastly, we examined if the striatum represents individual sequences. During the paced sessions, activity patterns for different sequences were not distinguishable in either caudate nucleus or putamen (**Figure 3.13c**). However, during full speed performance trained sequences elicited distinct activity patterns in both regions (i.e. crossnobis dissimilarity>0: caudate nucleus: $t_{(25)}$=2.27, p=0.032; putamen: $t_{(25)}$=2.44, p=.022; **Figure 3.13c**). This effect was specific to the trained sequences, with untrained sequences still exhibiting undistinguishable patterns of activity at full speed. Thus, we found some evidence that trained motor sequences are represented in the form of distinct activity patterns in the striatum during full speed skilled performance.

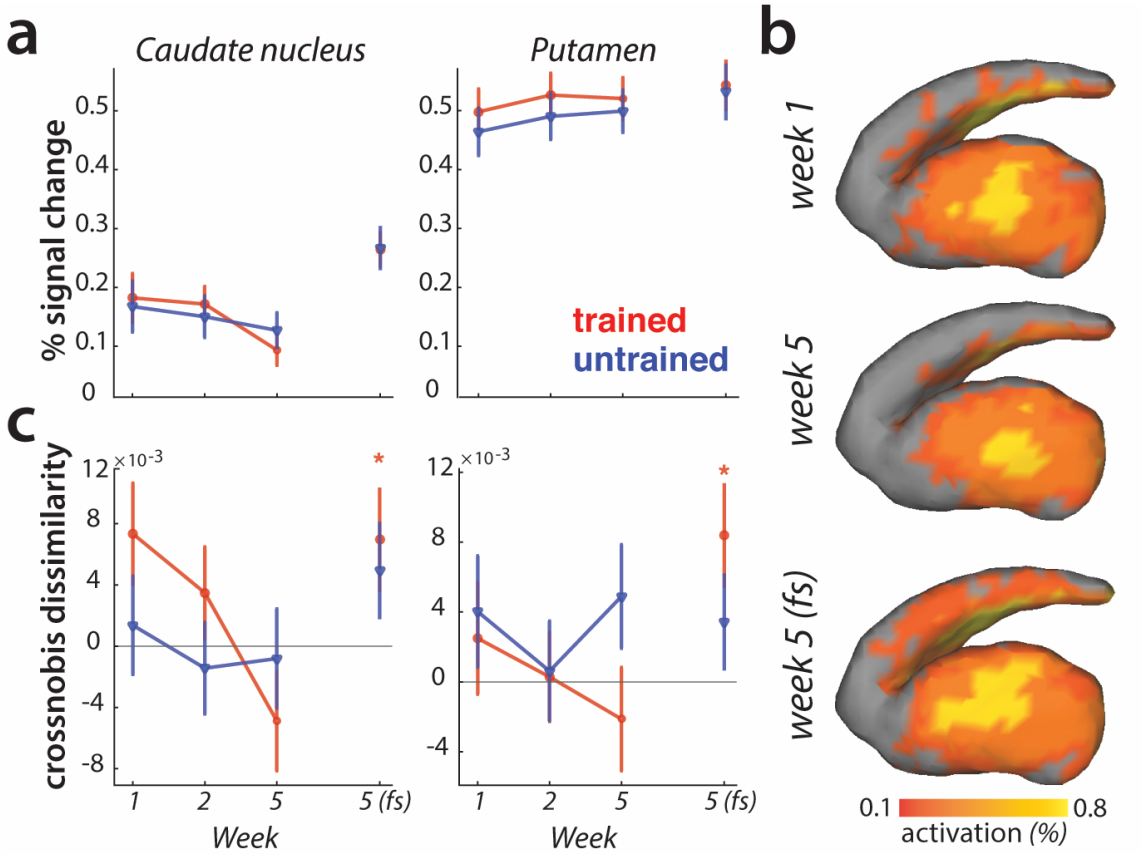

Figure 3.13. Striatal changes in activation and dissimilarities with learning.

a) Overall activation (percent signal change over resting baseline) for trained (red) and untrained (blue) sequences. Activation did not differ across sessions, or sequence types in the striatum. Error bars indicate the standard error of the group mean. **b)** Activation during performance of trained sequences in the striatum across weeks 1, 5 (paced speed) and 5 (full speed – *fs*), averaged across sequences and participants. **c)** Crossnobis dissimilarities between activation patterns of sequence pairs, calculated separately for trained and untrained patterns. Dissimilarities were not significantly different for trained or untrained sequences during paced performance. At full speed, sequence-specific activity patterns amongst trained sequences differed significantly in both caudate nucleus and putamen (* indicates $p<.05$). Error bars indicate the standard error of the group mean.

To examine whether the speed purely pulls the signal out of the noise better, or qualitatively changes the representation, we, similarly to the analyses in the cortical regions, performed the PCM correlation model across the paced and full speed sessions in week 5. The correlation between sequence-specific patterns in both regions was higher than 0 (putamen: $t_{(25)}$=9.56, p=8.0e^{-10}; caudate: $t_{(25)}$=6.37, p=1.1e^{-6}), but lower than 1 (putamen: $t_{(25)}$=8.85, p=3.6e^{-9}; caudate: $t_{(25)}$=5.86, p=4.1e^{-6}). Similarly as for the cortical regions, we found no differences between the caudate nucleus and putamen ($F_{(3,75)}$=0.19, p=.66), or sequence types (trained vs. untrained: $F_{(1,25)}$=0.05, p=.83). Thus, the sequence-specific representations activated during performance at high skill level (full speed) are at least partly activated even when performance slowed down. This suggests that moving faster engages similar representations as moving slower, but helps to increase the signal-to-noise ratio.

3.4 Discussion

Here we present a large longitudinal motor sequence learning study that allowed us to systematically investigate several previously proposed fMRI signatures of motor learning, including one new hypothesis concerning the change in multivariate activity patterns with learning. The existing literature, with its diversity of experimental protocols and analysis approaches, does currently not provide a consistent picture of learning-related changes. This inconsistency is exacerbated by the fact that most papers prioritize making new claims over re-examining previously established findings. Consequently, it is very hard to assess the replicability of most past findings. We address this issue here by a) producing a well-powered, longitudinal dataset that tackles some of the methodological inconsistencies (i.e. speed matching), b) pre-registering both design and hypotheses, and c) making data and analysis pipelines openly available, such that other hypotheses and analyses techniques can be freely tested.

Our findings reveal that parietal and premotor areas show widespread decreases in overall activation, as well as reorganization of sequence-specific patterns early in learning. Additionally, we observed that sequence specific patterns in these areas (as well as the

striatum) were more distinct during full speed performance. In contrast to this set of results, none of these learning-specific metrics were detected in M1, even after 5 weeks of training.

Our lack of any observable change in M1 activation contradicts some prior results, where increased activation in M1 was observed for matched performance after learning (Karni et al., 1995; Matsuzaka et al., 2007; Penhune and Doyon, 2002; Steele and Penhune, 2010; Vahdat et al., 2015), and does not align with reports of M1 stimulations influencing consolidation or storage of motor skills (in motor sequence tasks: Kang & Paik, 2011; Nitsche et al., 2003; Reis et al., 2009; Waters-Metenier, Husain, & Wiestler, 2014; in other motor tasks: Classen, Liepert, Wise, Hallett, & Cohen, 1998; Galea, Vazquez, Pasricha, Orban De Xivry, & Celnik, 2011; Hadipour-Niktarash, Lee, Desmond, & Shadmehr, 2007). We also found no support for a combination of increases and decreases of activation with training, which would lead to an overall change of the mean activity pattern (Steele and Penhune, 2010).

Instead, our results suggest that the pattern of neural activity in M1 does not change as participants become more skilled at producing motor sequences. This is consistent with a recent line of evidence demonstrating that M1 does not change activation with learning (Huang et al., 2013), and primarily encodes single movement elements, rather than sequences (Yokoi, Arbuckle, & Diedrichsen, 2018; Russo et al., 2019). Somewhat more surprisingly, we also observed no difference in overall M1 activation during full speed performance, when performance was considerably faster for trained sequences. This suggests that the activity increases related to faster movement speeds are compensated for by the shorter duration spent on the task.

Primary somatosensory cortex in many ways paralleled the results observed in M1. We observed no overall activation change, or change in the sequence-specific pattern correlation across sessions. The only exception was the observed shift in the mean activation pattern across sessions. One possible explanation is that feedback-related sensory activity in S1 undergoes some plastic changes with learning. This is consistent with a recent study demonstrating that S1, but not M1, is involved during consolidation of

motor skills (Kumar, Manning, & Ostry, 2019; for a review on somatosensory plasticity in motor learning see Ostry & Gribble, 2016).

In contrast to the limited evidence of learning-related changes in primary somatosensory and primary motor areas, higher order association areas (e.g. parietal and premotor cortices) displayed an array of learning-related changes. First, activation decreased in areas involved in sequence execution, with larger decreases for trained compared to untrained sequences. This result contrasts with other previous studies reporting increases in activation in premotor areas with learning (Grafton et al., 2002; Honda et al., 1998; Penhune and Doyon, 2002; Vahdat et al., 2015). Partially responsible for these inconsistencies may be a publication bias, favouring reports of signal increases over signal decreases with learning. For example, a recent metanalysis reanalyzed evidence for signal increases in the main text, while moving the (matched) evidence for signal decreases into the supplementary materials (Hardwick et al., 2013). Our data corroborates a number of recent studies reporting reduced activation in task-evoked premotor and parietal areas (Steele and Penhune, 2010; Wiestler and Diedrichsen, 2013; Wu et al., 2004).

The only activation increases for trained relative to untrained sequences were observed in areas that were suppressed below baseline during sequence execution. This has also been previously reported in a motor sequence learning study (Tamás Kincses et al., 2008), where deactivation was larger during performance of trained than random sequences. These areas include the precuneus, temporal parietal junction and the cingulate, regions commonly assigned to the default mode network (Raichle et al., 2001; Shulman et al., 1997). This group of regions is more activated during rest than during task performance, and has been associated with functions such as episodic memory retrieval and attention to internal states (Andrews-Hanna et al., 2010; Gusnard et al., 2001). Our observation of decreased inhibition of the default mode network likely reflects central attentional resources being freed up, allowing participants to engage in other mental processes (e.g., daydreaming) while performing the task. Thus, this release from initial deactivation is possibly task-irrelevant, reflecting increased automaticity with learning (Shamloo and Helie, 2016).

Overall, changes in average activation are relatively hard to interpret, as they could reflect a combination of numerous factors. As a more direct fMRI metric of plasticity, we suggest to inspect changes in the sequence-specific activity patterns, since these constitute a more likely fMRI correlate of the sequence-specific performance advantage observed after training. In this project, this provided us with two key insights of how activation patterns reorganize in association areas with learning. First, activity patterns associated with each of individual trained sequences, changed to a greater extent earlier in learning, and stabilized later. This finding resonates with several animal studies suggesting that the emergence of skilled behaviour is associated with early plasticity and later stabilization of neuronal activity patterns (Makino et al., 2017; Peters et al., 2017). Here we report a similar effect in humans, and advance these findings by demonstrating that this reorganization occurs at the level of sequence-specific patterns. In past studies using rodent models, sequence-specific patterns could not be dissociated from the overall activity pattern, as the animals were only trained on production of a single sequence. Additionally, by pacing participants' speed, we were able to cleanly dissociate changes in the organization of activity patterns from changes in the behavioural performance or variability. Second, activation patterns became more distinct for trained sequences at full speed. This indicates that the engagement of specific neuronal subpopulations for different sequences is particularly important when pushing the limit of performance.

While our study focused on the role of cortical areas in motor sequence learning, we also examined activation in the striatum, which has been suggested to play a critical role in skilled performance (Graybiel and Grafton, 2015; Kawai et al., 2015; Otchy et al., 2015). In contrast to previous fMRI studies (Coynel et al., 2010; Lehéricy et al., 2006; Reithler, van Mier, & Goebel, 2010), we did not find clear evidence for differences in overall activity, or shifts of the overall activity pattern with learning. Nonetheless, we observed distinguishable striatal activation patterns for different trained sequences at full speed, in line with a recent report showing distinguishable striatal patterns for performance of consolidated motor sequences (Pinsard et al., 2018). While by itself the finding of differential sequence-specific activity patterns is not evidence for a causal role of the striatum in the production of skilled behaviours, it is a necessary condition for such a functional role. Therefore, our results here are in line with the proposed involvement of the

striatum in motor sequence learning. Additionally, our results suggest that full speed performance might be particularly important for further studies of striatal multivariate activation to counteract the generally lower signal-to-noise ratio in this region.

An important feature of our design was that we collected imaging data in the trained state, both when performance was clamped to the initial speed, and when participants performed as fast as possible. Previous studies have usually included only one of these two options, making direct comparisons difficult (see Lutz et al., 2004 for an examination of various execution speeds on BOLD activity and Orban et al., 2010 in a motor learning context). Our results provide two important insights: first, in terms of the overall fMRI activation, the pattern of results remained the same for paced vs. full speed performance. This indicates that, in this specific case, the increased motor demands and the decreased time on task averaged out. In general, however, these two factors may not balance perfectly – therefore paced performance may be a better choice when comparing overall activation across sessions. Second, even though slow and paced performance in the trained state activated sequence-specific activation patterns, these were much stronger when performing at maximal speeds. Thus, for questions regarding the fine-grained patterns, it might be more suitable to challenge the system fully.

Of course, our list of inspected fMRI metrics of learning was not exhaustive. For instance, we did not investigate whether various fMRI correlates of learning predict behavioural outcomes, or how functional connectivity and network metrics change with learning, partly because of the absence of specific predictions. Pre-registration of hypotheses is especially important for these analyses, since the search space of possible tests becomes exponentially larger (e.g. correlating all possible brain metrics with all possible behavioural metrics; or using various metrics to assess inter-regional relationships). However, we hope that our dataset, upon its public release, can serve as a resource for other researchers to (re-)test novel predictions about learning related changes.

To conclude, the search for neural substrates of learning is a daunting task: the acquisition of longitudinal data sets is work intensive, and the large dimensionality of possible brain metrics makes the search difficult (Poldrack, 2000). Historically, the

question was simplified by studying activation increases in single areas as proxies for motor ‘engram’ localization (Berlot, Popp, & Diedrichsen, 2018). Here we found no evidence for such activation increases; instead we observed widespread and distributed decreases in activation across cortical areas. In contrast, subtler changes in the distributed patterns of fMRI activity have the potential to provide more direct metrics of plasticity. Increased pattern reorganization (across weeks), and larger pattern separation for trained sequences were found across prefrontal, parietal, and striatal regions. These metrics may be useful as general fMRI correlates of neural reorganization beyond the domain of motor learning.

3.5 References

Andrews-Hanna, J.R., Reidler, J.S., Sepulcre, J., Poulin, R., Buckner, R.L., 2010. Functional-Anatomic Fractionation of the Brain's Default Network. Neuron 65, 550–562.

Ashby, F.G., Turner, B.O., Horvitz, J.C., 2010. Cortical and basal ganglia contributions to habit learning and automaticity. Trends Cogn. Sci. 14, 208–215.

Bassett, D.S., Wymbs, N.F., Porter, M.A., Mucha, P.J., Carlson, J.M., Grafton, S.T., 2010. Dynamic reconfiguration of human brain networks during learning. Proc. Natl. Acad. Sci. 108, 7641–7646.

Bassett, D.S., Yang, M., Wymbs, N.F., Grafton, S.T., 2015. Learning-Induced Autonomy of Sensorimotor Systems. Nat. Neurosci. 18, 744–751.

Berlot, E., Popp, N.J., Diedrichsen, J., 2018. In search of the engram, 2017. Curr. Opin. Behav. Sci. 20., 56-60.

Beukema, P., Diedrichsen, J., Verstynen, T.D., 2019. Binding During Sequence Learning Does Not Alter Cortical Representations of Individual Actions. J. Neurosci. 39, 6968–6977.

Classen, J., Liepert, J., Wise, S.P., Hallett, M., Cohen, L.G., 1998. Rapid plasticity of human cortical movement representation induced by practice. J. Neurophysiol. 79, 1117–1123.

Coynel, D., Marrelec, G., Perlbarg, V., Pélégrini-Issac, M., Van de Moortele, P.F., Ugurbil, K., Doyon, J., Benali, H., Lehéricy, S., 2010. Dynamics of motor-related functional integration during motor sequence learning. Neuroimage 49, 759–766.

Dale, A.M., Fischl, B., Sereno, M.I., Dale, A.M., 1999. Cortical Surface-Based Analysis. Neuroimage 9, 179–194.

Dayan, E., Cohen, L.G., 2011. Neuroplasticity subserving motor skill learning. Neuron 72, 443–454.

Diedrichsen, J., Yokoi, A., Arbuckle, S.A., 2017. Pattern component modeling: A flexible approach for understanding the representational structure of brain activity patterns. Neuroimage 180, 119–133.

Doyon, J., Song, A.W., Karni, A., Lalonde, F., Adams, M.M., Ungerleider, L.G., 2002. Experience-dependent changes in cerebellar contributions to motor sequence learning. Proc. Natl. Acad. Sci. U. S. A. 99, 1017–22.

Fischl, B., Rajendran, N., Busa, E., Augustinack, J., Hinds, O., Yeo, B.T.T., Mohlberg, H., Amunts, K., Zilles, K., 2008. Cortical folding patterns and predicting cytoarchitecture. Cereb. Cortex 18, 1973–1980.

Floyer-Lea, A., Matthews, P.M., 2005. Distinguishable brain activation networks for short- and long-term motor skill learning. J. Neurophysiol. 94, 512–518.

Friston, K.J., Worsley, K.J., Poline, J.-P.B., Frith, C.D., Frackowiak, R.S.J., Holmes, a. P., Worsley, K.J., Poline, J.-P.B., Frith, C.D., Frackowiak, R.S.J., 1994. Statistical

parametric maps in functional imaging: A general linear approach. Hum. Brain Mapp. 2, 189–210.

Galea, J.M., Vazquez, A., Pasricha, N., Orban De Xivry, J.J., Celnik, P., 2011. Dissociating the roles of the cerebellum and motor cortex during adaptive learning: The motor cortex retains what the cerebellum learns. Cereb. Cortex 21, 1761–1770.

Grafton, S.T., Hazeltine, E., Ivry, R., 1995. Functional mapping of sequence learning in normal humans. J. Cogn. Neurosci. 7, 497–510.

Grafton, S.T., Hazeltine, E., Ivry, R.B., 2002. Motor sequence learning with the nondominant left hand: A PET functional imaging study. Exp. Brain Res. 146, 369–378.

Graybiel, A.M., 2016. The Basal Ganglia. Princ. neural Sci. 982–998.

Graybiel, A.M., Grafton, S.T., 2015. The striatum: Where skills and habits meet. Cold Spring Harb. Perspect. Biol. 7, 1–14.

Gusnard, D.A., Akbudak, E., Shulman, G.L., Raichle, M.E., 2001. Medial prefrontal cortex and self-referential mental activity: Relation to a default mode of brain function. Proc. Natl. Acad. Sci. U. S. A. 98, 4259–4264.

Hadipour-Niktarash, A., Lee, C.K., Desmond, J.E., Shadmehr, R., 2007. Impairment of retention but not acquisition of a visuomotor skill through time-dependent disruption of primary motor cortex. J. Neurosci. 27, 13413–13419.

Hardwick, R.M., Rottschy, C., Miall, R.C., Eickhoff, S.B., 2013. A quantitative meta-analysis and review of motor learning in the human brain. Neuroimage 67, 283–297.

Hazeltine, E., Grafton, S.T., Ivry, R., 1997. Attention and stimulus characteristics determine the locus of motor-sequence encoding. A PET study. Brain 120, 123–140.

Hikosaka, O., Sakai, K., Lu, X., Nakahara, H., Rand, M.K., Nakamura, K., Miyachi, S., Doya, K., 1999. Parallel neural networks for learning sequential procedures. Trends Neurosci. 22, 464–471.

Honda, M., Deiber, M.P., Ibáñez, V., Pascual-Leone, A., Zhuang, P., Hallett, M., 1998. Dynamic cortical involvement in implicit and explicit motor sequence learning. A PET study. Brain 121, 2159–2173.

Huang, Y., Zhen, Z., Song, Y., Zhu, Q., Wang, S., Liu, J., 2013. Motor Training Increases the Stability of Activation Patterns in the Primary Motor Cortex. PLoS One 8, e53555.

Hutton, C., Bork, A., Josephs, O., Deichmann, R., Ashburner, J., Turner, R., 2002. Image distortion correction in fMRI: A quantitative evaluation. Neuroimage 16, 217–240.

Jenkins, I.H., Brooks, D.J., Nixon, P.D., Frackowiak, R.S.J., Passingham, R.E., 1994. Motor sequence learning: A study with positron emission tomography. J. Neurosci. 14, 3775–3790.

Kang, E.K., Paik, N.J., 2011. Effect of a tDCS electrode montage on implicit motor sequence learning in healthy subjects. Exp. Transl. Stroke Med. 3, 2–7.

Karni, A., Meyer, G., Jezzard, P., Adams, M.M., Turner, R., Ungerleider, L.G., 1995. Functional MRI evidence for adult motor cortex plasticity during motor skill learning. Nature 377, 155–158.

Karni, A., Meyer, G., Rey-Hipolito, C., Jezzard, P., Adams, M.M., Turner, R., Ungerleider, L.G., 1998. The acquisition of skilled motor performance: fast and slow experience-driven changes in primary motor cortex. Proc. Natl. Acad. Sci. U. S. A. 95, 861–868.

Kawai, R., Markman, T., Poddar, R., Ko, R., Fantana, A.L., Dhawale, A.K., Kampff, A.R., Ölveczky, B.P., 2015. Motor Cortex Is Required for Learning but Not for Executing a Motor Skill. Neuron 86, 800–812.

Kumar, N., Manning, T.F., Ostry, D.J., 2019. Somatosensory cortex participates in the consolidation of human motor memory. PLoS Biol. 17, e3000469.

Lashley, K., 1950. In search of the engram. Society of Experimental Psychology, Symposium 4, 454-482.

Lehéricy, S., Bardinet, E., Tremblay, L., Van de Moortele, P.F., Pochon, J.B., Dormont, D., Kim, D.-S., Yelnik, J., Ugurbil, K., 2006. Motor control in basal ganglia circuits using fMRI and brain atlas approaches. Cereb. Cortex 16, 149–161.

Lehéricy, S., Benali, H., Van de Moortele, P.-F., Pélégrini-Issac, M., Waechter, T., Ugurbil, K., Doyon, J., 2005. Distinct basal ganglia territories are engaged in early and advanced motor sequence learning. Proc. Natl. Acad. Sci. U. S. A. 102, 12566–12571.

Lutz, K., Koeneke, S., Wüstenberg, T., Jäncke, L., 2004. Asymmetry of cortical activation during maximum and convenient tapping speed. Neurosci. Lett. 373, 61–66.

Ma, L., Wang, B., Narayana, S., Hazeltine, E., Chen, X., Robin, D.A., Fox, P.T., Xiong, J., 2010. Changes in regional activity are accompanied with changes in inter-regional connectivity during 4 weeks motor learning. Brain Res. 1318, 64–76.

Makino, H., Ren, C., Liu, H., Kim, A.N., Kondapaneni, N., Liu, X., Kuzum, D., Komiyama, T., 2017. Transformation of Cortex-wide Emergent Properties during Motor Learning. Neuron 94, 880–890.e8.

Matsuzaka, Y., Picard, N., Strick, P.L., 2007. Skill representation in the primary motor cortex after long-term practice. J. Neurophysiol. 97, 1819–1832.

Mattar, M., Wymbs, N.F., Bock, A.S., Aguirre, G.K., Grafton, S.T., Bassett, D.S., 2018. Predicting future learning from baseline network architecture. Neuroimage 172, 107–117.

Nitsche, M.A., Schauenburg, A., Lang, N., Liebetanz, D., Exner, C., Paulus, W., Tergau, F., 2003. Facilitation of implicit motor learning by weak transcranial direct current stimulation of the primary motor cortex in the human. J. Cogn. Neurosci. 15, 619–626.

Oosterhof, N.N., Wiestler, T., Downing, P.E., Diedrichsen, J., 2011. A comparison of volume-based and surface-based multi-voxel pattern analysis. Neuroimage 56, 593–600.

Orban, P., Peigneux, P., Lungu, O., Albouy, G., Breton, E., Laberenne, F., Benali, H., Maquet, P., Doyon, J., 2010. The multifaceted nature of the relationship between performance and brain activity in motor sequence learning. Neuroimage 49, 694–702.

Ostry, D.J., Gribble, P.L., 2016. Sensory Plasticity in Human Motor Learning. Trends Neurosci. 39, 114–123.

Otchy, T.M., Wolff, S.B.E., Rhee, J.Y., Pehlevan, C., Kawai, R., Kempf, A., Gobes, S.M.H., Ölveczky, B.P., 2015. Acute off-target effects of neural circuit manipulations. Nature 528, 358–363.

Penhune, V.B., Doyon, J., 2002. Dynamic cortical and subcortical networks in learning and delayed recall of timed motor sequences. J. Neurosci. 22, 1397–1406.

Penhune, V.B., Steele, C.J., 2012. Parallel contributions of cerebellar, striatal and M1 mechanisms to motor sequence learning. Behav. Brain Res. 226, 579–591.

Peters, A.J., Lee, J., Hedrick, N.G., Neil, K.O., Komiyama, T., 2017. Reorganization of corticospinal output during motor learning. Nat. Neurosci. 20, 1133.

Picard, N., Matsuzaka, Y., Strick, P.L., 2013. Extended practice of a motor skill is associated with reduced metabolic activity in M1. Nat. Neurosci. 16, 1340–1347.

Pinsard, B., Boutin, A., Gabitov, E., Lungu, O., Benali, H., Doyon, J., 2018. Consolidation alters motor sequence-specific distributed representations. bioRxiv 376053.

Poldrack, R.A., 2000. Imaging brain plasticity: Conceptual and methodological issues - A theoretical review. Neuroimage 12, 1–13.

Poldrack, R.A., Sabb, F.W., Foerde, K., Tom, S.M., Asarnow, R.F., Bookheimer, S.Y., Knowlton, B.J., 2005. The neural correlates of motor skill automaticity. J. Neurosci. 25, 5356–5364.

Raichle, M.E., MacLeod, A.M., Snyder, A.Z., Powers, W.J., Gusnard, D.A., Shulman, G.L., 2001. A default mode of brain function. Proc. Natl. Acad. Sci. U. S. A. 98, 676–682.

Reis, J., Schambra, H.M., Cohen, L.G., Buch, E.R., Fritsch, B., Zarahn, E., Celnik, P.A., Krakauer, J.W., 2009. Noninvasive cortical stimulation enhances motor skill acquisition over multiple days through an effect on consolidation. Proc. Natl. Acad. Sci. U. S. A. 106, 1590–1595.

Reithler, J., van Mier, H.I., Goebel, R., 2010. Continuous motor sequence learning: Cortical efficiency gains accompanied by striatal functional reorganization. Neuroimage 52, 263–276.

Russo, A.A., Khajeh, R., Bittner, S.R., Perkins, S.M., Cunningham, J.P., Abbott, L.F., Churchland, M.M., 2020. Neural Trajectories in the Supplementary Motor Area

and Motor Cortex Exhibit Distinct Geometries, Compatible with Different Classes of Computation. Neuron 107, 745–758.e6.

Seidler, R.D., Purushotham, A., Kim, S.G., Ugurbil, K., Willingham, D., Ashe, J., 2005. Neural correlates of encoding and expression in implicit sequence learning. Exp. Brain Res. 165, 114–124.

Seidler, R.D., Purushotham, A., Kim, S.G., Uğurbil, K., Willingham, D., Ashe, J., 2002. Cerebellum activation associated with performance change but not motor learning. Science (80-.). 296, 2043–2046.

Shamloo, F., Helie, S., 2016. Changes in default mode network as automaticity develops in a categorization task. Behav. Brain Res. 313, 324–333.

Shulman, G.L., Fiez, J.A., Corbetta, M., Buckner, R.L., Miezin, F.M., Raichle, M.E., Petersen, S.E., 1997. Common blood flow changes across visual tasks: II. Decreases in cerebral cortex. J. Cogn. Neurosci. 9, 648–663.

Steele, C.J., Penhune, V.B., 2010. Specific Increases within Global Decreases : A Functional Magnetic Resonance Imaging Investigation of Five Days of Motor Sequence Learning 30, 8332–8341.

Tamás Kincses, Z., Johansen-Berg, H., Tomassini, V., Bosnell, R., Matthews, P.M., Beckmann, C.F., 2008. Model-free characterization of brain functional networks for motor sequence learning using fMRI. Neuroimage 39, 1950–1958.

Toni, I., Krams, M., Turner, R., Passingham, R.E., 1998. The time course of changes during motor sequence learning: A whole- brain fMRI study. Neuroimage 8, 50–61.

Ungerleider, L.G., Doyon, J., Karni, A., 2002. Imaging Brain Plasticity during Motor Skill Learning. Neurobiol. Learn. Mem. 564, 553–564.

Vahdat, S., Lungu, O., Cohen-Adad, J., Marchand-Pauvert, V., Benali, H., Doyon, J., 2015. Simultaneous Brain-Cervical Cord fMRI Reveals Intrinsic Spinal Cord Plasticity during Motor Sequence Learning. PLoS Biol. 13, e1002186.

Walther, A., Nili, H., Ejaz, N., Alink, A., Kriegeskorte, N., Diedrichsen, J., 2016. Reliability of dissimilarity measures for multi-voxel pattern analysis. Neuroimage 137, 188–200.

Waters-metenier, S., Husain, M., Wiestler, T., 2014. Bihemispheric Transcranial Direct Current Stimulation Enhances Effector-Independent Representations of Motor Synergy and Sequence Learning 34, 1037–1050.

Wiestler, T., Diedrichsen, J., 2013. Skill learning strengthens cortical representations of motor sequences. Elife 2, e00801.

Wu, T., Kansaku, K., Hallett, M., 2004. How Self-Initiated Memorized Movements Become Automatic: A Functional MRI Study. J. Neurophysiol. 91, 1690–1698.

Wymbs, N.F., Grafton, S.T., 2015. The human motor system supports sequence-specific representations over multiple training-dependent timescales. Cereb. Cortex 25, 4213–4225.

Xiong, J., Ma, L., Wang, B., Narayana, S., Duff, E.P., Egan, G.F., Fox, P.T., 2009. Long-term motor training induced changes in regional cerebral blood flow in both task and resting states. Neuroimage 45, 75–82.

Yin, H.H., Mulcare, S.P., Hilário, M.R.F., Clouse, E., Holloway, T., Davis, M.I., Hansson, A.C., Lovinger, D.M., Costa, R.M., 2009. Dynamic reorganization of striatal circuits during the acquisition and consolidation of a skill. Nat. Neurosci. 12, 333–341.

Yokoi, A., Arbuckle, S.A., Diedrichsen, J., 2018. The role of human primary motor cortex in the production of skilled finger sequences. J. Neurosci. 38, 1430–1442.

Yokoi, A., Diedrichsen, J., 2019. Neural Organization of Hierarchical Motor Sequence Representations in the Human Neocortex. Neuron 103, 1178–1190.e7.

Yousry, T.A., Schmid, U.D., Alkadhi, H., Schmidt, D., Peraud, A., Buettner, A., Winkler, P., 1997. Localization of the motor hand area to a knob on the precentral gyrus. A new landmark. Brain 120, 141–157.

CHAPTER 4

4 Combining repetition suppression and pattern analysis provides new insights into the role of M1 and parietal areas in skilled sequential actions

4.1 Introduction

The ability to learn and produce complex sequences of movements is essential for many everyday activities, from tying shoelaces to playing instruments. Searching for where these acquired skills are represented in the brain has been one of the central questions in motor neuroscience (Lashley, 1950). One prominent issue in this debate is whether skilled sequence execution relies on representations in premotor and supplementary motor areas, or whether the sequences are represented in the primary motor cortex (M1) (see Dayan and Cohen, 2011; Berlot et al., 2018 for reviews). We recently conducted a systematic longitudinal 5-week training study (Berlot et al., 2020) employing functional magnetic resonance imaging (fMRI) to assess brain changes with motor sequence learning. We observed no overall change in overall activity with learning in M1, and no changes in the sequence-specific activity patterns. In contrast, clear learning-related changes in both overall activity and fine-grained activity patterns were observed in premotor and parietal areas, suggesting learning-related changes occur outside of M1. Consistent with this idea, activity patterns in M1 seem to reflect individual movement elements, but not the sequential context (Russo et al., 2020; Yokoi et al., 2018; Yokoi and Diedrichsen, 2019). This suggests that M1 does not represent learnt motor sequences, but must rely on inputs from other areas to select the next correct movement element.

Using the technique of repetition suppression, however, Wymbs and Grafton (2015) provided evidence for learning-related changes during motor sequence learning in M1. Repetition suppression (RS) refers to the observation that a stimulus repetition evokes

reduced neuronal activity compared to its initial presentation (Gross, Schiller, Wells, Gerstein, 1967). It is commonly used as a tool for investigating brain representation (Buckner et al., 1998; Henson et al., 2003; see Segaert et al., 2013 for review) following the logic that if regional activation reduces upon repetition, the underlying neuronal population must represent some aspect of the stimulus that repeated (Grill-Spector et al., 2006). Wymbs and Grafton (2015) found learning-related changes in RS across several regions, including M1, where they reported a non-monotonic change in RS over weeks – early increase, followed by a decrease, and again an increase in RS, which they suggested indicates skill-specific specialization in M1. Altogether, their results indicate that M1's activity patterns are malleable when learning motor sequences. This stands in stark contrast to the above-mentioned studies that used pattern dissimilarity analyses and found no evidence of sequential representation in M1.

We reasoned that this discrepancy between RS and pattern analysis may reflect the fact that different underlying components of activity patterns might bring about the suppression of activity observed on repetition, some of which may not be directly related to a sequence identity (Alink et al., 2018; Grill-Spector et al., 2006). To understand RS effects in more detail, we need to know what aspects of the underlying representations reduce from the first to the second repetition. We therefore designed a paradigm that allowed us to investigate changes in brain representation using both tools – RS and multivariate pattern analysis. We trained healthy volunteers to produce motor sequences over 5 weeks and tested their performance during high-field (7 T) MRI scanning. Participants performed trained and untrained sequences, each sequence twice in a row, allowing us to conduct both pattern and RS analysis on the same data. Replicating previous results, we observed significant learning-related changes in M1 for RS, but not for pattern dissimilarities. In contrast, both metrics showed learning-related changes in premotor and parietal regions. Using pattern analysis, we then decomposed the activation patterns in the first and second repetition to determine which representational aspects underlie the RS effects in the different regions. Finally, we performed control analyses to test whether observed effects could be attributed to learning-related improvements in the execution speed.

4.2 Methods

4.2.1 Participants

Twenty-seven participants took part in the experiment. Data of one participant were excluded because the field map was distorted in one of the four scans, resulting in 26 participants whose data was analyzed (17 females, 9 males). Their mean age was 22.2 years (SD = 3.3 years). Criteria for study inclusion were right-handedness and no prior history of psychiatric or neurological disorders. They provided written informed consent to all procedures and data usage before the study started. The experimental procedures were approved by the Ethics Committee at Western University.

4.2.2 Apparatus

Finger sequences were performed using a right-hand MRI-compatible keyboard device (**Figure 4.1a**). The keys of the device had a groove for each fingertip, with keys numbered 1-5 for thumb-little finger. The keys were not depressible, so participants performed isometric finger presses. The force of the presses was measured by the force transducers underneath each finger groove (FSG-15N1A, Sensing and Control, Honeywell; dynamic range 0-25 N; update rate 2 ms; sampling 200 Hz). For the key to be recognized as pressed, the applied force had to exceed 1 N.

4.2.3 Experimental design – behaviour

Participants were trained over a five-week time period to perform six 9-digit finger sequences (**Figure 4.1b**). They were split into two groups, with trained sequences of one group being the untrained sequences of the second group, and vice versa (see **Figure 4.4b** for all of the chosen sequences). The chosen sequences for both groups were matched as closely as possible on several features: starting finger, number of repetitions per finger, and first-order finger transitions. The decision to split participants into two groups was made

to ensure that none of the observed effects could be due to the specific set of sequences chosen.

On day 1 of the study, participants were acquainted with the apparatus and the task performed in the scanner. To ensure no sequence-specific learning would take place prior to scan 1, we used finger sequences different from the trained and untrained sets which participants did not encounter at any later stage of the experiment.

During the behavioural training sessions, participants were trained to perform the six sequences. They received visual feedback on the correctness of their presses online with each digit turning green for correct, and red for incorrect press (**Figure 4.1a**). They were instructed to perform the sequences as fast as possible while keeping the overall accuracy >85%. The details of the training protocol, as well as a few other design features (which were not assessed for this paper) have been described elsewhere (Berlot et al., 2020).

Figure 4.1. Experimental paradigm.

a) Experimental setup – finger sequences composed of 9 digits were executed on a keyboard device. Participants received visual feedback on correctness of their presses – digits turned green for correct presses, red for incorrect presses. **b)** Group-averaged performance on trained sequences over the 5-week behavioural training protocol. Red shade indicates the standard error of the group mean. **c)** Group-averaged performance during the scanning sessions. Trained sequences are in red, untrained in blue. Dark colour indicates first execution, light second execution. White bars indicate the group mean performance. **d)** Experimental paradigm inside the scanner. Each sequence was presented twice in a row. Trials started with a 1s preparation time in which the sequence was presented, followed by a 3.5s period of main phase, when the sequence was also execution, followed by 0.5s of inter-trial interval (ITI). The plotted timeseries for an insert of the design is group-averaged evoked activation of M1. Shaded error bars indicate the standard error of the group mean.

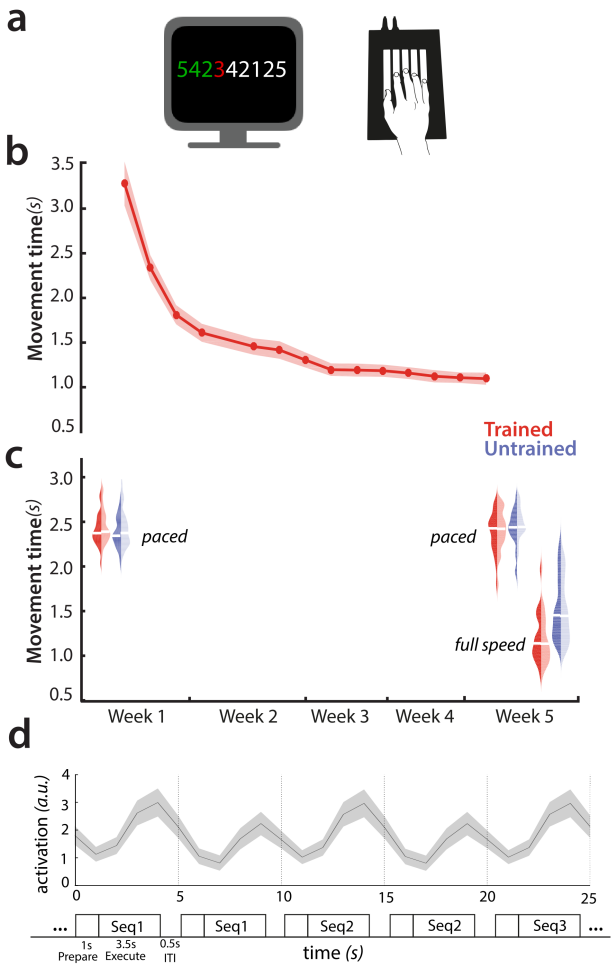
a
5423 42125
b
Movement time (s)
3.5
3.0
2.5
2.0
1.5
1.0
0.5
c
Trained
Untrained
Movement time (s)
paced
paced
full speed
Week 1
Week 2
Week 3
Week 4
Week 5
d
activation (a.u.)
0
5
10
15
20
25
Seq1
Seq1
Seq2
Seq2
Seq3
1s Prepare
3.5s Execute
0.5s ITI
time (s)

4.2.4 Experimental design – imaging

Longitudinal studies assessing learning have to tackle the challenge that performance changes with learning, and that it is not clear whether brain changes reflect the acquisition of new skills, or are caused indirectly by the changed behaviour (Poldrack, 2000). For motor learning, the higher speed of execution could lead to different brain activation, unrelated to learning. Pacing participants to perform at the same speed for trained and untrained sequences, and across sessions, presents a possible solution for this problem. On the other side, pacing participants at a slower speed might not tap into the same neural circuitry as skilled behaviour. For this reason, we decided to include both approaches; sessions with paced performance and a session where participants performed at full speed.

Participants underwent a total of 4 MRI scanning sessions (**Figure 4.1c**) while executing trained and untrained sequences. The first session served as a baseline prior to the start of the training protocol (in week 1), where the "trained" and "untrained" sequences were both untrained and seen for equivalent amounts of time. The second session was conducted in week 2, and the last two after training protocol was completed – in week 5. In scanning sessions 1-3, participants' performance inside the scanner was paced with a metronome, whereas in session 4, they performed as quickly as possible. For the purpose of this paper, we analyzed data of scanning session 1 (prior to training – paced), 3 (after learning – paced) and 4 (after learning – unpaced) (**Figure 4.1c**), allowing us to examining learning- and performance-related changes. Session 4 allows for the closest comparison to the previous RS study (Wymbs and Grafton, 2015) which also employed a full-speed performance design.

Each scanning session consisted of eight functional runs with event-related design randomly intermixing trials containing the 6 trained and the 6 untrained sequences (totalling 72 trials per functional run). Each sequence was executed for two trials in a row (**Figure 4.1d**). In this way, our design did not differentiate between repetition suppression and expectation suppression (Kok et al., 2012; Summerfield et al., 2008). In contrast to perceptual studies, however, in motor studies the influence of the expectation of a repetition is likely much less important. After the informative cue, preparatory processes are executed in a full awareness of whether the sequence is repeated from last trial, no matter if that

repetition was expected or not. Thus, repetition effects in motor control will always contain an element of expectation. For this reason, we chose repetition to be a predictable feature of our experimental design.

Each trial started with a 1-s preparation time with nine digits of the sequence presented on the screen (**Figure 4.1d**). A 'go' signal was presented afterwards. In scans 1-3, a pink line appeared underneath the sequence and started expanding, indicating the pace at which participants were to press. In scan 4, participants executed the sequence as fast as possible after the go cue. After execution, they received feedback on their overall performance – 3 points for correct and 0 for incorrect performance. Each trial lasted for 5 s total, with a 0.5-s inter-trial interval (**Figure 4.1d**). Five periods of 10 s rests were added throughout each functional run to provide a better estimate of baseline activation. These rests were added randomly, but never between the first and second execution of the same sequence. In total, each scanning session lasted for approximately 75 minutes.

4.2.5 Image acquisition

Data were acquired on a 7-Tesla Siemens Magnetom MRI scanner with a 32-receive channel head coil (8-channel parallel transmit). At the beginning of the first scan, we acquired anatomical T1-weighted scan for each participant. This was obtained using a magnetization-prepared rapid gradient echo sequence (MPRAGE) with voxel size of 0.75x0.75x0.75 mm isotropic (field of view = 208 x 157 x 110 mm [A-P; R-L; F-H], encoding direction coronal). Data during functional runs were acquired using the following sequence parameters: GRAPPA 3, multi-band acceleration factor 2, repetition time [TR] = 1.0 s, echo time [TE] = 20 ms, flip angle [FA] = 30 deg, slice number: 44, voxel size: 2x2x2 mm isotropic. To estimate magnetic field inhomogeneities, we acquired a gradient echo field map with the following parameters: transversal orientation, field of view: 210 x 210 x 160 mm, 64 slices, 2.5 mm thickness, TR = 475 ms, TE = 4.08 ms, FA = 35 deg. The dataset is publicly available on OpenNeuro (accession number ds002776).

4.2.6 Preprocessing and first-level analysis

Data preprocessing was carried out using SPM12. Preprocessing of functional data included correcting for geometric distortions using the acquired field map data, and head motion correction (3 translations: x, y, z; 3 rotations: pitch, roll yaw). The data across sessions were all aligned to the first run of the first session, and then co-registered to the anatomical scan.

Preprocessed data were analysed using a general linear model (GLM; Friston et al., 1994). We defined a regressor for each of the performed 12 sequences (6 trained, 6 untrained), separately for their first and second execution – resulting in a total of 24 regressors per run. The regressor was a boxcar function defined for each trial, and convolved with a two-gamma canonical hemodynamic response function (time to peak: 5.5 s, time to undershoot: 12.5 s). All instances of sequence execution were included into estimating regressors, regardless of whether the execution was correct or erroneous. This analysis choice was also taken by Wymbs and Grafton (2015), thus allowing a more direct comparison of repetition suppression results. Even when the error trials were excluded (i.e. removing all error trials as well as second execution trials when the first execution was erroneous), our results remained unchanged. Ultimately, the first level analysis resulted in activation images (beta maps) for each of the 24 conditions per run, for each of the four scanning sessions.

4.2.7 Surface reconstruction and regions of interest

Individual subject's cortical surfaces were reconstructed using FreeSurfer (Dale et al., 1999). Individual surfaces were aligned and spherically registered to match a template atlas (Fischl et al., 1999). Subsequently surfaces were resampled to FreeSurfer's Left-Right symmetric template (fs_LR.164k.spec) in the connectome workbench distribution (v.1.3.2, Marcus et al., 2011) .

These surfaces were used to define the regions of interest (ROI), which were defined on the group surface template using aligned probabilistic cytoarchitectonic maps

(Fischl et al., 2008) and then projected into the individual brains. Specifically, our ROIs included areas covering the primary motor cortex and secondary associative regions. The primary motor cortex (M1) was defined by including nodes with the highest probability of belonging to Brodmann area (BA) 4 which in addition corresponded to the hand knob area (Yousry et al., 1997). The dorsal premotor cortex (PMd) was included as the lateral part of the middle frontal gyrus. The anterior part of the superior parietal lobule (SPLa) was defined to include anterior, medial and ventral intraparietal sulcus. The subsequent analyses carried in the space of the original functional data acquisition for each individual subjects by determining the voxel that lay between the individual pial and white matter surfaces.

Additionally to the ROI analysis we also a continuous searchlight analysis (Oosterhof et al., 2011). A searchlight was defined for each surface node, encompassing a circular neighbourhood region containing 120 voxels. The voxels for each searchlight were found in exactly the same way as for the ROI definition. As a slightly coarser alternative to searchlights, we also defined a regular tessellation of the cortical surface separated into small hexagons, and extracted the functional data in the same way.

4.2.8 Evoked activation and repetition suppression

We calculated the percent signal change for execution of each sequence relative to the baseline activation for each voxel. The calculation was split between the first and second execution (**Figure 4.1d**).

To calculate repetition suppression, the activation during the first execution was subtracted from the elicited activation during the second execution. Thus, negative values of this difference contrast represented relative suppression of activation on the second execution, i.e. repetition suppression. For most subsequent analyses, the obtained values of activation and repetition suppression were averaged separately for trained and the untrained sequences. For ROI analysis, the volume maps were averaged across the predefined regions (M1, PMd, SPLa) in the native volume space of each subject. Additionally, for

visualization the volume maps were projected to the surface for each subject, and averaged across the group in Workbench space.

4.2.9 Dissimilarities between activity patterns for different sequences

To evaluate which regions displayed sequence-specific representation, we calculated Crossnobis dissimilarities between the evoked beta patterns of individual sequences. To do so, we first multivariately prewhitened the beta values – i.e. we standardized them by voxels' residuals and weighted by the voxel noise covariance matrix. We used optimal shrinkage towards a diagonal noise matrix following the Ledoit and Wolf (2004) procedure. Such regularized prewhitening has been found to increase the reliability of dissimilarity estimates (Walther et al., 2016). Next, we calculated the crossvalidated Mahalanobis dissimilarities (i.e. the Crossnobis dissimilarities) between evoked regional patterns of different pairs of sequences, resulting in a total of 66 dissimilarities. This was performed twice: once by combining the activation patterns across the two executions and second time by separately obtaining dissimilarities between evoked patterns split per execution. The obtained dissimilarities were then averaged overall, as well as separately within the pairs of trained sequences, and the untrained sequences. This analysis was conducted separately for each ROI and using a surface searchlight approach (Oosterhof et al., 2011). In the searchlight approach, dissimilarities were calculated amongst the voxels of each searchlight, with the resulting dissimilarities values assigned to the centre of the searchlight.

4.2.10 Changes in dissimilarities with repetition

We then related the change in dissimilarities with repetition to the changes in overall activity. Activation pattern for each sequence can be characterized as a point in a high-dimensional space, with each axis referring to the activation of a voxel. As a measure of the overall activation, we used the length of the activity vector from the origin (rest), and as dissimilarities the lengths of the vectors between different conditions. Unbiased

estimates of the length of activity vectors relative to rest were derived from the crossvalidated second-moment matrix. The square root of each diagonal element (variance of evoked pattern) indicates the length of the activity vector, relative to rest. The square root of crossnobis dissimilarity (variance – covariance between patterns) is the length of the vector between the two patterns. The crossnobis dissimilarities were average across the conditions before taking the square root transform, separately for each execution. Similarly, overall activity vector length was averaged across conditions to obtain an overall activity vector length for executions 1 and 2.

Using the obtained average activity vector length and dissimilarities per execution, we assessed whether repetition suppression simply scaled the entire activity pattern downward. To do so, we computed the ratio of activity vector length change: $\frac{\mathrm{act}_{\mathrm{exe2}}}{\mathrm{act}_{\mathrm{exe1}}}$. Based on this value, we computed what dissimilarities would be predicted on the second execution if representation decreased proportional to the decrease in activation ($\mathrm{diss}_{\mathrm{pred}} = \frac{\mathrm{act}_{\mathrm{exe2}}}{\mathrm{act}_{\mathrm{exe1}}}$ x $\mathrm{diss}_{\mathrm{exe1}}$). This was then contrasted with the observed dissimilarities on execution 2 ($\mathrm{diss}_{\mathrm{exe2}} - \mathrm{diss}_{\mathrm{pred}}$). A positive difference indicates that dissimilarities decrease relatively less with repetition than the reduction in average activation. This suggests a relatively sharper representation on the second execution. In contrast, a negative difference would reflect a further reduction in dissimilarities relative to that obtained in activation. This would suggest that with repetition, representation decreases relatively more than activation.

4.2.11 Pattern component analysis: modelling representational components

To determine what specific features of the patterns might change across the two executions, we decomposed the pattern component modelling toolbox (PCM; Diedrichsen et al., 2011, 2017). PCM models the covariance structure (second moment matrix) of regional activity patterns according to different representational hypotheses. In our experiment based on presented sequences, we defined five representational components.

First finger

Both trained and untrained sequences started with one of three possible fingers: thumb, middle or little finger. The first finger component predicts that activity pattern for sequences that start with the same finger are identical. For sequences starting with a different first finger, the prediction was based on the covariance of the natural statistics of hand movement (Ejaz et al., 2015).

All fingers

The sequences were slightly different in terms of which fingers were involved. The 'all fingers' component simply characterized how often each finger occurred in each sequence. If two sequences consisted exactly of the same presses (just in a different order), they were predicted to be identical. The predicted covariance was again weighted by the natural statistics of hand movement (Ejaz et al., 2015).

Sequence type

This component split the performed sequences based on whether they were trained or untrained, predicting one regional activity patterns for all the trained and a different activity pattern for all the untrained sequences.

Trained sequence identity

This component modelled any differences between the 6 trained sequences.

Untrained sequence identity

Similar as the trained sequence identity, this component predicted a unique activity patterns for each untrained sequence.

The overall predicted second moment matrix (G) was then a convex combination of the component matrices (G_c), each weighted by a positive component weight exp (Θ_i).

$$G = \sum_c \exp(\Theta_c)\, G_c$$

The construction of the model components was done separately for the two groups of participants, as different sequences constituted 'trained' or 'untrained' sequences for the two groups. The subsequent steps of model fitting and evaluation were carried together for all subjects.

We formulated a model family containing all possible combinations of the five chosen components (Yokoi and Diedrichsen, 2019). This resulted in 32 combinations, also containing the 'null' model that predicted no differences amongst any of the sequence patterns. We evaluated all of the 32 models using a crossvalidated leave-one-subject-out scheme. The components weights were fitted to maximize the likelihood of the data the data of subject 1,...,N-1. We then evaluated the likelihood of the observed regional activity patterns of subject N under that model. The resultant cross-validated likelihoods were used as model evidence for each model (see Diedrichsen et al. 2017). The log model Bayes Factor BF_m, the difference between the crossvalidated log-likelihood of each model and the null model, characterises the relative evidence for that model.

In addition to the model family of the chosen components, we also fit a 'noise-ceiling' model to assess maximal $logBF_m$ that would be achievable for a group model (Diedrichsen et al., 2017; Nili et al., 2014). For each of the two groups, we predicted the second moment matrix of a left-out subject based on n-1 subjects in the same group. This metric of inter-subject consistency was then combined across the subjects of the two groups.

To integrate the results across models, we used model averaging. Assuming a uniform prior probability across models, we first computed the posterior probability of each model and region directly from the log-Bayes factors:

$$posterior_m = \frac{\exp\left(logBF_m\right)}{\sum_{j=1}^{m} \exp\left(logBF_j\right)}$$

In this expression, the denominator normalizes the log-Bayes factors across 32 models to ensure they sum to 1. The obtained posterior probability was used in calculation of two

subsequent metrics: 1) component log-Bayes factor, and 2) variance accounted for by each component. The log-Bayes factor for each component (first finger, all fingers, etc.) was calculated as the log of the ratio between the posterior probability for the models containing the component (c=1) versus the models that did not (c=0).

$$logBF_c = log\left(\frac{\frac{1}{N_{m:c=1}}\sum_{m:c=1} posterior_m}{\frac{1}{N_{m:c=0}}\sum_{m:c=0} posterior_m}\right)$$

where $N_{m:c=1}$ ($N_{m:c=0}$) denotes the number of models (not) containing the component (Shen and Ma, 2019). The component log-Bayes factor is monotonically related to the posterior probability of model components.

To determine the amount of pattern variance accounted for by each component (across the models), we normalized the trace of each model component to be 12 (number of conditions) prior to fitting. Thus, the fitted component weight exp ($\Theta_{i,m}$) indicates the amount of variance accounted for by the component *i* in the context of model *m*. The model-averaged amount of variance accounted for by each component c was then calculated as:

$$variance_c = \sum_{m=1}^{32} posterior_m \ \exp(\Theta_{c,m})$$

Important to note is that the estimated variance is always positive, such that this quantity cannot be used to test whether a component is present at all. On the other hand, the log-Bayes factor does not take into account the actual weighting of the component in explaining the activity patterns. In univariate models, the average variance accounted for is tightly related to the evidence for that component- however this is not necessarily the case in the multivariate setting. While component *c1* can be crucial to account for the covariance between the patterns, it may actually play a relative small role in predicting the activity patterns. Thus, both the component Bayes factor and the averaged explained variance provide informative, albeit slightly different, measures of the importance of a component.

4.2.12 Statistical analyses of repetition suppression and dissimilarities

We employed a within-subject design. For each subject's data, we calculated repetition suppression (RS) and dissimilarities, separately for trained and untrained sequences. This was done for each region and session. To statistically quantify how RS and dissimilarities changed with learning (across sessions for trained / untrained sequences), we performed a session x sequence type ANOVA on those metrics, in predefined ROIs. Afterwards, we used a two-tailed paired t-test to assess the effect of sequence type per session. We additionally performed a three-way session x region x sequence type ANOVA to examine if the learning-related effects differed across regions. For the analysis of dissimilarities split by execution (execution 1 vs. 2), we calculated, per subject, the expected crossnobis dissimilarities for execution 2 of the cortical surface regions. The observed dissimilarities on the second execution were contrasted with those by using a two-tailed paired t-test.

4.2.13 Statistical analyses of pattern component modelling

We report the component log-Bayes factors, averaged across subjects. Additionally, the log-Bayes factors were submitted to a one-sample t-test against 0 (two-tailed). To quantify the change in component variance across executions, we calculated, per subject, the percent reduction in component variance from execution 1 to 2. The relative reduction in variance with repetition was contrasted across components by using a two-tailed paired t-test.

4.3 Results

4.3.1 Changes in repetition suppression with learning

To examine learning-related changes in repetition suppression and pattern analysis, we calculated both metrics on fMRI activation patterns both pre- and post-learning (i.e. weeks 1 and 5). Relative to rest, sequence execution activated primary motor cortex (M1), primary somatosensory cortex (S1), dorsal and ventral premotor cortex (PMd and PMv),

supplementary motor area (SMA) and the anterior superior parietal lobules (SPLa; **Figure 4.2a**). In general, activity was higher for the first than for the second execution (**Figure 4.2b**). Repetition suppression was calculated as the difference in activity between the two executions of the same sequence (Exe 2 – Exe 1). Negative values indicate a relative reduction in activation with repetition, i.e., repetition suppression (RS). Already in week 1, prior to learning, RS was observed in nearly all regions displaying task-evoked activation (**Figure 4.2c**). Only in regions that showed de-activation during task performance (blue shades in **Figure 4.2b**), did we observed positive difference values between the executions (areas in red shades in **Figure 4.2c**). This indicates that, both the amount of activation and the amount of deactivation reduced with repetition.

We statistically quantified how RS changed across weeks (specifically between sessions 1 and 4) for three predefined regions of interest: SPLa, PMd, and M1 (**Figure 4.2d**, see **Figure 4.2e-f** for a breakdown of activation per execution). The increase in RS across session was higher for trained than untrained sequences in all regions, as confirmed by a significant session x sequence type interaction in each region (PMd: $F_{(1,25)}$=5.29, p=0.030; SPLa: $F_{(1,25)}$=4.62; p=0.041). The increase in RS was particularly strong in M1 (M1: $F_{(1,25)}$=24.74; p=3.9e^{-5}). Indeed, the three-way interaction of region x session x sequence type was significant ($F_{(2,50)}$=9.19, p=3.9e^{-4}). To summarize the RS results, all regions showed evidence of an increase of sequence-specific representation with learning, with a particularly strong effect in M1.

Figure 4.2. Changes in repetition suppression and dissimilarities with learning.

a) Group-averaged evoked activation, measured as percent signal change over resting baseline in week 1, averaged across all sequences and projected to an inflated representation of the left hemisphere, i.e. hemisphere contralateral to the performing hand. **b)** Group-averaged activation for each execution (Exe1, Exe2), in the baseline session (Session 1 – Week 1) and after training (Session 4 – Week 5) represented on a flattened representation of the left hemisphere. CS stands for the central sulcus. **c)** The difference in evoked activation between the two executions. Blue represents relative suppression of activation on the second, relative to the first, execution. Regions of interest: primary motor cortex (M1), dorsal premotor cortex (PMd), anterior superior parietal lobule (SPLa). **d)** Repetition suppression in the predefined regions of interest, separately for trained (red) and untrained (blue) sequences. Error bars reflect the standard error of the group mean. More negative values indicate more suppression during second execution, relative to the first. * signals $p<.05$. **e)** Elicited activation measured in percent signal change over resting baseline for trained sequences on first (dark) and second (light) execution. RS is calculated as the difference between activation across executions, i.e. Exe2-Exe1. **f)** Elicited activation split by execution for untrained sequences. **g)** Average dissimilarity between evoked patterns for all pairs of sequences, in week 1, averaged across the group. Pattern dissimilarity was computed using a searchlight approach, by calculating the average crossnobis dissimilarity of activation patterns between all sequence pairs in each searchlight. **h)** Average dissimilarity between activation patterns of different sequence pairs in weeks 1 and 4. **i)** Dissimilarities between trained (red) and untrained (blue) sequence patterns, across weeks 1 and 5. Error bars reflect the standard error of the group mean. * signals $p<.05$.

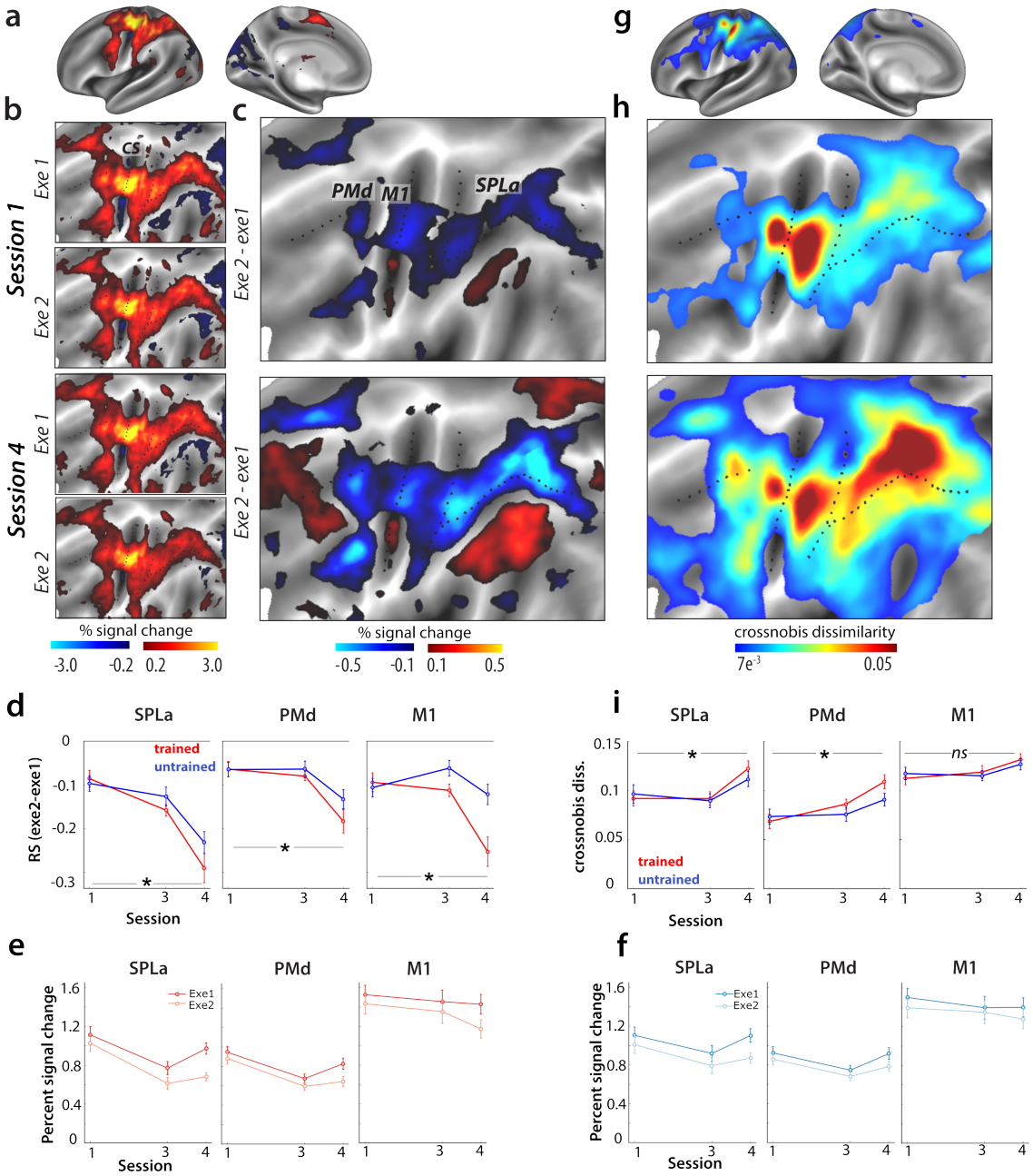
a
b
c
g
h
Session 1
Session 4
Exe 1
Exe 2
CS
Exe 2 - exe1
PMd
M1
SPLa
% signal change
-3.0 -0.2 0.2 3.0
% signal change
-0.5 -0.1 0.1 0.5
crossnobis dissimilarity
7e-3 0.05
d
SPLa
PMd
M1
RS (exe2-exe1)
trained
untrained
Session
i
crossnobis diss.
ns
e
Percent signal change
Exe1
Exe2
f

4.3.2 Changes in pattern dissimilarities with learning

As another measure of sequence-specific representations, we tested whether the regions that displayed RS also showed distinguishable fine-grained activity patterns for each sequence. As a measure of pattern dissimilarity, we calculated the average crossvalidated Mahalanobis dissimilarity (i.e., crossnobis dissimilarity) between activation patterns of all possible sequence pairs. Overall, regions with dissimilar activity patterns for the different sequences corresponded to regions which also exhibited RS effects (**Figure 4.2g-h**). Additionally, both metrics (RS and pattern dissimilarities) increased from session 1 to 4, with the effect particularly pronounced in the parietal cortex (**Figure 4.2c, i**). Thus, based on visual inspection, RS and pattern dissimilarity metrics seem to provide consistent evidence for the development of sequence-specific representations with learning in an overlapping set of regions.

However, when quantifying the change in pattern dissimilarities across weeks in predefined ROIs, we observed important differences from RS. In SPLa and PMd, pattern dissimilarities increased more for trained than untrained sequences across sessions (**Figure 4.2i**), as quantified by a significant interaction in a session x sequence type ANOVA (SPLa: $F_{(1,25)}$=4.80; p=.038, PMd: $F_{(1,25)}$=5.29, p=.030). In contrast, the week by sequence type interaction was not significant in M1 (**Figure 4.2i**; $F_{(1,25)}$=2.13, p=.16). This indicates that while PMd and SPLa show learning-related changes on the level of pattern dissimilarities, these are absent in M1. The three-way interaction (region x session x sequence type) on the observed dissimilarities was indeed significant ($F_{(2,50)}$=3.39, p=0.041), confirming the difference between regions.

4.3.3 Pattern dissimilarities reduce with repetition

Within the same dataset, we observed learning-related changes in RS in M1, but no change in pattern dissimilarities with learning. While the increase in pattern dissimilarities (**Figure 4.2h**), as well as direct evidence for pattern changes across weeks (Berlot et al., 2020), clearly argue that sequence-specific learning occurs in premotor and parietal areas and not in M1, RS provides evidence for the development of sequence-specific representations in all these regions. How can this discrepancy be explained? To resolve this question, we need

to understand how the role that each area plays during skilled sequence performance changes from the first to the second execution. We first inspected pattern dissimilarities for each of the two executions separately (execution 1, execution 2) in the trained state (Week 5 / Session 4). We observed that, on average, pattern dissimilarities in week 5 decreased with repetition in most cortical regions (**Figure 4.3a**). This decrease was particularly pronounced around the central sulcus, including M1 (**Figure 4.3b**).

Of course some decrease in dissimilarities would be expected given the decrease of overall activity with repetition (**Figure 4.2d**). We therefore compared the decrease in dissimilarities to what would be predicted if activation decreased proportionally for all sequences. First we calculated the relative decrease in activity – i.e. the ratio of the activity during the second execution over the activity during the first. This ratio was applied to the observed dissimilarities on the first execution, yielding a prediction of what dissimilarities would be expected for the second execution, if representation scaled with activation. This calculation was applied to activity patterns to each of the parcels on a regularly tessellated cortical surface (**Figure 4.3c**). Around the central sulcus, i.e. including M1, the observed dissimilarities on the second execution were significantly lower than what was predicted from the reduction in overall activity (**Figure 4.3c**). In contrast, observed dissimilarities on the second execution in parietal areas were quite close to the prediction based on dissimilarities scaling proportionally with average activity.

To quantify whether the reduction in dissimilarities differed qualitatively across regions, we subjected the difference between the observed dissimilarities on 2nd execution from those predicted under the scaling model to a one-way ANOVA with the main effect of region, which was significant ($F_{(2,50)}$=7.42, p=1.5e^{-3}). Post-hoc t-tests revealed that this was driven by a significantly larger deviation from scaling in M1 as compared to SPLa ($t_{(25)}$=3.55, p=1.56e^{-3}). M1 and PMd did not differ from one another ($t_{(25)}$=1.25, p=.22). There was a significant difference between PMd and SPLa ($t_{(25)}$=2.65, p=.013), indicating a more 'scaling-like' representation in SPLa. Altogether this indicates that representational change with repetition differed across regions: proportional scaling of representation in parietal regions, and violation of proportional scaling in M1, where a much more pronounced decrease of dissimilarities was observed.

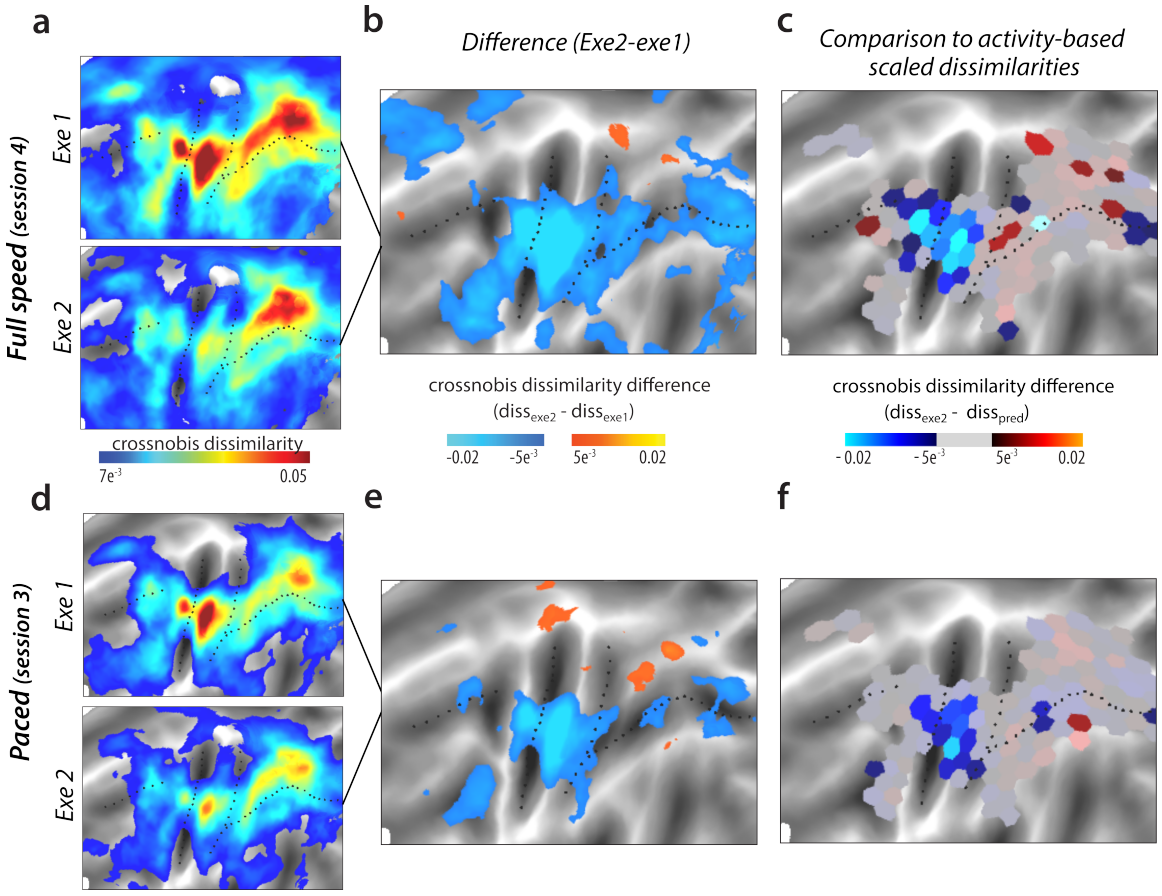

Figure 4.3. Representational change with repetition of sequence execution.

a) Dissimilarities between pairs of sequences in session 4, split by first and second executions. **b)** Difference in pattern dissimilarities between executions 1 and 2. Blue hues reflect relatively lower dissimilarities on the second execution. **c)** Difference between the observed dissimilarity during execution 2 and the predicted distance based on the reduction of activation with repetition. Blue hues indicate lower dissimilarities than predicted, red higher. The difference between the two was significant with $p<.05$ in tessels which are fully visible (i.e. not greyed out). **d-f)**: Same as **a-c** but for the paced speed session, i.e. session 3. Same thresholds were applied to the visualizations as the respective figures from a-c.

4.3.4 Decomposing representations across executions 1 and 2

Analysis of average dissimilarities across executions revealed a compression of representation in M1, but not in parietal regions. This analysis, however, does not reveal which aspects of the representations are responsible for this regional difference. To investigate exactly how the representation changed, we decomposed the representations during each execution into several underlying representational components. Differences in the sequence patterns could reflect differences in various characteristics, or features (**Figure 4.4a**). Specifically, based on previous results (Yokoi et al., 2018; Yokoi and Diedrichsen, 2019), we hypothesized that the covariance (or similarity) between activity patterns can be explained with the following 5 components (**Figure 4.4b**, see section 4.2.11 for details): *1) first finger:* a pattern component determined by the starting finger, *2) all fingers*: a pattern component that simply adds the finger-specific patterns regardless of their sequence, *3) sequence type*: trained and untrained sequences have different average patterns, *4) trained sequence identity*: the trained sequences differ amongst each other, *5) untrained sequence identity*: the untrained sequences differ amongst each other. Using pattern component modelling (Diedrichsen et al., 2017), we constructed a model family, which consisted of all possible combinations of those 5 components, totalling $2^5 = 32$ models. These models were then fit to the observed regional covariance structure (second moment matrices; **Figure 4.4c**), separately for executions 1 and 2. In all regions and across both executions, several models accounted for observed data well, with model fits as good as the noise ceiling model (M1: 21 models for exe 1, 24 for exe 2; PMd: 16 for exe 1 and 2, SPLa: 16 for exe 1 and 2), showing that overall these models accounted well for the observed data. To integrate the results across models, we used Bayesian model averaging to estimated which components were most important to explain the patterns.

In M1, the regional representation on the first execution was accounted for by the individual movement elements (all fingers), with especially high weight on the first finger (**Figure 4.4d**). This replicates the previous findings showing that M1's representation during sequence production tasks can be fully explained by the starting finger (Yokoi et al., 2018; Yokoi and Diedrichsen, 2019). In these two studies, the number of times each of the five fingers was pressed was held constant across all sequences. In the current study,

we did not match this number. Thus, the subsequent finger presses, encoded in the 'all finger' component, also accounted for substantial variance, independent of the exact ordering of these movements.

To statistically quantify these effects, we calculated component Bayes factors for individual components. In M1, the Bayes factors were significant for both first and all finger factors (first finger: BF=6.8, $t_{(25)}$=3.1, p=4.8e^{-3}; all fingers: BF=9.6, $t_{(25)}$=4.4, p=1.7e^{-4}). In contrast, the component Bayes factors were not significant for any sequence-related feature – neither sequence type (BF_c=3.2, t=1.9, p=.07), nor sequence identity: of trained sequences (BF_c=1.6, $t_{(25)}$=1.5, p=.16) or untrained sequences (BF_c=0, $t_{(25)}$=-0.2, p=.85). Thus, the pattern analysis clearly shows that activity patterns during the first execution in M1 can be explained by a superposition of individual movements, without any evidence of a sequence representation.

In SPLa and PMd, the variance explained during the first execution was well accounted for by sequence type (SPLa: BF_c=16.3, $t_{(25)}$=6.0, p=3.0e^{-6}, PMd: BF=15.5, $t_{(25)}$=5.94, p=3.3e^{-4}), and trained sequence identity (SPLa: BF_c=5.4, $t_{(25)}$=3.4, p=2.5e^{-3}; PMd: BF_c=4.6, $t_{(25)}$=2.8, p=.011). There was no significant evidence for representation of untrained sequence identity in either of the regions (SPLa: BF_c=0.8, PMd: BF=0.1; $t_{(25)}$<=1.1, p>=.28). In comparison to M1, the variance related on individual movements – either the first finger or all fingers were weaker across PMd and M1. In PMd the first finger still accounted for some variance (BF_c=4.1), but this was further reduced in SPLa (BF_c=0.5).

In M1, the pattern component related to the first finger drastically reduced by 93% with repetition (**Figure 4.4d**). The reduction in variance explained by the first finger component was larger than for the all finger component, which reduced by 75% (paired t-test: $t_{(25)}$=9.03, p=2.4e^{-9}). This indicates that the drastic reduction of average dissimilarities in M1 with repetition is mostly due a pronounced first-finger effect during the first execution that almost vanishes on the second execution. This was further confirmed with a significant correlation between the amount of first finger suppression and reduction in dissimilarities ($r_{(25)}$=0.43, p=0.027). In other words, participants who displayed further

reduction of the first finger effect also showed stronger reduction in observed dissimilarities.

Large reductions in first finger effect were also observed in session 4 in PMd (by 81%) and SPLa (by 83%). In contrast, the representation of sequence type and trained sequence identity in these areas clearly reduced less (PMd: sequence type: 44%, trained sequence: 64%; SPLa: sequence type: 49%, trained sequence: 55%). To statistically quantify whether the first finger effect reduced more than trained sequence component, we performed a paired t-tests on the percentage reduction across the two components. The results of tests were indeed significant for both PMd ($t_{(25)}$=7.96, p=2.6^{-8}) and SPLa ($t_{(25)}$=12.8, p=1.7e^{-12}).

In summary, SPLa's regional activation patterns were better accounted for by components related to the sequence identity than to the first finger, which also reduced much less with repetition. This likely explains why the average dissimilarities did not compress with repetition in SPLa regions as much as in M1. With repetition, the proportion of different components to overall regional representation remained relatively stable in SPLa (**Figure 4.4e**), but changed substantially in M1 in that the dominant first-finger representation on the first execution nearly disappeared on the second execution. This was affirmed by an execution x ROI (SPLa, M1) ANOVA comparing the relative amount of variance accounted for by the first finger component. Both main effects were significant (execution: $F_{(1,25)}$=66.39, p=1.68e^{-8}, region: $F_{(1,25)}$=85.98, p=1.44e^{-9}), as well as the interaction between the two ($F_{(1,25)}$=42.33, p=8.16e^{-7}). Thus, the decrease in M1's first finger representation on repetition was more pronounced than that of SPLa. PMd's representation was in-between those of M1 and SPLa – more variance was accounted for by the first finger than in SPLa, but less than in M1.

Figure 4.4. Component decomposition of regional representation across executions 1 and 2.

a) Executed 9-digit sequences. **b)** Candidate component models used to assess regional representations across first and second executions. Each row and column indicate a specific sequence, and values in the matrices reflect the correspondence across sequences on that component, with yellow indicating higher correspondence. **c)** Regional representations during the first execution of sequences, as assessed by the crossvalidated second moment matrix, averaged across subjects of group 1. Similar as for models, each row and column reflect an activation pattern for an individual sequence. Regions: primary motor cortex (M1) and anterior superior parietal lobule (SPLa). **d)** Variance explained by candidate model components on executions 1 (black) and 2 (grey) during the full speed session in M1, PMd (dorsal premotor cortex) and SPLa. Error bars reflect the standard error of the group mean. **e)** Relative contribution of variance explained in d) across the different components. The total variance explained across the different components (i.e. sum of the bars in d) was normalized across the two executions to display the relative shift of importance of different representational components. **f-g)**: Same depiction as **d-e** for the results of activity patterns during the paced scanning session.

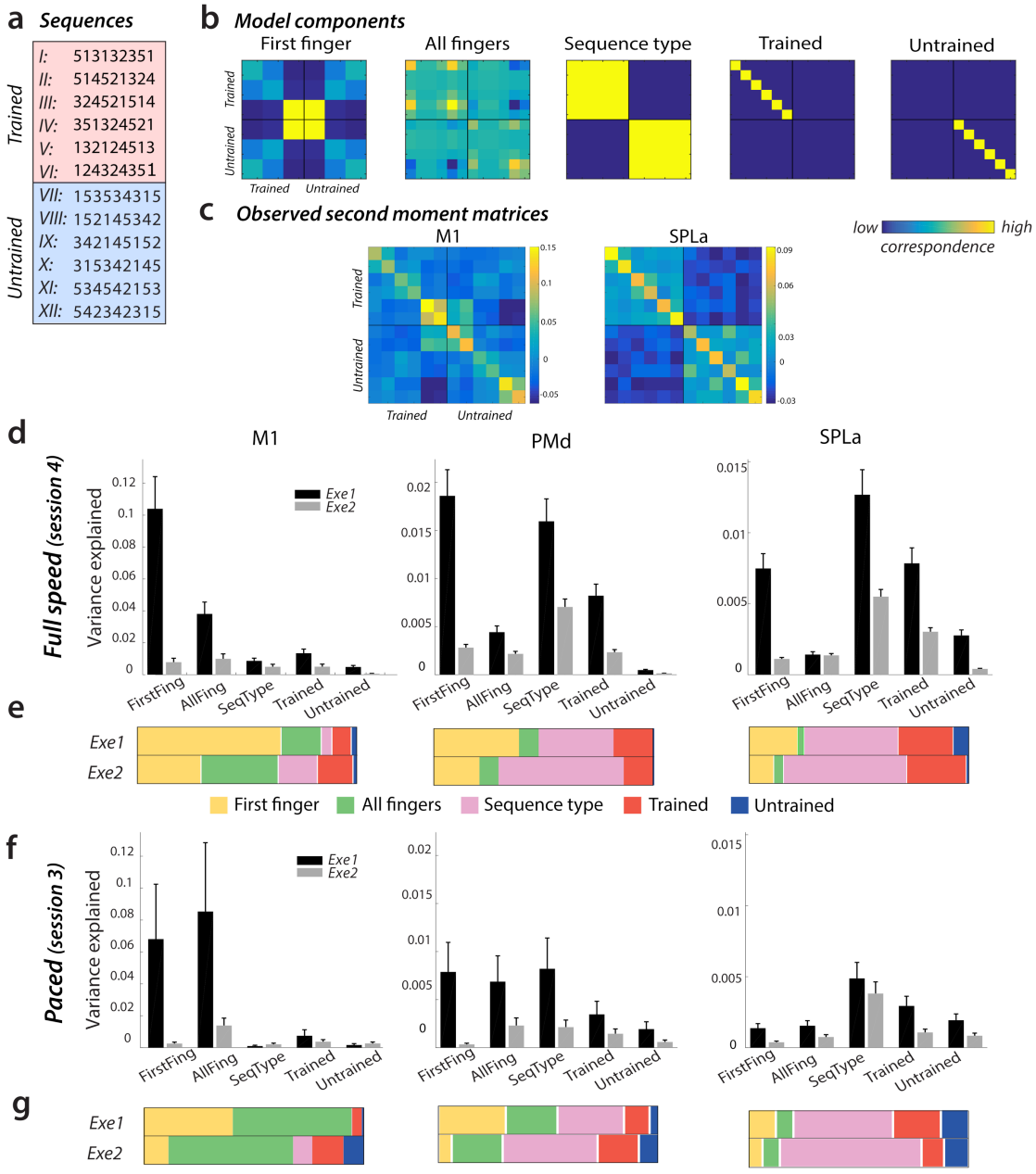
a Sequences
Trained
I: 513132351
II: 514521324
III: 324521514
IV: 351324521
V: 132124513
VI: 124324351
Untrained
VII: 153534315
VIII: 152145342
IX: 342145152
X: 315342145
XI: 534542153
XII: 542342315
b Model components
First finger
All fingers
Sequence type
Trained
Untrained
c Observed second moment matrices
M1
SPLa
low
high
correspondence
d
Full speed (session 4)
Variance explained
M1
PMd
SPLa
Exe1
Exe2
FirstFing
AllFing
SeqType
Trained
Untrained
e
First finger
All fingers
Sequence type
Trained
Untrained
f
Paced (session 3)
g

4.3.5 Effect of speed on repetition effects

It is important to note that the speed of execution differed between trained and untrained sequences in session 4 (**Figure 4.1c**). This speed difference could conflate the observed effect of learning. To control for this factor, we had designed the study to include an extra session, session 3, which was also performed after learning was completed, but with paced performance. Specifically, the movement speed in session 3 was matched between trained and untrained sequences, as well as to performance observed in session 1.

We have previously reported that after learning, crossnobis dissimilarities for trained sequences are affected by the speed of execution. Specifically, the dissimilarities between trained sequences were lower for paced session (session 3) than full speed session 4 in PMd and SPLa, but not in M1, where there was no distinction between trained and untrained dissimilarities in either session (Berlot et al., 2020; **Figure 4.2i** – comparison session 3-4). Similarly, RS in PMd and SPLa was also less pronounced in session 3. The RS did not differ significantly between trained and untrained sequences in session 3 ($t_{(25)}$<=1.22, p>=.23; **Figure 4.2d**). In M1, the difference in RS was also strongly reduced, but remained just above the significance threshold ($t_{(25)}$=2.1, p=0.046). Additionally, the change in RS from session 1 to session for trained and untrained sequences were non-significant. Thus, while the speed of performance clearly influenced the strength of RS across regions, it nevertheless appears that M1's RS cannot be fully explained by differences in speed between trained and untrained sequences.

Next, we compared whether the speed of execution affects the decrease in dissimilarities on repetition. As for the full speed performance, we observed that dissimilarities decreased on the second execution (**Figure 4.3d-e**). As reported for the full speed performance, the reduction in dissimilarities was more pronounced in M1 as compared to SPLa ($t_{(25)}$=2.80, p=9.6e^{-3}).

Finally, we assessed whether the reduction in representational components on repetition (especially the finger effect in M1) is observed even during paced performance. Overall, our PCM modelling accounted for less variance during the paced performance compared to full speed performance (**Figure 4.4d,f**). We have previously reported that the

patterns of activity are much more distinguishable and have higher signal-to-noise ratio during the full speed session compared to paced performance (Berlot et al., 2020), which likely accounts for this difference.

Interestingly, the overall amount of the first- vs. all-finger components varied with speed. During full speed performance the first finger component accounted for a larger part of the pattern variance than during paced performance (**Figure 4.4d-g**). This was confirmed by an significant interaction of a session x component (first / all fingers) ANOVA in M1 ($F_{(1,25)}$=17.3, p=3.3e^{-4}). Nevertheless, a similar reduction of the first-finger effect in M1 was observed for the paced session as for the full speed session (first finger reduction by 92%, all finger by 66%; $t_{(25)}$ = 3.12, p=4.5e^{-3}), suggesting that the decrease of the first finger weight on repetition did not depend on the speed of execution. The reductions in first finger effect were larger than for trained sequence components also in PMd and SPLa (PMd: $t_{(25)}$=2.34, p=0.02; SPLa: $t_{(25)}$=8.11, p=1.8e^{-8}). Altogether this confirms that the larger reduction of the first finger effect with repetition does not depend on the speed of performance.

4.4 Discussion

There are two common ways of looking at brain representations – MVPA and RS. In MVPA-types of analyses, differences in multivoxel activity patterns across conditions are interpreted to reflect that the region represents conditions as distinct. In RS, activity reduction on repetition is interpreted as the region representing the stimulus dimension along which the repetition occurred (Grill-Spector et al., 2006). For example, if a region shows less activity every time the colour of a visual stimulus repeats (rather than the shape, texture, etc.), it would provide evidence for a role of the region in the analysis of colour. The question on the relation between RS and pattern dissimilarities measures has been addressed before especially in visual neuroscience (Sapountzis et al., 2010; Epstein and Morgan, 2012; Hatfield et al., 2016; Mattar et al., 2018; Davis and Poldrack, 2013), but the two have not been directly compared before in the motor domain.

We combined the two methods to investigate changes during motor sequence learning. Using pattern analysis, several fMRI studies have failed to provide evidence that M1 obtains a motor sequence representation with learning (Wiestler and Diedrichsen, 2013; Yokoi et al., 2018; Berlot et al., 2020). In contrast, a study using RS (Wymbs and Grafton, 2015) reported learning-related changes even for M1, which suggests a development of sequence-dependent representation. Here we report that both techniques showed the development of sequence-specific representations in premotor and parietal cortices. In contrast, the two metrics provided discrepant insights into M1 – we observed some evidence for learning-related changes using RS, but not pattern dissimilarities. Additional control analyses suggest that this difference was not completely driven by the difference in the speed of execution, although higher speed of execution increased RS across regions.

As Wymbs & Grafton (2015), we found changes in RS in M1 across learning sessions, as well as a difference between trained and untrained sequences in sessions post-training. However, the specific evolution of the changes differed between the two studies. Wymbs and Grafton reported a complex increase-decrease-increase pattern of RS in M1 depending on the level of the training of the sequence. In contrast, we report higher RS for trained than untrained sequences after training. There are a number of important differences in the design of the two studies which could have contributed to the observed differences in results. For instance, their design only employed full speed performance, the probability of sequence repetition was lower, and the training was longer and had three groups of sequences (highly, medium, and lightly trained) rather than just two (trained and untrained). Further studies, directly manipulating these differences, are needed to reconcile the findings reported here relative to the previous report of Wymbs & Grafton (2015).

To assess in more detail what aspects of regional representation are sensitive to repetition, we decomposed regional representations into different underlying components (e.g. first finger, combination of all fingers, sequence identity, etc.), separately for the first and second execution. We observed that M1 mainly represents the first finger in a sequence. This component diminishes dramatically on repetition. In contrast, the representation of sequence type and identity, which accounted for most of the variance in

parietal areas, remained more stable across the two executions. Activation patterns in PMd reflected a mixture of sequence-related representations (as in parietal regions), which remained stable with repetition, and representations related to single movements (as in M1), which diminished with repetition. Altogether, our results suggest that RS acts differently on different components of neuronal representations. Depending on the representational composition of each region, RS can therefore be more or less pronounced. Specifically, regions that represented more transient information about a sequence (first finger) shows particularly strong suppression of dissimilarities with repetition, while regions that represent more persistent information (sequence type and identity) show a more proportional reduction of representation with activity.

Our findings can be summarized in the following – admittedly rather speculative – model of how parietal/premotor areas and M1 interact during skilled motor sequence performance. During the first execution, premotor and parietal regions contain information about the specific sequence that needs to be executed (**Figure 4.5**). Premotor regions also reflect the starting finger of the sequence. These regions send signals to M1, pre-activating the neural circuits for the movement of the first finger. This replicates a previous finding that the difference between M1's activation patterns is explained by the starting finger, rather than true sequence representation (Yokoi et al., 2018). The finding is also consistent with results from neurophysiology (Averbeck et al., 2002) and magneto-encephalography (MEG; Kornysheva et al., 2019) showing that the first action in a sequence is most highly activated in premotor and motor areas during the preparatory period.

Upon repetition, activation reduces across all regions. The decomposition analysis indicates that the sequence identity component in premotor and parietal regions reduces only moderately, suggesting that the sequence representation is always necessary to successfully guide M1 through the correct sequences of actions. In contrast, the pre-activation of the first finger reduced dramatically, possibly reflecting reduced planning needs on repetition (Ariani et al., 2020). Thus, the especially pronounced RS effect in M1 may be due to the fact that fMRI activity here is driven to a large degree by the initial input from other regions that prepares this region for the first execution of a sequence. On the second execution, the need for this pre-activation may be substantially reduced.

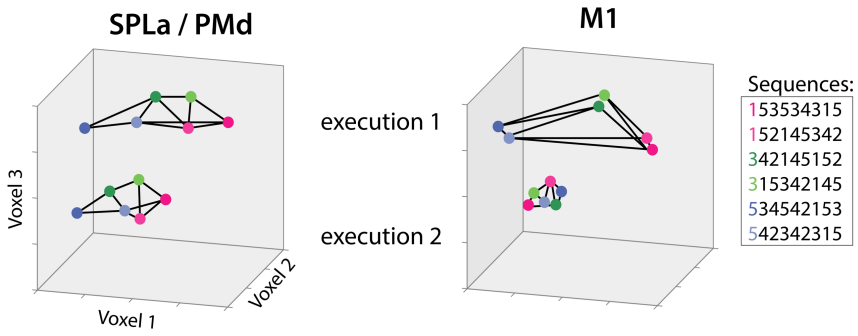

Figure 4.5. Conceptual depiction of changes in representation across regions and with repetition.

Different dots represent activation patterns for different finger sequences. Regions: anterior superior parietal lobule (SPLa), dorsal premotor cortex (PMd), primary motor cortex (M1). Activation levels of three hypothetical voxels are indicated across the three axes.

Overall, our results suggest that M1 does not represent individual trained sequences with learning, despite increased RS. Instead, it appears to represent individual finger presses. Nonetheless, we did find some evidence that RS in M1 was stronger for trained than untrained sequences. The effect was statistically not particularly strong in session 3, and we were not able to conclusively show that it was not, at least partially, caused by the trained vs. untrained differences in MT in session 4. Overall, however, our data is more in favour of the presence of a real effect than for its absence. If true, could the remaining effect be driven by a true learned sequence representation in M1? Since fMRI activity reflects a combination of the input to a cortical region and recurrent activity (Logothetis, 2002), but not the output spiking (Picard et al., 2013), we suggest that M1's sensitivity to sequence type reflects differences in the received input to M1, with more efficient communication from higher-order areas on repetition of trained sequences. Some support for this idea comes from a recent study demonstrating layer-specific effects in M1 (Persichetti et al., 2019). By measuring changes in cerebral blood volume across layers, the authors demonstrated that superficial M1 layers (which reflect M1's inputs) show RS, whereas deep layers' activation (which is more indicative of M1's outputs) is enhanced during repetition. Since the BOLD signal is biased towards the superficial vascular signals, our activation results more likely reflect inputs into M1.

Still, rather than input from other areas, increased RS in M1 could reflect sequence dependency at a subvoxel resolution (Grill-Spector and Malach, 2001; Grill-Spector et al., 2006), which cannot be detected by pattern analyses. A prior electrophysiology study provided some support for this, demonstrating differential M1's responses to trained relative to random sequences (Matsuzaka et al., 2007). However, this study did not show differential activation for different trained sequences, thus no sequence representation as defined here. Moreover, recent electrophysiological studies have also shown that M1 does not represent the sequential context (Russo et al., 2020; Zimnik and Churchland, 2021). Altogether, this makes it unlikely that the RS observed in M1 reflects sequence dependency.

Our proposed model makes a number of predictions that could be tested using a combination of techniques. For layer-specific fMRI studies, we would predict that the first

finger effect in M1 can be mostly found in the superficial layers, reflecting cortico-cortico communication. For MEG or intracranial EEG studies (Ghuman et al., 2008; Gilbert et al., 2010; Korzeniewska et al., 2020) we would predict that the difference between trained and untrained sequences would be mainly present at the start of the sequence, an effect that would strongly reduce on repetition. Addressing these questions will advance our understanding of motor sequence on neural circuitry underlying production of skilled actions.

We demonstrated that RS may not only reflect a suppression of a specific representation in a region, but that the role of the region, and hence the structure of the representation, can change qualitatively from the first to the second repetition. While the representation of the skilled motor sequences remained relatively stable in parietal and premotor regions, the M1's representation changed, with a strongly reduced activation related to the beginning of the sequence. These results emphasize that employing RS only using the average regional activation sometimes provides incomplete, and possibly misleading, insights into regional representation. Instead, the combination of RS with pattern analyses can illuminate how representations change with repetition, and may provide a deeper understanding of brain circuits and their function.

4.5 References

Alink, A., Abdulrahman, H., Henson, R.N., 2018. From neurons to voxels - repetition suppression is best modelled by local neural scaling. Nat. Commun. 9, 1–10.

Ariani, G., Pruszynski, J.A., Diedrichsen, J., 2020. Motor planning brings human primary somatosensory cortex into movement-specific preparatory states. bioRxiv.

Averbeck, B.B., Chafee, M. V, Crowe, D.A., Georgopoulos, A.P., 2002. Parallel processing of serial movements in prefrontal cortex. PNAS 99, 13172–13177.

Barron, H.C., Vogels, T.P., Emir, U.E., Makin, T.R., O'Shea, J., Clare, S., Jbabdi, S., Dolan, R.J., Behrens, T.E.J., 2016. Unmasking Latent Inhibitory Connections in Human Cortex to Reveal Dormant Cortical Memories. Neuron 90, 191–203.

Berlot, E., Popp, N.J., Diedrichsen, J., 2018. In search of the engram, 2017. Curr. Opin. Behav. Sci. 20.

Berlot, E., Popp, N.J., Diedrichsen, J., 2020. A critical re-evaluation of fMRI signatures of motor sequence learning. Elife 9, 1–24.

Buckner, R.L., Goodman, J., Burock, M., Rotte, M., Koutstaal, W., Schacter, D., Rosen, B., Dale, A.M., 1998. Functional-Anatomic Correlates of Object Priming in Humans Revealed by Rapid Presentation Event-Related fMRI 20, 285–296.

Dale, A.M., Fischl, B., Sereno, M.I., Dale, A.M., 1999. Cortical Surface-Based Analysis. Neuroimage 9, 179–194.

Davis, T., Poldrack, R.A. 2013. Measuring neural representations with fMRI: Practices and pitfalls. Ann. N. Y. Acad. Sci. 1296, 108-134.

Dayan, E., Cohen, L.G., 2011. Neuroplasticity subserving motor skill learning. Neuron 72, 443–454.

Diedrichsen, J., Ridgway, G.R., Friston, K.J., Wiestler, T., 2011. Comparing the similarity and spatial structure of neural representations: A pattern-component model. Neuroimage 55, 1665–1678.

Diedrichsen, J., Yokoi, A., Arbuckle, S.A., 2017. Pattern component modeling: A flexible approach for understanding the representational structure of brain activity patterns. Neuroimage 180, 119-133.

Ejaz, N., Hamada, M., Diedrichsen, J. ouml rn, 2015. Hand use predicts the structure of representations in sensorimotor cortex. Nat. Neurosci. 18, 1034–1040.

Epstein, R.A., Morgan, L.K. 2012. Neural responses to visual scenes reveals inconsistencies between fMRI adaptation and multivoxel pattern analysis. Neuropsyhologia 50, 530-543.

Fischl, B., Sereno, M.I., Tootell, R.B., Dale, A.M. 1999. High-resolution intersubject averaging and a coordinate system for the cortical surface. Hum. Brain Mapp. 8, 272-284.

Fischl, B., Rajendran, N., Busa, E., Augustinack, J., Hinds, O., Yeo, B.T.T., Mohlberg, H., Amunts, K., Zilles, K., 2008. Cortical folding patterns and predicting cytoarchitecture. Cereb. Cortex 18, 1973–1980.

Friston, K.J., Worsley, K.J., Poline, J.-P.B., Frith, C.D., Frackowiak, R.S.J., Holmes, a. P., Worsley, K.J., Poline, J.-P.B., Frith, C.D., Frackowiak, R.S.J., 1994. Statistical parametric maps in functional imaging: A general linear approach. Hum. Brain Mapp. 2, 189–210.

Fritsche, M., Lawrence, S.J.D., de Lange, F.P., 2020. Temporal tuning of repetition suppression across the visual cortex. J. Neurophysiol. 123, 224–233.

Grafton, S.T., Hamilton, A.F.D.C., 2007. Evidence for a distributed hierarchy of action representation in the brain. Hum. Mov. Sci. 26, 590–616.

Grill-Spector, K., Henson, R., Martin, A., 2006. Repetition and the brain: Neural models of stimulus-specific effects. Trends Cogn. Sci. 10, 14–23.

Grill-Spector, K., Malach, R., 2001. fMRI-adaption: A tool for studying fucntional properties of human cortical neurons. Acta Psychol. 107, 293–321.

Gross, C.G., Schiller, P.H., Wells, C., Gerstein, G.L., 1967. Single-unit activity in temporal association cortex of the monkey. J. Neurophysiol. 30, 833–843.

Hatfield, M.,, McCloskey, M., Park, S. 2016. Neural representation of object orientation: A dissociation between MVPA and repetition suppression. NeuroImage 139, 136-148.

Henson, R.N., Ganel, T., Otten, L.J., 2003. Electrophysiological and Haemodynamic Correlates of Face Perception, Recognition and Priming. Cereb. Cortex 13, 793–805.

Kok, P., Jehee, J.F.M., de Lange, F.P., 2012. Less Is More: Expectation Sharpens Representations in the Primary Visual Cortex. Neuron 75, 265–270.

Kornysheva, K., Bush, D., Meyer, S.S., Sadnicka, A., Barnes, G., Burgess, N., 2019. Neural Competitive Queuing of Ordinal Structure Underlies Skilled Sequential Action. Neuron 101, 1166–1180.e3.

Lashley, K., 1950. In search of the engram.

Ledoit, O., Wolf, M., 2004. Honey, I shrunk the sample covariance matrix. J. Portf. Manag 30, 110-119.

Logothetis, N.K., 2002. The neural basis of the blood-oxygen-level-dependent functional magnetic resonance imaging signal. Philos. Trans. R. Soc. B Biol. Sci. 357, 1003–1037.

Matsuzaka, Y., Picard, N., Strick. 2007. Skill Representation in the Primary Motor Cortex After Long-Term Practice. J. Neurophysiol. 971, 1819–1832.

Mattar, M.G., Olkkonen, M., Epstein, R.A., Aguirre, G.K. 2018. Adaptation decorrelates shape representations. Nat Commun. 9, 1-9.

Nili, H., Wingfield, C., Walther, A., Su, L., Marslen-Wilson, W., Kriegeskorte, N., 2014. A Toolbox for Representational Similarity Analysis. PLoS Comput. Biol. 10, e1003553.

Noppeney, U., Price, C.J., 2004. An fMRI Study of Syntactic Adaptation. J. Cogn. Neurosci. 16, 702–713.

Oosterhof, N.N., Wiestler, T., Downing, P.E., Diedrichsen, J., 2011. A comparison of volume-based and surface-based multi-voxel pattern analysis. Neuroimage 56, 593–600.

Persichetti, A.S., Avery, J.A., Huber, L., Merriam, E.P., Martin, A., 2019. Layer-Specific Contributions to Imagined and Executed Hand Movements in Human Primary Motor Cortex. Curr. Bio. 30, 1–5.

Picard, N., Matsuzaka, Y., Strick, P.L., 2013. Extended practice of a motor skill is associated with reduced metabolic activity in M1. Nat. Neurosci. 16, 1340–7.

Poldrack, R.A., 2000. Imaging brain plasticity: Conceptual and methodological issues - A theoretical review. Neuroimage 12, 1–13.

Russo, A.A., Khajeh, R., Bittner, S.R., Perkins, S.M., Cunningham, J.P., Abbott, L.F., Churchland, M.M., 2020. Neural Trajectories in the Supplementary Motor Area and Motor Cortex Exhibit Distinct Geometries, Compatible with Different Classes of Computation. Neuron 107, 745–758.e6.

Sapountzis, P., Schluppeck, D. Bowtell, R., Pierce, J.W. 2010. A comparison of fMRI adaptation and multivariate pattern classification analysis in visual cortex. Neuroimage, 49, 1632-1640.

Segaert, K., Weber, K., de Lange, F.P., Petersson, K.M., Hagoort, P., 2013. The suppression of repetition enhancement: A review of fMRI studies. Neuropsychologia 51, 59–66.

Shen, S., Ma, W.J., 2019. Variable precision in visual perception. Psychol. Rev. 126, 89–132.

Shmuelof, L., Zohary, E., 2005. Dissociation between Ventral and Dorsal fMRI. Neuron, 47, 457–470.

Summerfield, C., Trittschuh, E.H., Monti, J.M., Mesulam, M.M., Egner, T., 2008. Neural repetition suppression reflects fulfilled perceptual expectations. Nat. Neurosci. 11, 1004–1006.

Walther, A., Nili, H., Ejaz, N., Alink, A., Kriegeskorte, N., Diedrichsen, J., 2016. Reliability of dissimilarity measures for multi-voxel pattern analysis. Neuroimage 137, 188–200.

Weiner, K.S., Sayres, R., Vinberg, J., Grill-Spector, K., 2010. fMRI-adaptation and category selectivity in human ventral temporal cortex: Regional differences across time scales. J. Neurophysiol. 103, 3349–3365.

Wiestler, T., Diedrichsen, J., 2013. Skill learning strengthens cortical representations of motor sequences. Elife 2013, 1–20.

Wymbs, N.F., Grafton, S.T., 2015. The human motor system supports sequence-specific representations over multiple training-dependent timescales. Cereb. Cortex 25, 4213–4225.

Yokoi, A., Arbuckle, S.A., Diedrichsen, J., 2018. The role of human primary motor cortex in the production of skilled finger sequences. J. Neurosci. 38, 1430–1442.

Yokoi, A., Diedrichsen, J., 2019. Neural Organization of Hierarchical Motor Sequence Representations in the Human Neocortex. Neuron 103, 1178–1190.e7.

Yousry, T.A., Schmid, U.D., Alkadhi, H., Schmidt, D., Peraud, A., Buettner, A., Winkler, P., 1997. Localization of the motor hand area to a knob on the precentral gyrus. A new landmark. Brain 120, 141–157.

Zimnik, Andrew J., Churchland, M.M., 2021. Independent generation of sequence elements by motor cortex. Nat. Neurosci. 1–13.

CHAPTER 5

5 General Discussion

5.1 Final summary

The overarching goal of my thesis was to assess the functional brain architecture involved in production and learning of sequences of finger movements. To this end, high-field functional neuroimaging was employed to assess brain activation in humans during production of finger movements. The use of advanced multivariate analyses techniques allowed assessment of what aspects of finger movements are represented across brain regions.

In **Chapter 2**, we assessed the functional architecture of individuated finger movements and their passive stimulation, particularly focussing on the ipsilateral sensorimotor cortices, the function of which is less well understood in motor control. As a baseline, examination was first focussed on the contralateral hemisphere. Results showed that finger representations were equally strong across the active and passive conditions, exemplifying the importance of sensory feedback in dexterous hand control (Pruszynski et al., 2016). In contrast, ipsilateral sensorimotor cortices exhibited stronger representations for the active than the passive condition. This implies that the sensorimotor areas do not receive the sensory feedback of the ipsilateral hand, and are instead engaged during active components of movements, such as planning and movement initiation. This qualitative difference observed across the hemispheres also suggests that ipsilateral representations are unlikely to originate from a passive spill-over from their contralateral counterparts.

In **Chapter 3**, we studied brain changes that accompany learning of sequences of finger movements. A longitudinal approach was used for this which included a five-week training period and four interspersed scanning sessions. A number of learning-related changes were observed for premotor and parietal regions. In those regions, the overall amount of

activation decreased across weeks and sequence-specific activation patterns reorganized, especially early in learning. On the contrary, none of the examined metrics changed with learning in M1. This provides evidence that behavioural improvements achieved with motor sequence learning are largely driven by reorganization of brain circuits outside of M1, upstream in the motor hierarchy.

In **Chapter 4**, we combined multivariate pattern analysis and repetition suppression tools to further investigate learning-related changes. While both metrics increased with learning in parietal regions, they diverged in M1. Repetition suppression (RS) increased for trained sequences across weeks, whereas pattern dissimilarities did not. This provided a discrepancy between the insights gained from RS compared to pattern analysis on whether sequence-specific changes occur in M1. However, more fine-grained analyses of representational components across repetitions revealed that M1 does not directly represent sequences. On the first execution, M1 primarily reflects the starting finger of the sequence. On repetition, this starting finger component dramatically decreases, with more equal representation of all fingers constituting a sequence. Conversely, parietal regions consistently represented individual sequences even across repetition.

Taken together, this series of projects demonstrates a functional distinction between M1 and higher-order association regions during production of individuated finger movements, as well as learning of sequential finger movements. Already in Chapter 2, this distinction was apparent with premotor and parietal ipsilateral regions representing active and passive finger parameters to similar degrees, whereas primary sensorimotor cortices showed a clear distinction with more pronounced representations of active finger movements. This distinction was even more pronounced in Chapters 3 and 4, where even after extensive training, M1 only represented movement sequences in terms of their constituent single finger parameters; whereas activity patterns in premotor and parietal areas changed substantially, reflecting the development of sequence-specific representations. All of this points to an important distinction and hierarchical division between M1, with its stable architecture supporting individual finger execution, and associative regions, which reflect more abstract parameters of movements and are amenable to change.

Importantly, these insights would not have been gained without using advanced functional neuroimaging analysis techniques that are aimed to reveal representations rather than just activation. In Chapter 2, only examining average elicited activation would not have revealed the distinction between active and passive finger components in the ipsilateral hemisphere, since both elicited similar amounts of deactivation relative to baseline. Conversely, representational analysis revealed a clear disparity between the two. In Chapter 3, overall activation decreased in premotor and parietal regions across all sessions, but analysis of sequence-specific activity patterns revealed a distinction across sessions, with multivariate patterns reorganizing earlier in learning (weeks 1-2), and stabilizing later in training (weeks 2-5). Chapter 4 then explicitly compared multivariate analysis tools to repetition suppression (RS), an alternative representational method. This example of the two techniques used in common serves to show how combining advanced analysis tools can provide more nuanced insights into the functional roles of different regions. Altogether, this set of studies emphasizes the importance of using analysis approaches that move beyond only estimating the average regional activation and take into consideration multivariate patterns of activity across conditions to better understand the function of brain circuitry.

5.2 Limitations

The search for neural substrates of learning is a daunting task and embarking on a longitudinal study is time-consuming and often unforgiving: late realizations of potential design limitations come, well, too late. There are a number of limitations of the presented chapters on learning which are discussed below.

An important feature of our design was to include sessions where participants performed at equal, paced speed for both trained and untrained sequences, as well as an additional session at the end of training where they were allowed to execute sequences as fast as possible. This was our compromise to the learning and performance conundrum in longitudinal approaches (highlighted in section 1.4.3 of Chapter 1). Paced performance allowed us to compare the overall evoked activity across sessions, as well as contrast

activity between trained and untrained sequences. This was essential to obviate the confound of whether overall activity changes with learning or speed alone. However, the session where participants performed at full speed revealed several important advantages. It was only in this session that we observed higher pattern dissimilarities for trained than untrained sequences in associative regions. Moreover, only at full speed did we see significant pattern dissimilarities between trained sequences in the basal ganglia. This suggests that the full speed session provided higher signal-to-noise ratio to better distinguish sequence-specific patterns. Thus, had we included the full speed design across all weeks, it is possible we would have observed how and when activity patterns for trained sequences become distinguishable. It would also have allowed for more careful representational decomposition of regional activity patterns across sessions, which would have provided additional insights into how different features of performed sequences (all vs. first fingers, sequence type vs. sequence identity) emerge. At present this was most achievable with the final, full speed session. As practical advice for future research, the speed of execution should be controlled when assessing average activation change with learning, but when interested in more representational changes, sacrificing this control of performance is likely worth the added power and sensitivity to delineate multivariate changes.

Another limitation was our choice of untrained sequences. The set of untrained sequences did not change across weeks, making them thus 'minimally trained'. It is possible, therefore, that the distinction between trained and untrained sequences would have been larger for the examined metrics, had we used a new, random, set of sequences in each scanning session. Nonetheless, having the same set of sequences across sessions allowed us to assess the stability of sequence-specific patterns for untrained sequences, which would have been impossible with changing sequences. Of course, having both random as well as untrained sequences would have been optimal, but this would have led to longer scanning sessions, or less data obtained for each sequence.

Perhaps the biggest limitation of our training study is its duration. Five weeks of training might seem a long time when considering the feasibility of such a study in a span of a PhD or other experiments in the field (with the only longer training paradigm being

the study by Wymbs & Grafton, 2015). However, five weeks is by no means 'long' compared to real-life acquisitions of expertise, such as intentional practice in sports or music. Expert performers of motor skills usually practice for at least 10 years and perform millions of trials (Ericsson et al., 1993). Therefore, we cannot exclude the possibility that sequence-specific representations in M1 would develop for longer durations of training. Some studies of musicians support this idea. For instance, it has been shown that the representations of fingers in sensorimotor cortices are enlarged in violinists for their left (fingering) hand, but not for their right hand (Elbert et al. 1995). Moreover, there are reports of anatomical enlargement of M1's hand area in musicians (Amunts et al., 1997), providing a link between extensive usage of fingers and M1's anatomy. Notwithstanding, research also demonstrates that professional expertise leads to changes in other higher-order brain regions than M1. There are reports of decreased and more focused activation patterns across premotor and parietal regions in professional musicians relative to controls (Lotze et al., 2003), implying increased efficiency of these regions with practice, similar to what I report in this thesis. Additionally, musical expertise modulates higher-order brain functioning across fronto-temporal networks (Oechslin et al., 2013). Altogether this implies that extensive training leads to widespread changes in brain function, and not just in regions related to motor execution. This focus on M1 as the locus of expertise might come about because overt execution-related improvements are most easily observable with practice. This does not necessarily translate directly to brain changes on the execution level of M1, a fallacy I will come back to later in the discussion (section 5.4).

5.3 Extensions of current work

5.3.1 Plasticity of the ipsilateral hemisphere

Chapter 2 addressed the question of how the ipsilateral hemisphere represents individual finger movements (and their sensory feedback), while Chapters 3 and 4 focussed exclusively on the contralateral hemisphere. Yet, inspecting how the ipsilateral hemisphere represents complex movements and is modulated by learning might be particularly

interesting for two reasons. One, it has been shown that the ipsilateral hemisphere is relatively more involved in complex actions compared to simple actions (Verstynen et al., 2005). Two, motor skills are known to generalize across hands with performance improving even on hand that is not directly trained, which is referred to as intermanual transfer of learning (Lee et al., 2010; Sakai et al., 2003; Wiestler et al., 2014). Some models of intermanual transfer suggest that this occurs when, during training, the activity spreads through transcallosal connections from the trained contralateral cortex to the ipsilateral hemisphere, hence causing learning of the untrained hand (Lee et al., 2010). An alternative set of models predicts that learning occurs mostly in the hemisphere contralateral to the trained hand, but that these learnt representations are accessed when the untrained, ipsilateral hand is tested, resulting in the improved performance (Parlow and Dewey, 1991). Since we did not assess the performance of the untrained hand in the scanner, we cannot directly test these two model types.

While not covered in the published version of Chapter 3, during the analysis efforts I investigated how the ipsilateral hemisphere changed with learning (**Figure 5.1**). First, the average activity of the ipsilateral M1 was suppressed below the resting baseline during production of finger sequences in all sessions, whereas premotor (PMd) and parietal (SPLa) regions showed significant activation. Second, the activation elicited in associative regions was larger for movements of the contralateral hand, compared to the ipsilateral hand. This pattern of results matches with what we reported for single finger movements – there we observed that the contralateral hemisphere was more activated for both active movement and passive finger stimulation than the ipsilateral hemisphere. Third, activation in ipsilateral PMd and SPLa was modulated by learning – similar to their contralateral homologs, their activation decreased across sessions with paced performance (sessions 1-3), and more-so for trained than untrained sequences. This distinction between trained and untrained sequences was also preserved in the full speed session. Thus, while activation in the ipsilateral associative regions showed similar learning-related effects as in the contralateral hemisphere, those regions were less involved than the contralateral hemisphere. Further studies should employ performance of both hands during brain imaging to better decipher what the role of ipsilateral hemisphere is in learning transfer across hands.

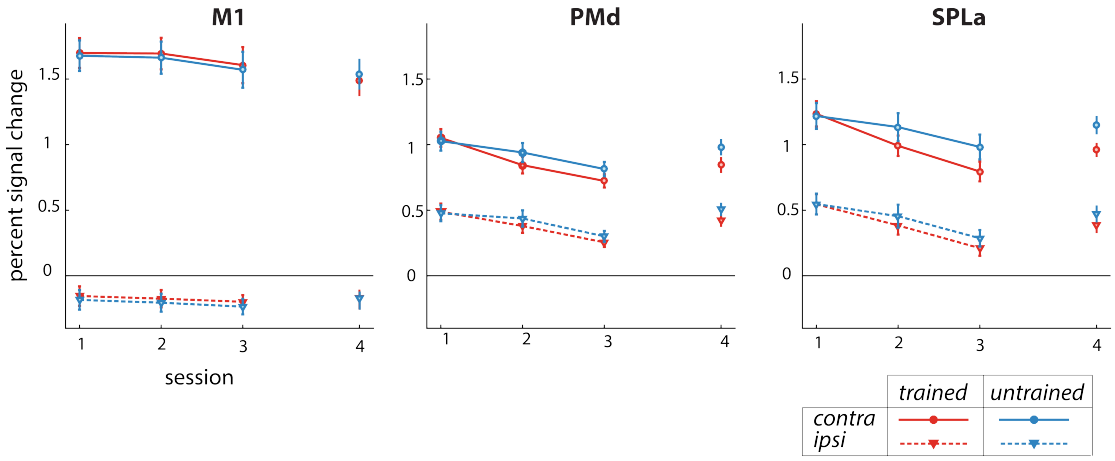

Figure 5.1. Changes in activation during motor sequence learning across contralateral and ipsilateral hemispheres.

Activation across scanning sessions, as measured by percent signal change over resting baseline. Regions: primary motor cortex (M1), dorsal premotor cortex (PMd), anterior superior parietal lobe (SPLa). Solid lines are for contralateral hemisphere to the performing hand, dashed lines for ipsilateral, red for trained and blue for untrained sequences. Error bars reflect the standard error of the group mean.

5.3.2 Relating representations across regions

Chapters 2 and 3 characterized learning-related changes of different brain regions. Changes in brain regions are, however, not independent of one another. On the contrary, brain regions constantly interact. Thus, how communication between brain regions changes with learning is an important question, which was not investigated in this thesis. But more broadly in the field, a number of studies have examined how connectivity between brain regions changes as a function of motor learning. Reported results include decreases in the correlation between visual and motor regions with motor sequence learning (Bassett et al., 2015), suggesting a growing autonomy of motor and visual systems with growing expertise. Interestingly, individual differences in the baseline connectivity between visual and motor systems seem predictive of the future learning ability, suggesting that the connectivity of brain systems plays a role in behavioural adaptability (Mattar et al., 2018). Besides, a number of other connectivity changes have been reported with learning: increasing number of connections between specific areas, increased connection strength, more efficient transfer of information across regions, reconfiguration of how brain regions are connected with one another, etc. (Mantzaris et al. 2013; Heitger et al. 2012; see Bassett & Mattar 2017 for a review). Altogether, these studies exemplify the importance of considering the system as a whole, and not purely as segregated regions.

The most common approach in these studies is to assess interactions between brain regions by analyzing how their univariate responses co-vary (univariate functional connectivity; Biswal et al. 1995). In other words, activity of different regions is first averaged on the regional level, and then correlated across regions. Further metrics, such as those derived from graph connectivity approaches (Bullmore and Sporns, 2009) can then be performed on the obtained inter-regional correlation values. However, as demonstrated in all of the chapters of this thesis, patterns of responses within regions are multidimensional, or multivariate, and contain information that can be lost by averaging across all voxels in a region (Mur et al., 2009). Therefore, just as studies examining only the average BOLD responses can be blind to information contained in multivariate patterns of activity, such functional connectivity approaches do not measure fluctuations in information represented in multivariate patterns. An important question to pursue in the

future is how multivoxel information interact across regions. The importance of this question has been recognized in the neuroimaging field in recent years, with several papers advocating for moving beyond a univariate metric of connectivity to instead capture the multivariate nature of regional interactions (Anzellotti et al., 2017; Anzellotti and Coutanche, 2018; Basti et al., 2020). Therefore, the next frontier is to use multivariate connectivity metrics on longitudinal data to shed further light on how the relationship between the representations of different brain regions changes with learning.

5.4 Future avenues in studying sequential motor skills

The presented chapters on motor sequence learning (Chapters 3 and 4) provide evidence of widespread learning-related changes in associative regions of the neocortex. However, no such effects were observed in M1, which speaks against the idea that a motor engram forms in this region with learning (Berlot et al., 2018). This might be surprising to many, especially given the focus M1 has received in the motor learning literature. Instead of this conceptualization, our data are more compatible with the view that motor sequence learning is supported by an emergence of sequential representations upstream in higher-order association regions. Chapter 4 provided some evidence for a distinction between premotor and parietal areas – with parietal regions primarily representing individual sequences, whereas premotor regions also contained information on the constituent fingers, especially the starting finger, of the executed sequences. Apart from that, however, we cannot provide more detailed insights into what flavour these 'sequence representations' in cortical association regions come in. It seems that our pursuits in further delineating the circuitry involved in motor sequence learning have come to a halt. Why might this be? In this section, I will expose four common fallacies (applicable also to this thesis) that might be standing in the way of our pursuits: one, focussing on the execution time as the measure of learning; two, directly mapping learning processes onto brain regions; three, inferring latent processes from the brain location where we observe learning-related changes; four, preconceived ideas of motor sequence organization influencing our experimental designs and analyses. Last, I will suggest some novel paradigms to further probe how motor sequences are organized in the brain.

5.4.1 Fallacy 1: Learning is not a monolith

The most pronounced behavioural improvement in virtually any motor learning study is the speed of execution, which is commonly plotted as a learning curve (**Figure 5.2a upper**). However, instead of a singular improvement in the 'execution' process, it is more plausible that the change in speed is caused by multiple processes. In other words, learning is not a monolith construct. The plotted learning curve is most likely composed of a number of latent learning curves (**Figure 5.2a lower**). In order to draw those underlying processes, we need a richer description of the skilled behaviour, since a single behavioural index (e.g. execution time) cannot yield insights into multiple processes. One indicator could be the preparation time necessary for accurate performance (Haith et al., 2016), which has been shown to reduce with learning (Ariani and Diedrichsen, 2019). Besides preplanning, an important aspect of skillful movement is the ability to plan future responses during ongoing movements. This ongoing planning during execution has been demonstrated to improve with learning (Ariani et al., 2020a). It would be important to consider also executive processes, such as working memory and attention, which likely play an important role in motor sequence learning (McDougle and Collins, 2020). Additional indicators of latent processes might include the facilitation under repetition (Ariani et al., 2020b), the influence of sensory feedback on performance, and transfer of learning, either across stimuli or effectors (Wiestler et al., 2014). A more careful delineation of how such latent processes change with practice would further our understanding of how overt execution-related changes come about. The next step would be to formalize these different latent processes in a coherent model of motor sequence learning. Multi-process models have been extremely successful in explaining the dynamics and different facets of error-based learning (adaptation) (Joiner et al., 2017; Shadmehr et al., 2010; Smith et al., 2006), and could serve as an inspiration for developing models of motor sequence learning.

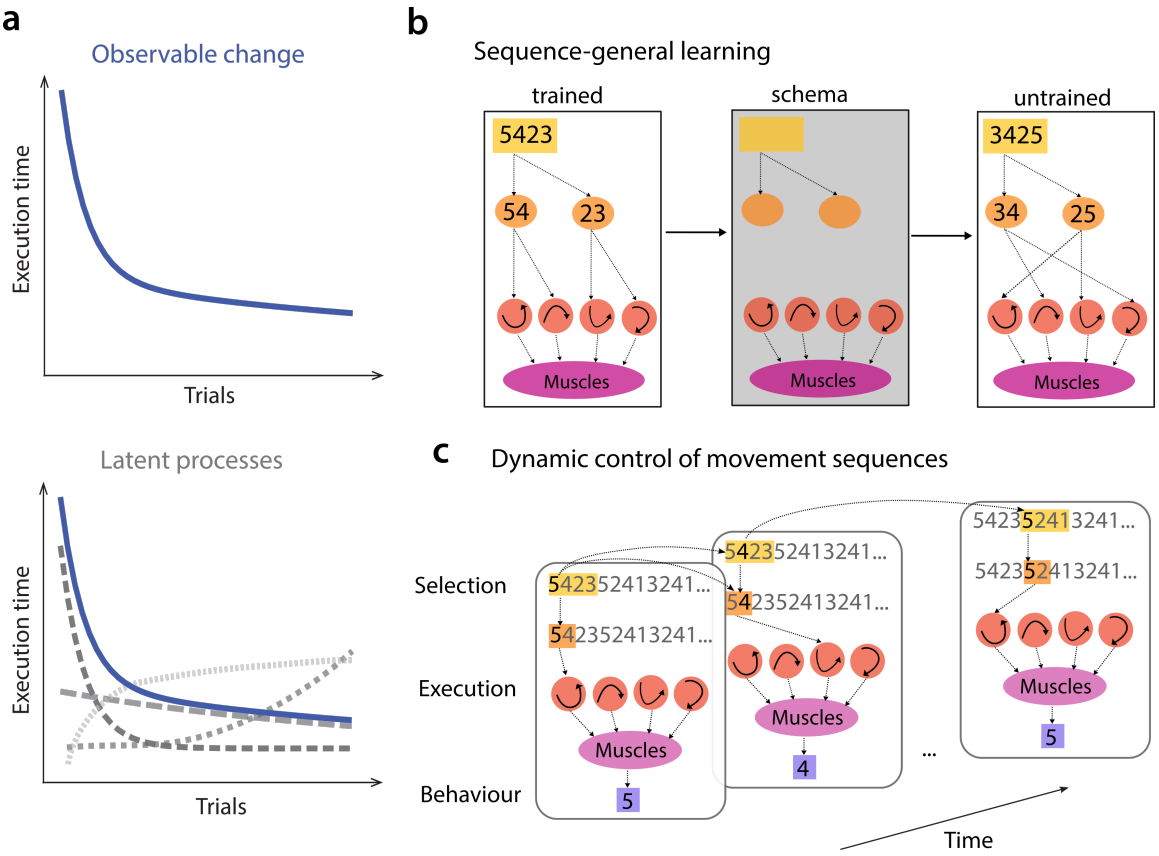

Figure 5.2. Challenges and new approaches in studying motor sequence learning.

a) Decomposing the learning curve: Observable improvements in behaviour improvements with motor sequence learning are plotted in blue – the execution time for a given sequence decreases with training. This improvement can likely be explained by several latent processes, presented in different gray lines in the lower graph. **b)** One possibility for sequence-general improvements in behaviour is a creation of an abstract schema representation, which facilitates performance for untrained sequences. **c)** Studying how sequential behaviour unfolds in continuous performance instead of separate trials with discrete sequences. Open questions include how communication occurs across different levels of hierarchy, and over time (dotted arrows).

5.4.2 Fallacy 2: No one-to-one mapping between anatomy and function

Thinking of behavioural improvements as a singular process can lead to a single-process search for brain correlates of learning. However, asking 'where does learning occur in the brain?' will not provide a meaningful answer. Instead, having models of latent processes is a first step to enable us to draw links between skill improvements and changes in brain representation. Still, these links might not allow for a one-to-one mapping of the 'what' (function) to the 'where' (anatomy). This attempt to directly map function onto anatomy is the second fallacy to keep in mind and attempt to overcome.

There are at least two possible violations of a direct one-to-one mapping between function and anatomy. One, a latent process could be instigated through an interplay between regions, instead of processes within a single region. In Chapter 4 we postulated, albeit speculatively, that the interaction between PMd and M1 might be responsible for the observed reduction of M1's activity upon repetition of trained, rather than untrained, sequences. Functionally, the communication between PMd and M1 could be related to preparing the start of the sequence, while being sensitive to the sequential context. Thus, a latent process could be instigated through a communication between regions, rather than within-region processing. Further studies are needed to test this prediction more directly, which could include approaches on representational connectivity, as discussed in section 5.3.2.

Yet another violation of the one-to-one mapping is the case when a brain region is involved in several processes. An empirical example for this comes from Chapter 4, where a decomposition of regional representations revealed that they were best described as a combination of features. For instance, PMd's representation was most prominently explained by a combination of a sequence and a first finger representation. This exemplifies that multiple latent processes possibly engage different subspaces of the same network. In summary, the answers to how latent processes of learning map onto the brain could come in non-straightforward ways that might not follow our preconceived ideas.

5.4.3 Fallacy 3: Reverse inference in interpreting results

Related to the mixed selectivity of regional representation is the fallacy of inferring a latent process is inferred from where activation is observed – e.g. execution from M1's activity, planning from PMd, etc. This was also implicitly done throughout the thesis (**Figure 1.2** in Chapter 1), where I equated the 'execution' level with M1. While the logic of reverse inference is not problematic per se, it is flawed when a specific region is involved in more than one process. In other words, if M1's activity were modulated *if and only if* when execution processes were active, the two could be equated, but we know this is not the case. Studies have shown that within M1, execution and planning can occur simultaneously in separate neural subspaces (Ames et al., 2019; Churchland et al., 2012). Thus, M1 should not be equated with the 'execution' layer. In a similar vein, the fact that we see most prominent learning-related changes outside of M1 in higher-order cortical regions should not be taken as evidence that the sequence learning task is more 'cognitive' than 'motor' in nature (Wong and Krakauer, 2019). Instead of using such reverse inference to interpret the results or jump to conclusions, it would be more useful to use such intuitions as a launching pad for more specific testable hypotheses in follow-up experiments.

5.4.4 Fallacy 4: Preconceived notions in experimental designs

The fourth fallacy relates to the fact that our preconceived ideas of how motor sequences might be organized affect our experimental designs and, through that, our inspection of brain representations. We might hypothesize that motor sequences are organized in a hierarchical fashion (with sequences, chunks, individual elements) and we design our experiment accordingly (i.e. with different sequences and chunks that individuals execute). This then allows us to search for 'chunk' and 'sequence' representations in the brain. However, brain regions do not sit around caring about 'sequence identity' or 'chunks', or any other feature we as experimenters define our stimuli as. These are just semantic labels we give to brain regions to make sense of our data. Yet, replacing first-principle thinking about brain processes with analysis labels is too often a very convenient and tempting shortcut. More concerning than labelling alone is that we might not have a strong

alternative hypothesis of what these brain regions might reflect. Both our work (Chapters 3 and 4) and previous work (Yokoi and Diedrichsen, 2019) has shown that while there is evidence for a hierarchical distinction between M1 and association regions, it is harder to decipher the role of associative regions in execution of skilled motor sequences. This lack of further delineation amongst associative regions hints that the types of designs we use are limiting our understanding of how motor sequence learning is instantiated in the brain. In light of this, it is important to consider what aspects of our experimental designs could be improved to better capture the essence of real-life sequential skills.

In the next section, I will propose three possible avenues forward: 1) investigating sequence-general improvements, 2) probing how learning occurs using a bottom-up instead of a top-down approach, and 3) characterizing brain responses during continuous sequential behaviour.

5.4.5 Novel paradigms to probe sequence organization

First, our investigations in Chapters 3 and 4 focussed on sequence-specific learning. Sequence-specific learning is commonly delineated from sequence-general improvements, which refers to improvements in behaviour that generalize to novel, random sequences (e.g. Ariani and Diedrichsen, 2019; Wiestler et al., 2014). The rationale behind studying sequence-specific learning is that the specific order of elements within a sequence is an important aspect of the acquired skill. This aspect of learnt skill cannot generalize to random sequences constructed using a different order. However, we observed significant improvements in the performance of untrained sequences (see Figure 3.2 in Chapter 3). In fact, the sequence-general improvement accounts for 50% of the effect seen for trained sequences. Several factors likely contribute to this improvement, some of which might be related to participants becoming better at keyboard handling, more comfortable in the experimental set-up, less self-conscious in front of an experimenter, etc. One particular aspect could be important in furthering our understanding of skilled sequential behaviour. Namely, during learning of specific sequences, a more abstract representation could be formed, a sequence ‘schema’ (Bartlett, 1932; Piaget, 1923; Schmidt, 1975; Zhou et al.,

2021), which allows for rapid remapping and generalization of performance to untrained sequences (**Figure 5.2b**). What constitutes a motor sequence schema might be exposed by assessing the neural representations common to different sequences (as opposed to being sequence-specific). Additionally, further behavioural assays of when learning generalizes and when it does not transfer could shine further light on this more abstract aspect of motor sequence learning. After all, rapid transfer of abstract knowledge is likely one of the things which allows pianists to more rapidly learn new musical pieces or enables chefs to quickly grasp the means of a new cooking recipe.

Second, we should ask ourselves how our 'chunks' and 'sequences' map onto something like learning to play Chopin's Revolutionary Etude on piano. Instead of top-down predefined sets of sequences or chunks, learning a piano piece likely acts through a more bottom-up approach where continuous sets of actions need to be broken up into various representations, at different levels of complexities, which can support and improve performance. One way to inspect such learning would be by providing participants with a long continuous sequence that they would need to learn in their own time and manner. With an ever-growing amount of online studies, it might be possible to recruit enough participants to start addressing how individuals self-organize to learn a new skill (rather than feed them individual trials) (see Ten et al., 2020 as a recent example of an online category learning study). One important question that could be addressed is whether chunking and hierarchical organization emerge naturally with learning, even when the task is not structured in such a way. It could be that individuals indeed self-organize and discretize the continuous sequence early in learning to aid skill acquisition (Acuna et al., 2014; Ramkumar et al., 2016; Verwey and Dronkert, 1996). Alternatively, chunking could emerge later over time, after learning the initial statistical regularities of the sequence (Beukema and Verstynen, 2018; Nissen and Bullemer, 1987). Critically, such a task would allow a different viewpoint to inspect how sequential behaviour emerges rather than by a-priori creating predefined structured sets of chunks and sequences.

Third, employing a continuous sequential design might also be insightful for probing the underlying brain representations. Instead of presenting trial-separated individual sequences, we could employ a design where an individual would (after a

behavioural practice as explained above) perform the acquired continuous skill uninterrupted for a longer time. Such a design might necessitate the use of brain imaging techniques with higher temporal resolution than afforded by fMRI, for instance magnetoencephalography (Kornysheva et al., 2019) or electrocorticography (Henin et al., 2021). This would allow us to address several interesting questions: first, do we see a similar hierarchy between M1 vs. higher-order regions in terms of representing elemental actions to execute vs. bigger units? Can we better decompose representation in association regions, perhaps by inspecting how representations are linked over time? Are there regions, or subspaces within regions, that represent the future actions rather than the currently ongoing actions? How do these representational spaces communicate (dotted arrows in **Figure 5.2c**)?

Additionally, execution of longer continuous sequences might be pertinent to address whether representations of different brain regions are better explained in terms of discrete organization (of chunks and sequences), or continuous timescales. There is a growing body of literature demonstrating a hierarchical progression of the temporal window which is processed in a given region, with primary sensory regions operating on shorter timescales than higher-order association regions (Hasson et al., 2015; Murray et al., 2014). Applied to motor sequence execution it could be that different regions represent continuous actions in buffers of different lengths, with no 'storage' of chunks or sequences. One possibility is that such a paradigm could end up revealing seemingly contradictory evidence across behaviour vs. neuroimaging: while behaviourally, discrete chunks and sequence representations would naturally emerge, cortical association regions would end up being better accounted for by a continuous than a discrete hierarchical organization. An interesting hypothesis in that case to account for this apparent discrepancy would be that there is a gate-keeper, perhaps in the basal ganglia (Tremblay et al., 2010; Wymbs et al., 2012), which is sensitive to discrete chunks and through communication to the neocortex discretizes, or gates, the continuously unfolding information from cortical association regions to the execution level. There are of course many other possible findings that could emerge from using such a paradigm. Overall, assessing brain activation during continuous sequential behaviour could be a fruitful avenue forward, possibly providing us with

alternative, perhaps even counter hypotheses to our current hierarchical sequence organization model.

To summarize, in this section I have offered some suggestions on potential novel paradigms to probe organization of sequential behaviour. This is by no means indicative that the approaches implemented thus far (including in this thesis) are fundamentally flawed. On the contrary, our understanding of motor sequence learning has drastically advanced in the recent years. Nevertheless, we should strive towards novel approaches to push the frontiers and improve our understanding of real-life sequential skills. In "real life", things are for the most part hopelessly messy – learning cannot be easily approximated using single processes, split into trials or broken down into experimenter-defined 'sequences'. Still, I believe that the suggested paradigms might capture some of the core aspects of sequential skill learning, and could form new exciting paths to study acquisition of sequential behaviour.

5.5 Conclusion

Together, the findings from this thesis demonstrate a clear functional delineation in the roles that M1 and associative regions have in production of finger movements. M1 represents execution of individual elements of motor sequences, with the M1 contralateral to the performing hand having representations of the motor command and the incoming sensory feedback tightly integrated. In contrast, the ipsilateral M1 represents active components of movements, such as planning or action initiation, but not sensory feedback. After extensive practice of motor sequences, M1 still represents only elemental movements, while associative regions show substantial and widespread learning-related changes. Thus, fundamental improvements in behaviour observed in sequence learning are likely driven by evolving changes in neural representation in higher-order regions.

5.6 References

Acuna, D.E., Wymbs, N.F., Reynolds, C. a, Picard, N., Turner, R.S., Strick, P.L., Grafton, S.T., Kording, K., 2014. Multi-faceted aspects of chunking enable robust algorithms. J. Neurophysiol. 1849–1856.

Ames, K.C., Ryu, S.I., Shenoy, K. V., 2019. Simultaneous motor preparation and execution in a last-moment reach correction task. Nat. Commun. 10, 1–13.

Amunts, K., Schlaug, G., Jäncke, L., Steinmetz, H., Schleicher, A., Dabringhaus, A., Zilles, K., 1997. Motor cortex and hand motor skills: Structural compliance in the human brain. Hum. Brain Mapp. 5, 206–215.

Anzellotti, S., Caramazza, A., Saxe, R., 2017. Multivariate pattern dependence. PLoS Comput. Biol. 13, e1005799.

Anzellotti, S., Coutanche, M.N., 2018. Beyond Functional Connectivity: Investigating Networks of Multivariate Representations. Trends Cogn. Sci. 22, 258–269.

Ariani, G., Diedrichsen, J., 2019. Sequence learning is driven by improvements in motor planning. J. Neurophysiol. 121, 2088–2100.

Ariani, G., Kordjazi, N., Pruszynski, J.A., Diedrichsen, J., 2020a. The planning horizon for movement sequences. bioRxiv.

Ariani, G., Kwon, Y.H., Diedrichsen, J., 2020b. Repetita iuvant: Repetition facilitates online planning of sequential movements. J. Neurophysiol. 123, 1727–1738.

Bartlett, F.C., 1932. Remembering: A study in experimental and social psychology. Cambridge University Press.

Bassett, D.S., Mattar, M.G., 2017. A Network Neuroscience of Human Learning: Potential to Inform Quantitative Theories of Brain and Behavior. Trends Cogn. Sci. 21, 250–264.

Bassett, D.S., Yang, M., Wymbs, N.F., Grafton, S.T., 2015. Learning-Induced Autonomy of Sensorimotor Systems. Nat. Neurosci. 18, 744–751.

Basti, A., Nili, H., Hauk, O., Marzetti, L., Henson, R.N., 2020. Multi-dimensional connectivity: a conceptual and mathematical review. Neuroimage 221, 117179.

Berlot, E., Popp, N.J., Diedrichsen, J., 2018. In search of the engram, 2017. Curr. Opin. Behav. Sci. 20., 56–60.

Beukema, P., Verstynen, T., 2018. Predicting and binding: interacting algorithms supporting the consolidation of sequential motor skills. Curr. Opin. Behav. Sci. 20, 98–103.

Biswal, B., Yetkin, F.Z., Haughton, V.M., Hyde, J.S., 1995. Functional Connectivity in the Motor Cortex. Magn. Reson. Med. 537–541.

Bullmore, E., Sporns, O., 2009. Complex brain networks: Graph theoretical analysis of structural and functional systems. Nat. Rev. Neurosci. 10, 186–198.

Churchland, M.M., Cunningham, J.P., Kaufman, M.T., Foster, J.D., Nuyujukian, P., Ryu, S.I., Shenoy, K. V., Shenoy, K. V., 2012. Neural population dynamics during reaching. Nature 487, 51–56.

Elbert, T., Pantev, C., Wienbruch, C., Rockstroh, B., Taub, E., 1995. Increased Cortical Representation of the Fingers of the Left Hand in String Players. Science 270, 305–307.

Ericsson, K.A., Krampe, R.T., Tesch-Romer, C., 1993. The Role of Deliberate Practice in the Acquisition of Expert Performance, Psychological Review. 100, 363.

Haith, A.M., Pakpoor, J., Krakauer, J.W., 2016. Independence of Movement Preparation and Movement Initiation. J. Neurosci. 36, 3007–15.

Hasson, U., Chen, J., Honey, C.J., 2015. Hierarchical process memory: memory as an integral component of information processing. Trends Cogn. Sci. 19, 304–313.

Heitger, M.H., Ronsse, R., Dhollander, T., Dupont, P., Caeyenberghs, K., Swinnen, S.P., 2012. Motor learning-induced changes in functional brain connectivity as revealed by means of graph-theoretical network analysis. Neuroimage 61, 633–650.

Henin, S., Turk-Browne, N.B., Friedman, D., Liu, A., Dugan, P., Flinker, A., Doyle, W., Devinsky, O., Melloni, L., 2021. Learning hierarchical sequence representations across human cortex and hippocampus. Sci. Adv. 7, 4530.

Joiner, W.M., Sing, G.C., Smith, M.A., 2017. Temporal specificity of the initial adaptive response in motor adaptation. PLoS Comput. Biol. 13, e1005438.

Kornysheva, K., Bush, D., Meyer, S.S., Sadnicka, A., Barnes, G., Burgess, N., 2019. Neural Competitive Queuing of Ordinal Structure Underlies Skilled Sequential Action. Neuron 101, 1166–1180.e3.

Lee, M., Hinder, M.R., Gandevia, S.C., Carroll, T.J., 2010. The ipsilateral motor cortex contributes to cross-limb transfer of performance gains after ballistic motor practice. J Physiol 588, 201–212.

Lotze, M., Scheler, G., Tan, H.M., Braun, C., Birbaumer, N., 2003. The musician's brain : functional imaging of amateurs and professionals during performance and imagery. Neuroimage 20, 1817–1829.

Mantzaris, A. V., Bassett, D.S., Wymbs, N.F., Estrada, E., Porter, M.A., Mucha, P.J., Grafton, S.T., Higham, D.J., 2013. Dynamic network centrality summarizes learning in the human brain. J. Complex Networks 1, 83–92.

Mattar, M., Wymbs, N.F., Bock, A.S., Aguirre, G.K., Grafton, S.T., Bassett, D.S., 2018. Predicting future learning from baseline network architecture. Neuroimage 172, 107–117.

McDougle, S.D., Collins, A.G.E., 2020. Modeling the influence of working memory, reinforcement, and action uncertainty on reaction time and choice during instrumental learning. Psychon. Bull. Rev. 28, 20–39.

Mur, M., Bandettini, P.A., Kriegeskorte, N., 2009. Revealing representational content with pattern-information fMRI - An introductory guide. Soc. Cogn. Affect. Neurosci. 4, 101–109.

Murray, J.D., Bernacchia, A., Freedman, D.J., Romo, R., Wallis, J.D., Cai, X., Padoa-Schioppa, C., Pasternak, T., Seo, H., Lee, D., Wang, X.J., 2014. A hierarchy of intrinsic timescales across primate cortex. Nat. Neurosci. 17, 1661–1663.

Nissen, M.J., Bullemer, P., 1987. Attentional requirements of learning: Evidence from performance measures. Cogn. Psychol. 19, 1–32.

Oechslin, M.S., Ville, D. Van De, Lazeyras, F., Hauert, C., James, C.E., 2013. Degree of Musical Expertise Modulates Higher Order Brain Functioning 2213–2224.

Parlow, S.E., Dewey, D., 1991. The temporal locus of transfer of training between hands: an interference study. Behav. Brain Res. 46, 1–8.

Piaget, J., 1923. Le langage et la pensée chez l'enfant. Delachaux et Niestlé.

Ramkumar, P., Acuna, D.E., Berniker, M., Grafton, S.T., Turner, R.S., Kording, K.P., 2016. Chunking as the result of an efficiency computation trade-off. Nat. Commun. 7, 1–11.

Sakai, K., Kitagushi, K., Hikosaka, O., 2003. Chunking during human visuomotor sequence learning. Exp. Brain Res. 229–242.

Schmidt, R.A., 1975. A Schema Theory of Discrete Motor Skill Learning. Psychol. Rev. 82, 225–260.

Shadmehr, R., Smith, M.A., Krakauer, J.W., 2010. Error correction, sensory prediction, and adaptation in motor control. Annu. Rev. Neurosci. 33, 89–108.

Smith, M.A., Ghazizadeh, A., Shadmehr, R., 2006. Interacting adaptive processes with different timescales underlie short-term motor learning. PLoS Biol. 4, 1035–1043.

Ten, A., Kaushik, P., Oudeyer, P., Gottlieb, J., Universit, I., 2020. Humans monitor learning progress in curiosity-driven exploration. Psyarxiv.

Tremblay, P.L., Bedard, M.A., Langlois, D., Blanchet, P.J., Lemay, M., Parent, M., 2010. Movement chunking during sequence learning is a dopamine-dependant process: A study conducted in Parkinson's disease. Exp. Brain Res. 205, 375–385.

Verstynen, T., Diedrichsen, J., Albert, N., Aparicio, P., Ivry, R.B., 2005. Ipsilateral Motor Cortex Activity During Unimanual Hand Movements Relates to Task Complexity. J. Neurophysiol. 93, 1209–1222.

Verwey, W.B., Dronkert, Y., 1996. Practicing a Structured Continuous Key-Pressing Task: Motor Chunking or Rhythm Consolidation? J. Mot. Behav. 28, 71–79.

Wiestler, T., Waters-Metenier, S., Diedrichsen, J., 2014. Effector-Independent Motor Sequence Representations Exist in Extrinsic and Intrinsic Reference Frames. J. Neurosci. 34, 5054–5064.

Wong, A.L., Krakauer, J.W., 2019. Why Are Sequence Representations in Primary Motor Cortex So Elusive ? Neuron 103, 956–958.

Wymbs, N.F., Bassett, D.S., Mucha, P.J., Porter, M.A., Grafton, S.T., 2012. Differential Recruitment of the Sensorimotor Putamen and Frontoparietal Cortex during Motor Chunking in Humans. Neuron 74, 936–946.

Wymbs, N.F., Grafton, S.T., 2015. The human motor system supports sequence-specific representations over multiple training-dependent timescales. Cereb. Cortex 25, 4213–4225.

Yokoi, A., Diedrichsen, J., 2019. Neural Organization of Hierarchical Motor Sequence Representations in the Human Neocortex. Neuron 103, 1178–1190.e7.

Zhou, J., Jia, C., Montesinos-cartagena, M., Gardner, M.P.H., Zong, W., Schoenbaum, G., 2021. Evolving schema representations in orbitofrontal ensembles during learning. Nature 590.

APPENDIX

Appendix: Letter of information, Consent Form and Ethics Approval for experiments for Chapters 3-4.

LETTER OF INFORMATION FOR PARTICIPANTS
Neural correlates of skillful finger movements

Principal Investigator:
Jörn Diedrichsen, Ph.D.
Departments of Computer Science and Statistics
University of Western Ontario, London, Ontario

Introduction
We would like to invite you to take part in a study in motor control. The purpose of the research is to investigate how we learn and control complex movement skills. You are being asked to participate in this research, because we recruit participants without neurological disorders, with two functional upper limbs and with normal or corrected-to-normal vision. You should participate in this study only if you want to; you are not required to in any way. Before you decide whether you wish to take part, please read the information below. Please ask us if anything is unclear or you would like more information.

Research Procedures
If you agree to participate in this study, you will undergo multiple training and testing sessions. We will schedule the sessions during days that are most convenient for you. XX (3-10) of these of these sessions will involve behavioral training in the laboratory in the Brain and Mind Institute. XX (1-4) sessions will involve functional imaging at Robarts research institute for neuroimaging.

Behavioral training
In these sessions, you will be seated in front of a keyboard and will be asked to make a sequence of key presses in a pre-specified order as quickly as possible – sometimes you also have to press multiple finger at once in a coordinated pattern. After each movement, you will receive visual or auditory feedback on speed and accuracy. The testing is organized into blocks of trials of 3-6min length. After each block you will have the opportunity to take a break. In preparation of scanning we may also ask you to lie down on a plastic bed in the laboratory (the "mock" scanner), such that you can practice to perform the task while lying down.

Functional Imaging Procedures
An MRI machine uses a strong magnet and radio waves to make images of the body interior. You will be asked to lie on a long narrow couch for 45-90min while the machine gathers data. During this time you will be exposed to magnetic fields and radio waves. You will not feel either. You will, however, hear repetitive tapping noises that arise from the magnets that surround you. You will be provided with earplugs or headphones that you will be required to wear to minimize the sound and protect your hearing. You will also view a display on the backside of the scanner and have your fingers placed on the response keyboard that is securely placed on your lap. As in the behavioral sessions you will perform blocks of the motor task in runs of 4-10min length. After each block the scanner will stop briefly and you will be able to talk with the experimenter over intercom, receive feedback about your performance, and take a brief break if you wish. In the end of the experiment we will ask you to lie still in the scanner for approximately 10 min, such that we can obtain an anatomical image of your brain.

The space within the large magnet in which you lie is somewhat confined, although we have taken many steps to relieve the "claustrophobic" feeling. There are no known significant risks with this procedure at this time because the radio waves and magnetic fields, at the strengths used, are thought to be without harm. The exception is if you have a cardiac pacemaker, or a metallic clip in your body (e.g., an aneurysm clip in your brain), have severe heart disease, body piercings, tattoos containing metallic ink or slow release pharmaceutical skin patches.

There is a possibility that you will experience a localized twitching sensation due to the magnetic field changes during the scan. This is not unexpected and should not be painful. However, you can stop the exam at anytime. The magnetism and radio waves do not cause harmful effects at the levels used in the MRI machine. However, because the MR scanner uses a very strong magnet that will attract metal, all metallic objects must be removed from your person before you approach the scanner. In addition, watches and credit cards should also be removed as these could be damaged. (These items will be watched for you).

Risks

The behavioural part of the study has basically the same level of risk as working at a computer keyboard or practicing a musical instrument. The main risk is fatigue in the hand from the repetitive movement. The experimenter will offer you opportunity to take breaks during the experiment as often as you wish.

Part of your participation in this study will involve a research test with Magnetic Resonance Imaging (MRI) system, a common medical diagnostic tool that uses a strong magnetic field, a low frequency magnetic field, and a radio frequency field. No X-rays are used. As with any technology there is a risk of death or injury. For MRI the risk of death is less than 1 in 10 million and the risk of injury is less than 1 in 100,000. These risks do not arise from the MRI process itself, but from a failure to disclose or detect MRI incompatible objects in or around the body of the subject or the scanner room. It is therefore very important that you answer all the questions honestly and fully on the MRI screening questionnaire.

Almost all the deaths and injuries related to MRI scans have occurred because the MRI operator did not know that surgically implanted metal hardware (such as a cardiac pacemaker) was present inside the subject during the MRI scan. Other remote risks involve temporary hearing loss from the loud noise inside the magnet. This can be avoided with ear headphone protection that also allows continuous communication between the subject and staff during the scan.

For comparison, the risk of death in an MRI is similar to travelling 10 miles by car, while the risk of injury during an MRI is much less than the risks associated with normal daily activities for 1 hour. You may not be allowed to continue in this research study if you are unable to have a MRI scan because, for example, you have some MRI incompatible metal in your body, you may be pregnant or attempting to become pregnant, or you may have a drug patch on your skin that contains a metal foil. Should you require a medically necessary MRI scan in the future, the final decision as to whether you can be scanned will be made by a qualified physician considering all the risks and benefits.

MRI exclusion criteria

If you have any history of head or eye injury involving metal fragments, if you have some type of implanted electrical device (such as a cardiac pacemaker), if you have severe heart disease (including susceptibility to heart rhythm abnormalities), you should not have an MRI scan unless supervised by a physician. Additionally you should not have a MRI scan if you have conductive implants or devices such as skin patches, body piercing or tattoos containing metallic inks because there is a risk of heating or induction of electrical currents within the metal element causing burns to adjacent tissue.

Benefits and compensation

There is no direct benefit to you from participating in this study. The results from this study may help us to better understand the brain regions underlying human motor learning. Upon completion of all parts of the study, you will receive $10 for every hour of behavioral experiments and $20 for every hour of fMRI

experiments. Additionally you will receive bonuses for the points you make during the motor task. While the size of this reward depends on your performance, it usually is $5 per hour. If the study has to be stopped for any reason, compensation will be adjusted according to the fraction of the study that was completed.

Voluntary Participation / Withdrawal from Study
You should only participate in the study if you really want to; choosing not to take part will not disadvantage you in any way. At any time during the study, the experimenter may ask you to stop the study. This usually occurs for technical reasons. You also can withdraw from the study at any point in time if you feel uncomfortable, claustrophobic or tired –you just have to tell the experimenter that you wish to stop. Withdrawal will have no negative consequence for you or your academic status and you will be paid for your time that you have spend on the experiment up to that point. You can also withdraw your data from the study at any time, without negative consequence for yourself, your academic status, or your reimbursement.

Confidentiality
Any information obtained from this study will be kept confidential. Any data resulting from your participation will be identified only by a participant code, without any reference to your name or personal information. A sheet linking you name to the participant code will be stored in a securely locked filing cabinet in a room that will be accessible only to the experimenters. Five years after completion of the study these records will be destroyed. Representatives of the University of Western Ontario Health Sciences Research Ethics Board may require access to the study-related records or may follow up with you to monitor the conduct of the study. De-identified data will be kept past these five years for future usage.

Name of Sponsor / Conflict of Interest
The research is supported by a startup grant from Western University, and a Scholar award from the James S. McDonnell Foundation. Neither of the funders has played any role in study design or analysis. None of the **Investigators has a financial interest in the outcome of the study.**

Consent Form
You do not waive any legal rights by signing the consent form. You will be provided with a copy of this letter of information and the consent form.

LETTER OF INFORMATION FOR PARTICIPANTS
Neural correlates of skillful finger movements

I have read the letter of information, have had the nature of the study explained to me, and I agree to participate. All questions have been answered to my satisfaction.

Dated in London, this_____ day of_____,20___.

Name of Participant (Please print): _____

Signature of Participant: _____

Signature of Investigator: _____

Signature of Person Responsible
for Obtaining Consent:_____

Name of Person Responsible
for Obtaining Consent (Please print):_____

Date for Obtaining Consent: _____

CURRICULUM VITAE

Eva Berlot

Education

2016 – present	**University of Western Ontario** PhD in Neuroscience Supervisor: Jörn Diedrichsen, PhD
2014 – 2016	**Maastricht University** Research MSc in Cognitive Neuroscience, completed with distinction Supervisors: Elia Formisano, PhD, Federico De Martino, PhD
2011 – 2014	**University College London** BSc Psychology, completed with distinction Supervisor: Patrick Haggard, PhD

Honors and Awards

2020	Merit Abstract Award Organization for Human Brain Mapping Conference
2018	CoSMo summer school travel award (1,500 CAD)
2016 – 2020	Ontario Trillium Scholarship (160,000 CAD)
2016 – 2020	Western Graduate Research Scholarship (35,200 CAD)
2016	Ontario Graduate Scholarship (10,000 CAD) – declined due to conflict with Ontario trillium scholarship
2016	Sinapsa Travel Award (500 EUR)
2016	Cum Laude completion of research masters (Maastricht University)
2014 – 2016	Ad Futura Scholarship (24,000 EUR)
2014	Dean's Honor List for BSc completion (UCL)
2013	Wellcome Trust Biomedical Scholarship (1,600 GBP)

Publications

Berlot, E., Popp, N. J., Grafton, S. T., & Diedrichsen, J. (2020). Combining repetition suppression and pattern analysis provides new insights into the role of M1 and parietal areas in skilled sequential actions. *bioRxiv*.

Diedrichsen, J., **Berlot, E.**, Mur, M., Schütt, H. H., & Kriegeskorte, N. (2020). Comparing representational geometries using the unbiased distance correlation. *arXiv.*

Berlot, E., Popp, N.J., & Diedrichsen, J. (2020). A critical re-evaluation of fMRI signatures of motor sequence learning. *Elife, 9*, e55241.

Berlot, E., Arts, R., Smit, J., George, E., Gulban, O.F., Moerel, M., Stokroos, R., Formisano, E., & De Martino, F. (2020). A 7 Tesla fMRI investigation of human tinnitus percept in cortical and subcortical auditory areas. *NeuroImage: Clinical, 25*, 102166.

Berlot, E., Prichard, G., O'Reilly, J., Ejaz, N., & Diedrichsen, J. (2019). Ipsilateral finger representations in the sensorimotor cortex are driven by active movement processes, not passive sensory input. *Journal of Neurophysiology, 121*(2), 418-426.

Berlot, E., Formisano, E., & De Martino, F. (2018). Mapping frequency-specific tone predictions in the human auditory cortex at high spatial resolution. *Journal of Neuroscience, 38*(21), 4934-4942.

Berlot, E., Popp, N.J., & Diedrichsen, J. (2018). In search of the engram, 2017. *Current Opinion in Behavioral Sciences, 20*, 56-60.

Ferre, E., **Berlot, E.**, & Haggard, P. (2015). Vestibular contribution to aright-hemisphere network for bodily awareness: combining galvanice vestibular stimulation and Rubber Hand Illusion. *Neuropsychologia, 9*, 140-147.

Press, C., **Berlot, E.**, Bird, G., Ivry, R., & Cook, R. (2014). Moving time: The influence of action on duration perception. *Journal of Experimental Psychology, 143*, 1787-1793.

Selected Oral presentations

Berlot E., Popp, N., & Diedrichsen, J. (2020). Rethinking repetition suppression as a metric of learning. Presentation at Organization for Human Brain Mapping.

Berlot E., Popp, N., & Diedrichsen, J. (2020). fMRI signatures of motor sequence learning. Presentation at Motor Learning and Motor Control, SfN pre-meeting 2019, Chicago, USA.

Poster presentations

Berlot E., Popp, N., & Diedrichsen, J. (2020). Rethinking repetition suppression as a metric of learning. Poster at Organization for Human Brain Mapping.

Berlot E., Popp, N., & Diedrichsen, J. (2019). Motor plasticity revealed by changes in sequence-specific fMRI activity patterns across weeks of training. Poster at Society for Neuroscience, Chicago, USA.

Berlot, E., Mur, M., & Diedrichsen, J. (2019). Representational connectivity: comparing the sensitivity of connectivity metrics to noise. Poster at Organization for Human Brain Mapping, Rome, Italy.

Berlot, E., Popp, N., & Diedrichsen, J. (2018). Repetition suppression during movement execution reflects different mechanisms in the striatum than in the neocortex. Poster at Cognitive Computational Neuroscience, Philadelphia, USA.

Berlot, E., Popp, N., & Diedrichsen, J. (2018). What are the fMRI signatures for plasticity during motor sequence learning? Poster at Neural Control of Movement, Santa Fe, USA.

Berlot, E., Formisano, F., & De Martino, F. (2017). Mapping frequency-specific tone predictions at high spatial resolution. Poster at International Auditory Cortex Conference, Banff, Canada.

Berlot, E., Gulban, O.F., & De Martino, F. (2016). Tonotopy and functional connectivity in the auditory pathway of tinnitus patients: A 7 Tesla study. Poster for Organization for Human Brain Mapping, Geneva, Switzerland.

Teaching Experience

- Individual mentoring: supervision of undergraduate trainees working as research assistants (Eunice Park, Corey Mroczkowski) and for honors thesis project (Kayla Cooper)

- Presentation committee: providing feedback to Neuroscience graduate students on their presentations

Science Outreach

- Inspiring Young Women in STEM conference (2018) – organizer

- Science Rendezvous 2017 & 2018 – volunteer

- London Brain Bee 2017 & 2019 Competition – volunteer